Clinical Signs and Pathology Associated With Domoic Acid Toxicosis in Southern Sea Otters (*Enhydra lutris nereis*)

Melissa A. Miller[1,2]*, Megan E. Moriarty[1,2], Pádraig J. Duignan[2,3], Tanja S. Zabka[4], Erin Dodd[1], Francesca I. Batac[1], Colleen Young[1], Angelina Reed[1], Michael D. Harris[1], Katherine Greenwald[1], Raphael M. Kudela[5], Michael J. Murray[6], Frances M. D. Gulland[2], Peter E. Miller[7†], Kendra Hayashi[5], Catherine T. Gunther-Harrington[8], Martin T. Tinker[9] and Sharon Toy-Choutka[1]

[1] Marine Wildlife Veterinary Care and Research Center, California Department of Fish and Wildlife, Santa Cruz, CA, United States, [2] Karen C. Drayer Wildlife Health Center, One Health Institute, School of Veterinary Medicine, University of California, Davis, Davis, CA, United States, [3] The Marine Mammal Center, Sausalito, CA, United States, [4] Genentech, Inc., South San Francisco, CA, United States, [5] Department of Ocean Sciences, Institute for Marine Sciences, University of California, Santa Cruz, Santa Cruz, CA, United States, [6] Monterey Bay Aquarium, Monterey, CA, United States, [7] Institute of Marine Sciences, University of California, Santa Cruz, Santa Cruz, CA, United States, [8] Department of Medicine and Epidemiology, School of Veterinary Medicine, University of California, Davis, Davis, CA, United States, [9] Nhydra Ecological Consulting, Head of Saint Margarets Bay, NS, Canada

The marine biotoxin domoic acid (DA) is an analog of the neurotransmitter glutamate that exerts potent excitatory activity in the brain, heart, and other tissues. Produced by the diatom *Pseudo-nitzschia* spp., DA accumulates in marine invertebrates, fish, and sediment. Southern sea otters (*Enhydra lutris nereis*) feed primarily on invertebrates, including crabs and bivalves, that concentrate and slowly depurate DA. Due to their high prey consumption (25% of body weight/day), sea otters are commonly exposed to DA. A total of 823 necropsied southern sea otters were examined to complete this study; first we assessed 560 subadult, adult, and aged adult southern sea otters sampled from 1998 through 2012 for DA-associated pathology, focusing mainly on the central nervous system (CNS) and cardiovascular system. We applied what was learned to an additional cohort of necropsied sea otters of all demographics (including fetuses, pups, juveniles, and otters examined after 2012: n = 263 additional animals). Key findings derived from our initial efforts were consistently observed in this more demographically diverse cohort. Finally, we assessed the chronicity of DA-associated pathology in the CNS and heart independently for 54 adult and aged adult sea otters. Our goals were to compare the temporal consistency of DA-associated CNS and cardiovascular lesions and determine whether multiple episodes of DA toxicosis could be detected on histopathology. Sea otters with acute, fatal DA toxicosis typically presented with neurological signs and severe, diffuse congestion and multifocal microscopic hemorrhages (microhemorrhages) in the brain, spinal cord, cardiovascular system, and eyes. The congestion and microhemorrhages were associated with detection of high concentrations of DA in postmortem urine or gastrointestinal content and preceded histological detection of cellular necrosis or apoptosis. Cases of chronic

DA toxicosis often presented with cardiovascular pathology that was more severe than the CNS pathology; however, the lesions at both sites were relatively quiescent, reflecting previous damage. Sea otters with fatal subacute DA toxicosis exhibited concurrent CNS and cardiovascular pathology that was characterized by progressive lesion expansion and host response to DA-associated tissue damage. Acute, subacute, and chronic cases had the same lesion distribution in the CNS and heart. CNS pathology was common in the hippocampus, olfactory, entorhinal and parahippocampal cortex, periventricular neuropil, and ventricles. The circumventricular organs were identified as important DA targets; microscopic examination of the pituitary gland, area postrema, other circumventricular organs, and both eyes facilitated confirmation of acute DA toxicosis in sea otters. DA-associated histopathology was also common in cardiomyocytes and coronary arterioles, especially in the left ventricular free wall, papillary muscles, cardiac apex, and atrial free walls. Progressive cardiomyocyte loss and arteriosclerosis occurred in the same areas, suggesting a common underlying mechanism. The temporal stage of DA-associated CNS pathology matched the DA-associated cardiac pathology in 87% (n = 47/54) of cases assessed for chronicity, suggesting that the same underlying process (e.g., DA toxicosis) was the cause of these lesions. This temporally matched pattern is also indicative of a single episode of DA toxicosis. The other 13% of examined otters (n = 7/54) exhibited overlapping acute, subacute, or chronic DA pathology in the CNS and heart, suggestive of recurrent DA toxicosis. This is the first rigorous case definition to facilitate diagnosis of DA toxicosis in sea otters. Diagnosing this common but often occult condition is important for improving clinical care and assessing population-level impacts of DA exposure in this federally listed threatened subspecies. Because the most likely source of toxin is through prey consumption, and because humans, sea otters, and other animals consume the same marine foods, our efforts to characterize health effects of DA exposure in southern sea otters can provide strong collateral benefits.

INTRODUCTION

Domoic acid (DA) is an amino acid analog of kainic acid and glutamate that acts as a potent excitotoxin when ingested by humans and other animals. Along the North American Pacific Coast, DA is produced during blooms of the diatom *Pseudo-nitzschia* spp., including *P. australis* (Scholin et al., 2000; Trainer et al., 2000; Bargu et al., 2010). Domoic acid can accumulate in food webs (Lefebvre et al., 2002; Trainer et al., 2002; Kvitek et al., 2008) and persist in marine sediments (Sekula-Wood et al., 2009), enhancing exposure risks for humans and wildlife. Domoic acid-associated human deaths were first recognized along the east coast of North America in 1987 (Perl et al., 1990a,b; Teitelbaum et al., 1990). In California, DA was initially reported as a cause of avian mortality (Fritz et al., 1992; Work et al., 1993) and then as a cause of marine mammal mass-stranding (Scholin et al., 2000). Subsequent studies have confirmed health impacts in diverse marine wildlife (Shumway et al., 2003; Bejarano et al., 2008; Lefebvre et al., 2010; McHuron et al., 2013), clarified food web exposure patterns (Lefebvre et al., 2002; Goldberg, 2003;

Kvitek et al., 2008), and identified factors influencing *Pseudo-nitzschia* bloom dynamics and DA production (Bargu et al., 2010; Lewitus et al., 2012; McKibben et al., 2017).

Laboratory research has provided insight into the pathophysiology of DA (Tryphonas et al., 1990; Pulido et al., 1995; Sobotka et al., 1996; Giordano et al., 2007). Early observational studies focused on neurotoxicity (Tryphonas et al., 1990; Pulido et al., 1995; Silvagni et al., 2005), while later investigations documented cardiovascular pathology and other health impacts (Kreuder et al., 2005; Gill et al., 2007; Zabka et al., 2009; Moriarty et al., 2021a,b). Acute, subacute, and chronic effects of DA exposure are now recognized in people, wildlife, and laboratory animals (Sutherland et al., 1990; Goldstein et al., 2008; Pulido, 2008; Buckmaster et al., 2014). Severe, intermittent, or chronic sublethal DA exposure can cause cognitive and functional deficits such as impaired memory, poor spatial navigation, and temporal lobe epilepsy (Zatorre, 1990; Cendes et al., 1995; Sobotka et al., 1996; Goldstein et al., 2008; Thomas et al., 2010; Buckmaster et al., 2014; Ramsdell and Gulland, 2014; Grattan et al., 2018).

Sequestration of DA in fetal fluids can prolong maternal and fetal toxicosis (Ramsdell and Zabka, 2008; Goldstein et al., 2009; Lefebvre et al., 2018). Permanent neurobehavioral deficits from *in utero* or early postnatal DA exposure have been described in California sea lions (*Zalophus californianus*) (Goldstein et al., 2008; Ramsdell and Zabka, 2008; Thomas et al., 2010; Cook et al., 2015, 2016), primates (Burbacher et al., 2019), and rodents (Sobotka et al., 1996; Doucette et al., 2004; Levin et al., 2006; Lefebvre et al., 2017). Domoic acid has also been detected in milk from California sea lions, indicating lactational exposure (Rust et al., 2014).

Despite awareness of the effects of DA in Pacific coastal marine ecosystems (Lefebvre et al., 2016), little is known about the health and population impacts on California's smallest marine mammal: the southern sea otter (*Enhydra lutris nereis*). This federally listed threatened subspecies has a current population of approximately 3,000 individuals distributed along 500 km of the central California coast (Hatfield et al., 2019). Toxic *Pseudo-nitzschia* blooms are common throughout southern sea otter habitat (McCabe et al., 2016; McKibben et al., 2017), and cases of DA-associated fatal neurotoxic and cardiovascular disease have been reported in sea otters (Kreuder et al., 2005; Miller et al., 2020; Moriarty et al., 2021b).

The primary objective of this study was to establish a case definition for DA toxicosis in southern sea otters using insight gained from necropsy and microscopic examination of 823 individuals necropsied from 1998 through 2018. Our secondary objectives were to describe acute, subacute, and chronic lesions associated with DA toxicosis, estimate the DA post-exposure intervals based on lesion characteristics and stereotypical host tissue response patterns, and compare the temporal patterns in the CNS and cardiovascular system. Improved recognition of DA toxicosis can inform clinical care, facilitate estimates of population-level health impacts, and aid assessment of disease prevalence in relation to climate change and other environmental perturbations.

MATERIALS AND METHODS

Sample Population and Comprehensive Postmortem Evaluations

The sample population consisted of minimally decomposed southern sea otters from the central California coast that were necropsied from 1998 through 2018 (**Supplementary Table 1**). Criteria for diagnosing DA toxicosis were developed initially using a subgroup of 560 subadults, adults, and aged adults that were part of an in-depth review of sea otter mortality patterns from 1998 through 2012 (Miller et al., 2020). Provisional diagnostic criteria were assessed and further refined via examination of additional otters of all age classes (fetuses, pups, immatures, subadults, adults, and aged adults), and animals necropsied through 2018 (*n* = 263; **Supplementary Table 1**). Finally, we independently assessed and compared the chronicity of gross and microscopically apparent DA-associated pathology in the CNS and heart of 54 adult and aged adult southern sea otters with optimal tissue sampling (**Supplementary Tables 1**, **2**). The total sample size for all three phases of this study was 823 southern sea otters that were necropsied from 1998 through 2018.

When available, antemortem clinical data were reviewed to assess findings associated with DA toxicosis. Standardized protocols were utilized for gross necropsy, tissue and body fluid collection, histopathology, and diagnostic testing. The abdomen, thorax, brain, and heart were photographed during necropsy to facilitate comparison among sampled sea otters. All major organs and tissues were examined grossly and microscopically, including the brain, pituitary gland, trigeminal ganglia, heart, aorta, kidneys, eyes, lung, liver, spleen, pancreas, adrenal glands, gallbladder, stomach, intestines, rectum, omentum, lymph nodes, salivary glands, skeletal muscles, tongue, soft palate, tonsil, esophagus, thymus, thyroid, parathyroid, bladder, skin, gonads, and reproductive tract. Formalin-fixed tissues were trimmed using a standard protocol (**Supplementary Data Sheets 1, 2** and **Supplementary Images 1A,B**) so that lesions could be compared among cases.

Central nervous system (CNS) trimming of the brain for microscopic examination was initiated by a single coronal slice through the left and right cerebral hemisphere and diencephalon just caudal to the mammillary bodies (**Supplementary Data Sheet 1** and **Supplementary Image 1A**). Coronal slices were cut sequentially from this point both rostrally and caudally at approximately 4 mm thickness throughout the cerebrum, cerebellum, and brainstem, and standardized sections were collected for histopathology to facilitate comparison. The pituitary gland was bisected along the sagittal midline for histological examination (**Supplementary Data Sheet 1** and **Supplementary Image 1B**). Microscopic examination included the left and right rostral and caudal hippocampus, olfactory and entorhinal cortex, parahippocampal cortex, temporal cerebral cortex, rhinencephalon at the level of the lateral olfactory tract, pituitary gland, cerebellum, pons, medulla, ventricles, meninges, choroid plexus, and trigeminal ganglia. For some cases, the olfactory bulbs, spinal cord, brainstem, diencephalon, mesencephalon, and additional circumventricular organs (CVOs), including the area postrema, pineal gland, and median eminence, were also examined.

Cardiac trimming and histopathology were standardized to include the left and right atrioventricular free wall and valves, papillary muscles, interventricular septum, cardiac apex, and thoracic aorta (**Supplementary Data Sheet 1**). One or both eyes were bisected mid-sagittally at the optic nerve and examined microscopically (**Supplementary Data Sheet 1**). Trim sheets were completed so that each tissue could be identified during microscopic examination (**Supplementary Data Sheet 2**). Epidemiological assessment of DA-associated mortality patterns and comprehensive DA testing of body fluids and tissues from necropsied southern sea otters are summarized in separate publications (Miller et al., 2020; Moriarty et al., 2021b; Tinker et al., in Press; Miller et al., In final preparation).

Assessment of DA-Associated Pathology
The potential for DA toxicosis as a cause of death for each sea otter was determined using a preponderance of evidence

approach that included review of available case history, gross and microscopic assessment of the brain, heart, eyes, and other tissues, and biochemical tests (liquid chromatography-mass spectrometry and enzyme-linked immunosorbent assay) for DA in tissues and body fluids. Publications on the pathology of DA in other species aided lesion assessment (Teitelbaum et al., 1990; Tryphonas et al., 1990; Bruni et al., 1991; Pulido et al., 1995; Silvagni et al., 2005; Goldstein et al., 2008; Zabka et al., 2009; Lefebvre et al., 2010; Vranyac-Tramoundanas et al., 2011; McHuron et al., 2013; Buckmaster et al., 2014). Also considered, when available, were data on confirmed toxic *Pseudo-nitzschia* bloom events, DA-associated public safety seafood harvest closures, and DA-associated stranding of sympatric wildlife.

Variation in the level of detail available for each case (a common challenge for retrospective studies of free-ranging wildlife) affected the precision of diagnostic assessment. More informative cases had antemortem data, a shorter time interval between death and necropsy, biochemical testing for DA, and comprehensive necropsy and histopathology. Less precise cases had more limited clinical history, DA test results, histopathology and/or reduced sample quality due to minor postmortem scavenging or autolysis; however, diagnostic assessment was both possible and informative. Domoic acid case classification (Miller et al., 2020) reflected the level of confidence in the likelihood of DA toxicosis as a primary or contributing cause of death: probable cases had the highest confidence for DA toxicosis as a cause of death, while possible cases had indications of DA exposure but insufficient detail to confirm whether DA toxicosis contributed to mortality. Negative cases were considered unlikely to have DA toxicosis as a cause of death.

Prior epidemiological studies have identified DA exposure and systemic protozoal disease due to *Toxoplasma gondii* and/or *Sarcocystis neurona* as significant risk factors for fatal cardiomyopathy in southern sea otters (Kreuder et al., 2005; Miller et al., 2020; Moriarty et al., 2021b). Kreuder et al. (2005) pooled cases with moderate to severe non-suppurative myocarditis and those with significant non-inflammatory cardiac pathology. For the current study, a range of lesions including myocardial congestion, hemorrhage, cardiomyocyte vacuolation, apoptosis, necrosis or loss, interstitial edema, non-suppurative inflammation, vascular pathology, fibrosis, and microscopic hemorrhage (microhemorrhage) were assessed independently to distinguish cardiac lesions associated with DA toxicosis from those attributable to protozoal infection or other etiologies. Based on prior research (Miller et al., 2020), southern sea otters with purely suppurative myocarditis or endocarditis were grouped separately due to suspected or confirmed bacterial etiology. Cases were not classified based on the presence/absence of cardiac dilation, because experience from >20 years of southern sea otter postmortem examinations suggests that these differences represent stages within a continuum of cardiomyopathy expression.

Microscopic assessment of the CNS, heart, and eyes was performed in relation to the other tissues to document the systemic effects of DA toxicosis and identify criteria that could facilitate diagnosis. Gross and microscopic

pathology from the most definitive acute DA cases were compared with non-DA cases. We also identified lesions in sea otters similar to those that have been reported in other species with DA toxicosis. Due to the complex systemic effects of DA toxicosis, the possibility of repeated sublethal DA exposure, and potential interactions among concurrent health conditions, lesion patterns were reported conservatively as DA-associated pathology. Confirming the pathophysiological mechanisms underlying lesion development was beyond the scope of this descriptive, necropsy-based, retrospective study.

Estimating the Interval Between DA Exposure and Death Based on Lesion Chronicity

For a prior analysis of southern sea otter mortality patterns (Miller et al., 2020), estimates of DA lesion chronicity were pooled as acute/subacute for CNS lesions and subacute/chronic for cardiovascular lesions because more in-depth temporal assessment was not considered possible in wild sea otters with unknown DA exposure timing, frequency, and dose. However, as we gained an understanding of patterns of DA lesion development, progression, and healing responses, we were able to estimate acute, subacute, and chronic post-DA exposure intervals. These intervals were based on the gross and microscopic appearance of DA-associated CNS, cardiovascular, and ocular pathology, and uniform patterns of host response following toxic injury (Kumar et al., 2014). Estimates of lesion chronicity and post-DA exposure intervals were also guided by DA concentrations in postmortem tissues and body fluids, case histories, and descriptions of DA-associated pathology and lesion progression in other animals (Bruni et al., 1991; Pulido et al., 1995; Silvagni et al., 2005; Goldstein et al., 2008; Zabka et al., 2009; Lefebvre et al., 2010; Vranyac-Tramoundanas et al., 2011; Buckmaster et al., 2014). Based on the above criteria, acute lesions were estimated to have developed within a few hours to a few days prior to death, subacute lesions likely developed within a few days to approximately 6 months prior to death, and chronic pathology was considered the result of DA toxicosis occurring >6 months to years before death. Because the duration between DA exposure and death is unknown for wild sea otters, and recurrent DA exposure is possible given the pervasiveness of this toxin in the marine environment, these temporal criteria are estimates that should be further validated and refined through prospective research.

After identifying CNS and cardiac lesion patterns characteristic of each DA post-exposure chronicity category (acute, subacute, and chronic), we assessed the chronicity of gross and microscopic DA-associated pathology in the CNS and heart of 54 adult and aged adult southern sea otters with optimal tissue sampling. The relative chronicity of DA-associated pathology and the presence/absence of any mixed temporal patterns (e.g., acute pathology superimposed on pre-existing chronic lesions) were noted independently for the CNS and heart prior to comparison. Strong temporal associations, such as the presence of subacute pathology in both organ systems,

were considered indicative of a single event of DA toxicosis that concurrently affected the CNS and cardiovascular system. The presence of concurrent acute, subacute, and/or chronic DA-associated pathology in the CNS, heart, or both tissues was also evaluated, given its importance as potential evidence for recurrent DA toxicosis.

Documentation of *Pseudo-nitzschia* Uptake by Ingested Prey in Sea Otters Acutely Exposed to DA

Prey items from the gastrointestinal (GI) tracts of two sea otters were assessed for *Pseudo-nitzschia* diatom ingestion. Both sea otters died during toxic *Pseudo-nitzschia* blooms, had histopathology indicative of acute DA toxicosis, and had very high DA concentrations (5,000–56,200 ppb) in postmortem urine and gastric content. Minimally digested sand crabs (*Emerita analoga*) were recovered from the stomach of both sea otters at necropsy. The GI tracts of these sand crabs were dissected, pooled for each sea otter, and cleaned using a modified $KMnO_3$/HCl oxidation method to remove soft tissue (Miller and Scholin, 1998). Cleaned cells were resuspended in distilled water and filtered onto a Millipore filter (Millipore Sigma, Burlington, MA, United States). The dried filter was mounted to an aluminum stub, sputter-coated with gold-palladium, and viewed on a scanning electron microscope (SEM: model ISI WB-6; International Scientific Instruments, New Delhi, India) for the presence of *Pseudo-nitzschia* frustules (silica-based exoskeletons of diatoms). Free-living sand crabs were also collected during a toxic *Pseudo-nitzschia* bloom that was associated with marine mammal mass-mortality; the GI tracts of these crabs were also processed to confirm *Pseudo-nitzschia* ingestion as described above. Finally, an *in vitro* culture of *Pseudo-nitzschia australis* diatoms was cleaned, dried on a glass coverslip, and mounted to an aluminum stub prior to coating and SEM; this served as a positive control for *Pseudo-nitzschia* frustules.

RESULTS

A bimodal pattern of DA-associated clinical signs and pathology was observed in southern sea otters. Otters with acute DA toxicosis typically stranded with severe CNS signs, chronic cases presented predominantly with severe cardiovascular signs, and subacute cases showed either or both patterns. Detailed descriptions of clinical, gross, and histopathology findings are described below. Clinical, biochemical, and gross necropsy findings are summarized by chronicity category in **Table 1**, and DA-associated histopathology is summarized in **Table 2**. To optimize the utility of the summary tables and pathology image content of this manuscript for diagnosing potential DA cases, all figures and **Tables 1**, **2** are also available as separate, large, high-resolution, downloadable files in **Supplementary Presentation 1** in the Supplementary Materials. It is important to note that the figure order and numbering differs between the text of the manuscript, where the figures are cited in order of discussion, and

Supplementary Presentation 1, where the figures are arranged by 1) organ system (e.g., brain, heart, etc.), then 2) tissue subtype within each organ system (e.g., hippocampus, atrium, etc.), 3) from gross, broad-scale pathology findings to progressively higher magnification microscopic views that show lesions in detail, and 4) from acute to chronic with respect to the estimated post-exposure interval for DA toxicosis, so that the reader can visually assess lesion progression and resolution through time. The figures are arranged this way so that the most definitive findings for confirming a diagnosis of DA toxicosis are illustrated first, while helpful but less diagnostically definitive findings are found at the close of each section (e.g., in the CNS, diagnostic hippocampal lesions are presented prior to DA-associated cerebellar pathology.) Side-by-side images within figures also depict normal tissues along with progressive lesion development through time (acute, subacute, and chronic). To facilitate comparison between the lesion descriptions in each table and corresponding images, the **Supplementary Presentation Figures** are also cross-referenced in column 1 of the **Supplementary Presentation Tables 1** and **2**.

Domoic Acid-Associated Clinical Findings

Sea otters stranding alive with acute DA toxicosis were often in good to excellent nutritional condition (**Figures 1A,B**), with full GI tracts (**Figure 2A**). Clinically these animals often exhibited tremors, seizures, obtundation, hyper- or hypothermia, and visual deficits (**Table 1**). Other clinical signs included somnolence or unusual tameness, difficulties with ambulation and food prehension, and abnormal vocalization. These neurological signs could be caused by DA-associated neurotoxicity and/or the observed regional or systemic vascular pathology leading to fluid leakage, brain swelling, and cerebellar herniation.

In subacute and chronic cases, clinical signs could be continuous or episodic. Chronically affected individuals often exhibited abrupt cessation of normal behaviors (such as eating), remaining immobile and unresponsive for several minutes before resuming normal activity. Periods of reduced activity were sometimes accompanied by tremors. A few sea otters displayed unusual aggression or persistent biting and chewing on an extremity and were euthanized as potential rabies suspects; brain tissue screening for rabies was negative in all cases. Abrasions or scrapes on the nose, face, and paws, asymmetrical whisker wear, and self-trauma to the paws, penis, or tail were suggestive of significant neurological impairment, paresthesia, and/or ambulatory deficits. Some otters had clinical signs or gross pathology suggestive of spinal cord damage, including hind limb paraparesis, fecal impaction, and urine retention, all of which have been reported for other DA-affected species (Jian Wang et al., 2000; Pulido, 2008).

Live-stranded sea otters with subacute to chronic cardiomyopathy had radiographic evidence of cardiomegaly and enhanced pulmonary density, and clinical indications

TABLE 1 | Clinical, biochemical and gross findings suggestive of domoic acid toxicosis and DA-associated cardiomyopathy in southern sea otters (*Enhydra lutris nereis*).

Assessment Type	Acute (Hours to days)	Subacute (Days to <6 months)	Chronic (≥6 months to years)
	Central nervous system (CNS) signs & lesions dominate. Occasional deaths from acute cardiovascular impacts	May present with severe CNS and/or cardiovascular deficits <– – – – – – – – – – –>	Cardiovascular signs & lesions dominate. CNS signs may be present but less severe than cardiovascular pathology
External Examination	• Fair-excellent nutritional condition • Glossy, well-groomed pelage • +/− Perimortem neurological disease; abraded nose, face, paws, self-trauma, clear to mucoid oronasal fluid/hypersalivation	• +/− Perimortem neurological disease (abrasions nose, face, paws, self-trauma) • Signs overlap with acute & chronic cases • Variable nutritional condition • Pelage may be poorly groomed, dry • +/− Copious red or yellow-tinged, clear to mucoid oronasal fluid & pulmonary edema	• Signs of cardiac/respiratory failure • Declining (poor-fair) nutritional condition, often cachexic; empty GI tract • Pelage often poorly groomed, dry • +/− Peritoneal effusion, fluid wave • +/− Red or yellow-tinged, clear to mucoid oronasal fluid & pulmonary edema
DA Biochemical Results (urine, GI content)	• Often DA-positive, may be ≥ 300 ppb (≥500 ppb is highly suspect for DA) • *Pseudo-nitzschia* frustules in prey • Negative test does not rule out toxicosis, esp. if alive for hours/days before death	• DA test results variable, less informative • DA values may not correspond with lesion severity or chronicity	
Clinical Presentation	• Tremors, seizures, tameness, paresis, obtundation, aggression, self-trauma, blindness/visual deficits, hypersalivation	• +/− Chronic/recurrent neurological disease • Cardiopulmonary disease, dyspnea	• Cardiopulmonary disease, heart failure, effusion, dyspnea, emaciation • +/− Chronic/recurrent neurological disease
Brain	• Meninges, neuropil, & ventricles: Severe congestion +/− hemorrhage • +/− Neuropil pink, wet, translucent • +/− Variable brain swelling & herniation	• Meningeal & neuropil congestion gradually fades +/− hemorrhage • +/− Variable brain swelling & herniation • Neuropil pink, white to pale tan (late)	• Neuropil pale tan +/− brain atrophy • Hippocampus shrunken, flattened, asymmetrical, enlarged ventricle(s) • Minimal congestion, herniation, swelling
Cerebrospinal Fluid Volume*	• Mildly increased (normal ≤2 ml)	• Variable (mild-marked) increase (>2 ml)	
Cardiovascular System	• Myocardium may look brown, wet, translucent • +/− Heart, systemic veins & viscera appear mildly dilated & "full of blood", but organs not abnormally enlarged • +/− Grossly apparent hemorrhage in papillary muscles, ventricular myocardium • +/− Pleural, pericardial and peritoneal effusion (mild to moderate)	• Myocardium pale & mottled or streaked, especially apex, ventricles (L > R), brown discoloration mild/absent. • Atrial walls increasingly opaque • +/− Mild myocardial hemorrhage • Variable (none-severe) cardiac dilation • +/− Pleural, pericardial, peritoneal effusion	• Variable (mild to severe) cardiac & venous dilation +/− venous shunts (chest, abdomen) • Myocardium pale, tan or white spots or streaks, atrial walls often opaque • Severe congestion, cardiomegaly, hepatomegaly, chronic passive congestion • Moderate-severe peritoneal, pleural & pericardial effusion, hepatic capsular fibrin • Pulmonary edema +/− interstitial fibrosis
		• +/− Depressed, thin or transparent areas, especially near apex (myofiber loss)	
		• +/− Hepatic vein thrombosis	
	• +/− Arrhythmias, acute death, heart failure, pulmonary edema, dyspnea, cyanosis		

(Continued)

TABLE 1 | Continued

Assessment Type	Acute (Hours to days)	Subacute (Days to < 6 months)	Chronic (≥6 months to years)
Pericardial Fluid*	• **Volume mildly increased (Normal = 1.5-2 ml), may be strongly DA positive** • +/− pale brownish/reddish tinge	• **Volume moderately/markedly increased (~4-8 ml), may be DA-positive**	• **Volume markedly increased (often >8 ml)**
		• +/− fibrin strands interspersed in pericardial fluid	
Eyes	• **+/− Blindness/visual deficits** • **Hyphema (Unilateral or bilateral)**	• **+/− Blindness/visual deficits** **Hyphema (Unilateral or bilateral)**	• +/− Blindness/visual deficits • +/− Hyphema (Unilateral or bilateral)
Liver	• Moderate diffuse congestion	• Hepatomegaly (mild/moderate), hepatic passive congestion, +/− mild hemosiderosis • Serous ascites +/− fibrinous capsulitis • +/− Grossly apparent fibrin thrombi in hepatic vein & hepatic parenchymal necrosis	• Hepatomegaly (moderate/marked), hepatic passive congestion, hemosiderosis +/− Liver surface has irregular "cobblestone" appearance • Hemorrhagic ascites, fibrinous capsulitis • +/− Hepatic vein thrombi, hepatic necrosis
Kidneys and Bladder	• Moderate/marked diffuse congestion	• Variable congestion	• Moderate-marked congestion
		• +/− Dilated, urine-distended bladder	
Stomach and Intestines	• **Often food in GI tract, including minimally digested food in stomach**	• **+/− Partially digested food in GI tract**	• **GI tract often empty, atrophic**
	• +/− Ileus, intussusception, torsion	• +/− Serosal & mucosal congestion	
Female-Specific	• +/− Recent abortion, acute death while pregnant, stillborn fetus, pre-term fetus • +/− Signs of forced copulation during non-estrus period (while pregnant, possibly due to neurological disease) • **Uterus, placenta, fetus: Congestion, edema, brain or myocardial hemorrhage, meconium stains +/−uterine torsion** • None to mild mismatch between systemic adipose stores & muscle catabolism	• +/− Recent abortion, death while pregnant, stillborn fetus, +/− uterine torsion • +/− Signs of forced copulation during non-estrus period (due to neurological disease) • +/− Fetus: Congestion, edema, brain or myocardial hemorrhage, meconium stains • Variable mismatch between systemic adipose stores & muscle catabolism	• +/− Cardiac decompensation during pregnancy, recent abortion, stillborn fetus • +/− Pregnant but emaciated, or marked nutritional mismatch (ample systemic adipose but severe muscle catabolism) • +/− Fetus: Emaciation, congestion, edema, meconium stains (female attempted to reproduce despite progressive cardiac disease)
		• Perimortem fight trauma	
	• History of "rebooting" reproductive cycle, poor pup care or preweaning pup		
Male-Specific	• No testicular atrophy	• +/− Testicular atrophy	• Testicular atrophy
	• +/− Mild paraphimosis or self-trauma	• No paraphimosis or self-trauma	• No paraphimosis or self-trauma

Definitions: GI, gastrointestinal; PPB, parts per billion.
***Bold text**, most helpful criteria for DA case diagnosis and staging, when present. +/−, findings that are less consistently observed or less definitive.*
*Longer postmortem interval, blood loss & dehydration can decrease yield.

TABLE 2 | Histopathology findings suggestive of domoic acid (DA) toxicosis and DA-associated cardiomyopathy in southern sea otters (*Enhydra lutris nereis*).

Key Tissues	Acute (Hours to days)	Subacute (Days to < 6 months)	Chronic (≥6 months to years)
	Central nervous system (CNS) signs and lesions dominate. Occasional deaths from acute cardiovascular impacts.	May present with severe CNS and/or cardiovascular deficits. < – – – – – – – – – – – – >	Cardiovascular signs and lesions dominate. CNS signs may be present, but are often less severe than cardiovascular pathology.
Hippocampus, Entorhinal Cortex, Parahippocampal Gyrus	• **Marked diffuse congestion and multifocal microhemorrhages,** • **+/− spongiosis** +/− Perivascular fibrinoid changes in hippocampus and elsewhere without evidence of sepsis or endotoxemia • No/mild neuronal necrosis, shrinkage, dropout, astrogliosis on histopathology	• Pyramidal neurons: Necrosis, apoptosis, hyperchromic, shrunken, pale, elongated, dropout, especially cornu ammonis 2 region (CA2), entorhinal cortex, parahippocampal gyrus. Dentate neurons relatively spared. "Red dead" neurons relatively uncommon • Lesions commonly segmental, spread up and down CA over time (spans CA1-4 in severe cases), with most severe damage around CA2. Pyramidal neuron loss and gemistocytic astrocyte proliferation. • Perivascular and laminar spongiosis of molecular layer between CA and dentate granule cells with gliosis • Lesions often asymmetrical • Progressive neuropil vacuolation, +/− malacia near blood vessels and ventricles • Segmentally decreased pyramidal neuron density, focal retraction toward dentate, and flattening of pyramidal neuron curve, outer hippocampus, dilation of lateral ventricle • Ventricle walls appear irregular, "moth-eaten", with discontinuous ependyma • Progressive decrease in congestion, microhemorrhage, fibrinoid change	• Mild to complete segmental loss of pyramidal neurons (especially in CA2), mild gliosis, malacia. Smooth curve of CA pyramidal neurons becomes angular • Inflexion of dentate neurons often "points" toward area of most severe segmental pyramidal neuron damage (consistent tissue trimming is required) • Retraction of severely affected CA segments toward dentate neurons, flattened medial hippocampus, ventricle dilation • Hippocampi may appear shrunken, flattened, asymmetrical, with enlarged lateral ventricle • Ventricle walls appear irregular, "moth-eaten", with discontinuous ependyma • Chronic, mild, sublethal cases can be challenging to confirm, especially when autolysis or concurrent pathology are present • For severe chronic lesions, may see neuropil loss, cavitation, extracellular vacuoles; lesions often bilateral but may be asymmetrical • No severe congestion or microhemorrhage • Minimal/no discernible neuronal necrosis, shrinkage, dropout. Astrogliosis may persist
Pituitary	• **Moderate to marked congestion in pars distalis and pars nervosa with relative sparing of pars intermedia. Microhemorrhages in pars nervosa**	• +/− Vascular congestion in pars distalis and pars nervosa with relative sparing of pars intermedia, +/− edema and microhemorrhages in pars nervosa	• No abnormal pituitary congestion, edema, hemorrhage • +/− Scarring in pars nervosa
Area Postrema, Other Circumventricular Organs (CVOs)	• **Congested, spongiotic, +/− microhemorrhages**	• Mild to moderately congested, spongiotic, +/− neuronal necrosis or apoptosis, astrogliosis, damaged ventricle wall, microhemorrhage	• Adjacent ventricle may appear scarred, "moth-eaten", with discontinuous ependyma • +/−Scarring, gliosis, vacuolation

(Continued)

TABLE 2 | Continued

Key Tissues	Acute (Hours to days)	Subacute (Days to < 6 months)	Chronic (≥ 6 months to years)
Choroid Plexus, Ependyma, Ventricles, Sub-Ependymal Neuropil	• Congestion of choroid plexus • Ventricles may contain cell debris and acute hemorrhage • Sub-ependymal neuropil: +/– Congestion, microhemorrhage, spongiosis (especially lateral and third ventricles) • Ependyma and choroid: +/–acute necrosis/apoptosis, cells rounded, swollen, eosinophilic, sloughing	• Ventricles may contain cell debris and mild to severe hemorrhage • Sub-ependymal neuropil: Congestion, microhemorrhage, spongiosis, astrogliosis • Ventricles: Irregular contour, "moth-eaten" appearance, patchy ependymal lining, ependymal cells trapped below surface • Ventricle edges may adhere, forming scars • Ependyma, choroid: Lessening congestion, necrosis, apoptosis	• +/– Mild pallor, spongiosis and astrogliosis of sub-ventricular neuropil • Ventricles variably dilated with irregular contours, "moth-eaten" appearance • +/– Ventricles discontinuously lined by ependyma and acellular fibrils, bands of ependymal cells trapped below surface • Ventricle edges may adhere, forming scars
Diencephalon (Thalamus, Hypothalamus)	• Marked vascular congestion, microhemorrhage less prominent • +/– Perivascular spongiosis • Minimal/no discernible neuronal necrosis, dropout, astrogliosis	• Progressive development of multifocal large, well-defined vacuoles, especially near ventricles and neuronal nuclei • Congestion progressively fades • Perivascular spongiosis • Sparse neuronal necrosis/apoptosis, shrinkage, dropout, astrogliosis • Periventricular neuropil and ependyma may look spongiotic, scarred, "moth-eaten"	• Multifocal large, sharp-walled, well-defined vacuoles, especially near ventricles and neuronal nuclei • Periventricular neuropil and ependyma may appear scarred, "moth-eaten" • +/– Decreased neuronal density in some nuclei, +/– mild astrogliosis
Cerebellum, Pons, Medulla	• Marked diffuse vascular congestion, especially in meninges and molecular layer	• Marked diffuse vascular congestion, especially in molecular layer	• Periventricular neuropil and ependyma may appear scarred, "moth-eaten" • Sparse scarring and vacuolation
	• Purkinje cell layer: +/– mild laminar swelling of astrocytes and Purkinje cell loss	• Purkinje cell layer: +/– mild laminar swelling of astrocytes and Purkinje cell loss	
Olfactory Tracts, Olfactory Bulbs	• Marked congestion, mild/moderate spongiosis and laminar swelling of astrocytic foot processes, +/– microhemorrhages • Neurons and glia: Mild-moderate cytoplasmic vacuolation, minimal/no necrosis, shrinkage, dropout, astrogliosis	• Mild/moderate spongiosis and laminar swelling of astrocytic foot processes • Marked congestion +/– multifocal microhemorrhage (progressively fades) • Sparse neuronal necrosis, shrinkage, dropout, gemistocytic astrogliosis	• +/– Sparse, well-defined vacuoles along laminae (Swollen astrocytic processes) • +/– Mild gemistocytic astrogliosis
Spinal Cord	• Severe diffuse congestion, multifocal microhemorrhage • +/– Dilation of central canal, ependymal loss, minimal intraluminal hemorrhage • +/– Perivascular and periventricular spongiosis and microhemorrhage	• Dilation of central canal, ependymal loss, minimal intraluminal hemorrhage • +/– Patchy symmetrical neuronal necrosis • +/– Microhemorrhage, gemistocytic astrocytes, sparse dilated axon sheaths	• +/– Dilation and mural scarring of central canal, variable ependymal loss • +/– Sparse axonal loss, ballooning of axon sheaths, mildly decreased neuronal density • +/– Multifocal large, well-defined clear spaces, especially near ventricles

(Continued)

TABLE 2 | Continued

Key Tissues	Acute (Hours to days)	Subacute (Days to < 6 months)	Chronic (≥6months to years)
Cardiovascular and Pulmonary	• **Marked diffuse myocardial congestion and multifocal microhemorrhages: Perivascular, epi- and endocardium, coronary groove, papillary muscles** • **Coronary endothelial and vascular smooth muscle necrosis/apoptosis/ vacuolation, mural edema, hemorrhage** • +/− **Proteinacious interstitial edema** • +/− Bands of bunched cardiomyocytes, hyper-eosinophilic, glassy appearance • +/−Mild cardiomyocyte swelling, edema, vacuolation, necrosis, or apoptosis • Coronary vasculature: No hyalinization	• **Cardiomyocytes: Cytoplasmic vacuolation, eosinophilia, swelling, necrosis, apoptosis, myophagia** • **Multifocal cardiomyocyte loss with stromal collapse, fatty replacement, mild fibrosis, non-suppurative inflammation** • **Coronary arterioles: Smooth muscle necrosis/apoptosis. Walls of coronary arterioles increasingly hyalinized, hypocellular** **+/− sparsely mineralized** • Decreasing congestion, interstitial edema • Most severe lesions: apex, left ventricular free wall, septum, and papillary muscles • Ventricles: Often sub-endocardial/sub-epicardial lesion distribution	• **Moderate to severe multifocal cardiomyocyte loss, intersecting bands of stromal collapse, fatty replacement, stromal fibrosis** • **Large expanses of atrium may contain few cardiomyocytes, severe fatty replacement, no/mild inflammation** • Walls of coronary arterioles hyalinized, hypocellular, thickened, sparsely mineralized Endothelium may be bunched and rounded • Cardiomyocyte necrosis/apoptosis/cytoplasmic vacuolation less prominent • Lesions most severe apex, left ventricular free wall, atrium, papillary muscles, septum
Hepatobiliary	• Moderate diffuse congestion • +/− Mild acute venous dilation	• Hepatic passive congestion, atrophy of hepatic cords (especially centrilobular) • +/− Patchy hepatic necrosis and thrombosis	• Hepatic passive congestion, atrophy of hepatic cords (centrilobular to diffuse) • +/− Patchy hepatic necrosis and thrombosis
Eyes	• **Hyphema and severe diffuse vascular congestion (bilateral)**		• +/− Blindness/visual deficits • +/−Congestion, hyphema due to congestive heart failure
Female Reproductive System	• +/− **Bands and patches of myometrial hyper-eosinophilia, necrosis, apoptosis** • +/− **Myometrial arteries: Endothelial and smooth muscle necrosis or apoptosis, degeneration, edema, hemorrhage** • Placental congestion, hemorrhage, necrosis	• **Bands and patches of myometrial hyper-eosinophilia, necrosis, apoptosis** • **Myometrial vessels: Endothelial and smooth muscle cell necrosis or apoptosis, degeneration, edema, hemorrhage** • Placental congestion, hemorrhage, necrosis	• Placental congestion, hemorrhage, necrosis (associated with congestive heart failure)
Renal	• Moderate to marked diffuse congestion	• Variable congestion	• Moderate to marked congestion
Gastrointestinal		• +/− Moderate vascular congestion	

Definitions: CA, cornu ammonis of hippocampus.
Bold text, *most helpful criteria for DA case diagnosis and staging, when present.*
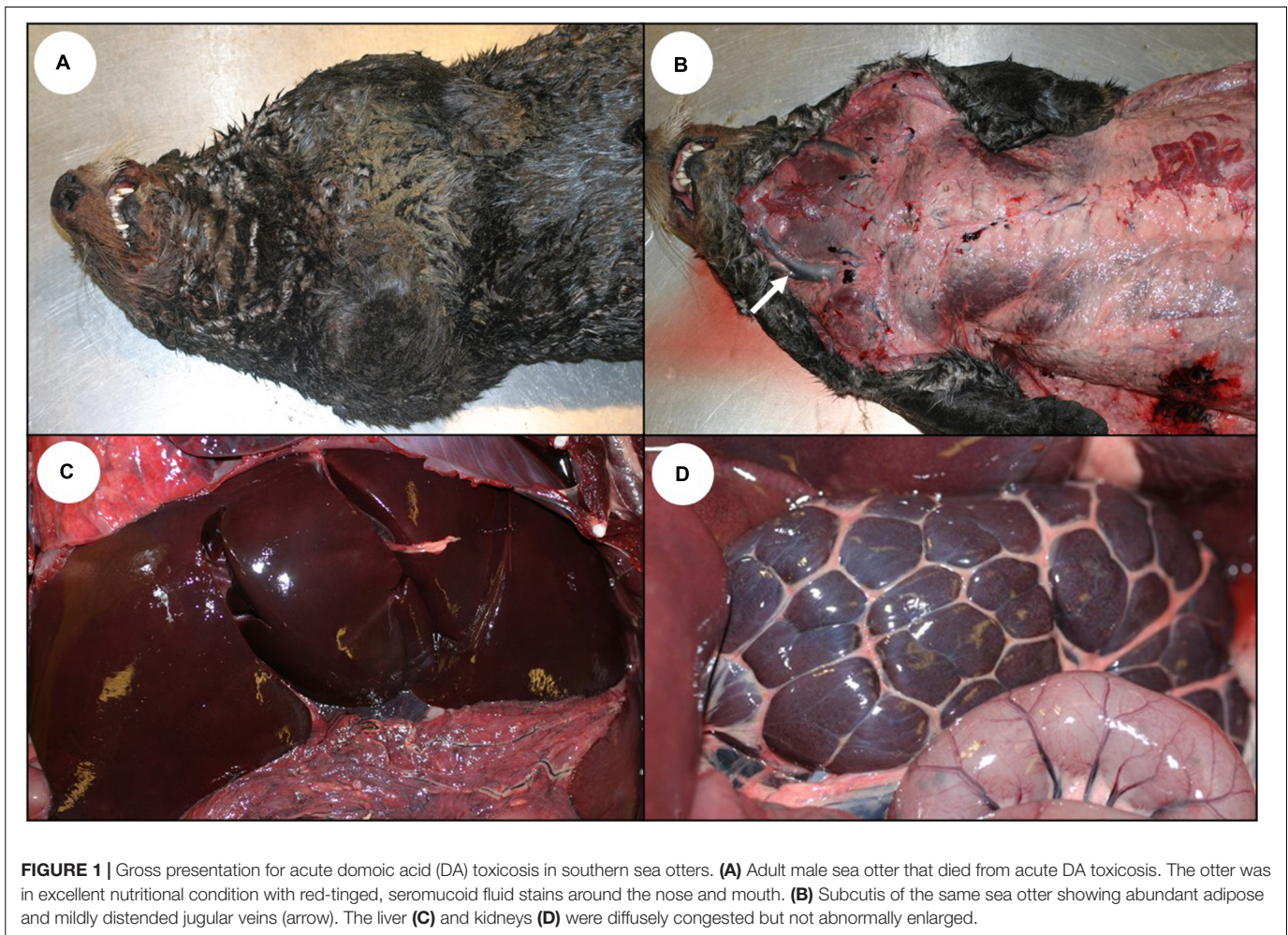*+/−, findings that are less consistently observed or less definitive.*

FIGURE 1 | Gross presentation for acute domoic acid (DA) toxicosis in southern sea otters. **(A)** Adult male sea otter that died from acute DA toxicosis. The otter was in excellent nutritional condition with red-tinged, seromucoid fluid stains around the nose and mouth. **(B)** Subcutis of the same sea otter showing abundant adipose and mildly distended jugular veins (arrow). The liver **(C)** and kidneys **(D)** were diffusely congested but not abnormally enlarged.

of congestive heart failure (**Table 1**): dyspnea, lethargy, anorexia, copious white or pink oronasal froth, and pleural, pulmonary, pericardial, and peritoneal edema (Moriarty et al., 2021a). Affected otters were emaciated with a poorly groomed pelage. Murmurs, pulse deficits, and abnormalities on electrocardiographic examination, such as reduced P wave amplitude, atrial and ventricular ectopy, and first- and second-degree atrioventricular block were also noted (Moriarty et al., 2021a), similar to reports for humans and other mammals with DA toxicosis (Perl et al., 1990a; Vranyac-Tramoundanas et al., 2011; Vieira et al., 2016).

Domoic Acid-Associated Pathology of the CNS and Cardiovascular Systems
Acute DA Toxicosis
Central nervous system
The earliest, most common, and most striking gross lesion in the CNS of sea otters with high DA concentrations (>500 ppb) in urine or GI content was severe diffuse brain, spinal cord, and meningeal congestion (**Table 1** and **Figures 3B,C**, **4A**; please also see **Figure 3A** as a normal comparison image). Affected brain tissue was pink, moist, and mildly translucent; postmortem cisternal taps commonly yielded >2 ml of cerebrospinal fluid

(CSF) (≤2 ml is normal at necropsy). Severe congestion was sometimes accompanied by diffuse brain swelling and herniation of the caudal cerebellar vermis through the occipital foramen (**Figures 3B**, **4A**), along with grossly apparent meningeal, neuropil, and ventricular hemorrhage (**Figures 3B,C**, **4A**).

On histopathology, severe diffuse congestion was observed in the meninges, hippocampus, diencephalon, entorhinal, olfactory and parahippocampal cortex, and the olfactory bulbs (**Table 2** and **Figure 4B**). Domoic acid-associated cerebellar congestion was easiest to see in the molecular layer (**Figure 5A**). Severe congestion was often accompanied by multifocal microhemorrhage (**Table 2** and **Figures 4B,C**, **6B–D**, **7A,B**, **8A,B**). In contrast, neuronal or glial necrosis or degeneration were minimal in sea otters with acute DA toxicosis (**Figures 6C,D**, **7A**).

Early vascular and perivascular CNS lesions included mural and perivascular edema, vacuolation and necrosis or apoptosis of arteriolar mural smooth muscle cells and endothelium, and occasional sloughed endothelium (**Table 2**). Microhemorrhages were common near small arterioles or engorged capillary beds (**Figures 6C,D**; please also see **Figure 6A** as a normal comparison image), especially in the cornu ammonis (CA) of the hippocampus. Intramural and perivascular
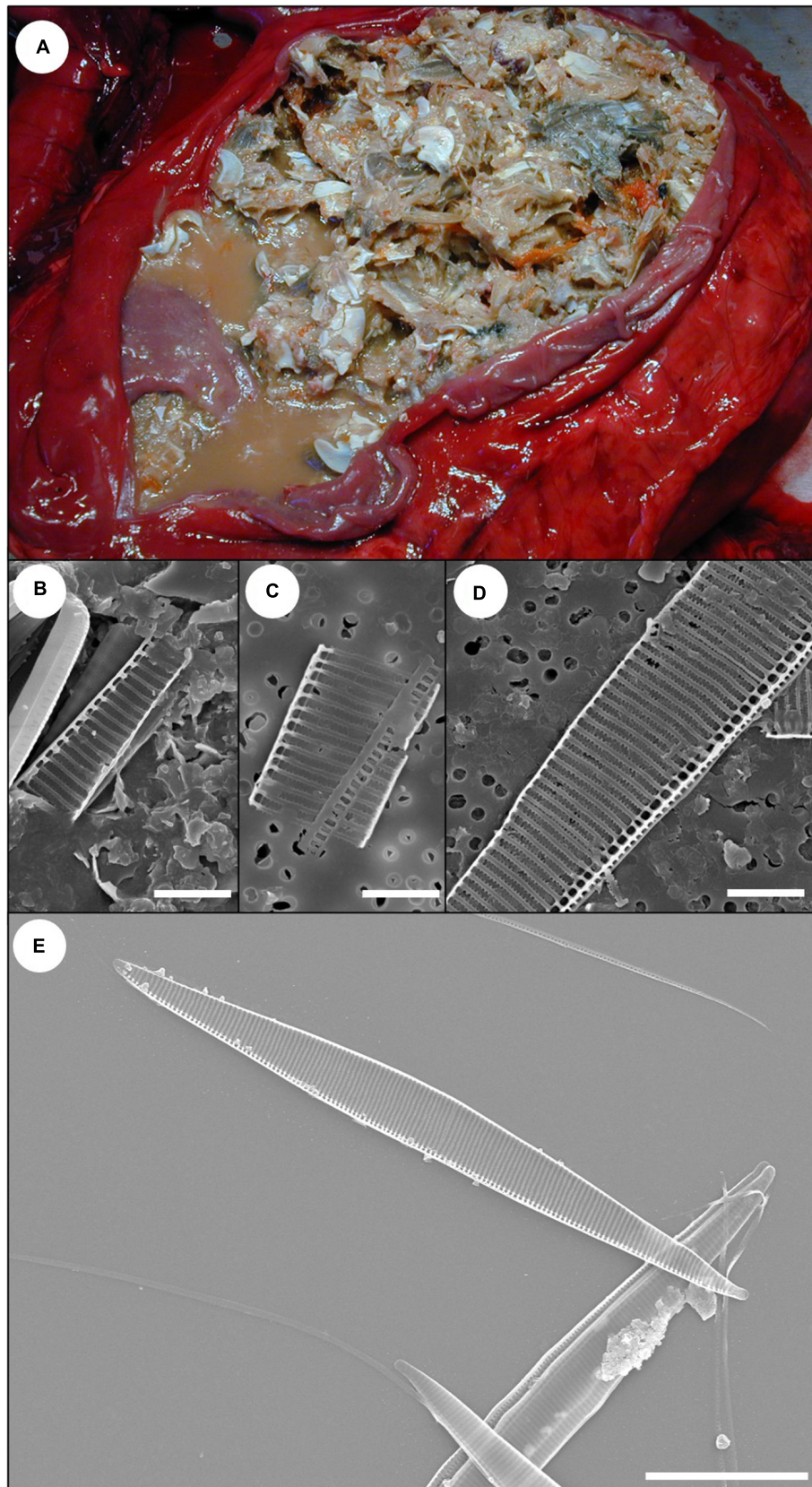
FIGURE 2 | *Pseudo-nitzschia* frustule detection in sand crabs (*Emerita analoga*) ingested by southern sea otters with acute domoic acid (DA) toxicosis. Sea otters with acute DA toxicosis often have full gastrointestinal (GI) tracts. Examination of the GI tracts of these prey items can reveal the presence of pennate frustules

(Continued)

(silica-based exoskeletons of diatoms), confirming that the prey consumed *Pseudo-nitzschia* diatoms that could have contained DA prior to predation by sea otters. **(A)** Full stomach from a sea otter that died of acute DA toxicosis during a toxic *Pseudo-nitzschia* bloom; postmortem stomach content and urine were strongly positive for DA (≥10,240 ppb). The stomach contained a mixture of small crabs, including sand crabs (*Emerita analoga*). The masses of tiny, bright orange spheres are crab eggs. Sea otters may preferentially consume crabs with eggs because their nutritional value is higher; these reproductive cycles can coincide with *Pseudo-nitzschia* blooms. **(B)** Scanning electron microscopy (SEM) micrograph of fragment of *Pseudo-nitzschia* frustule from cleaned GI tracts of free-living sand crabs collected during a toxic *Pseudo-nitzschia* bloom event (Bar = 4 µm). **(C)** SEM micrograph from the stomach content shown in **(A)**. A fragment of *Pseudo-nitzschia* frustule was obtained from the gastrointestinal tracts of sand crabs in this sample (Bar = 4 µm). **(D)** SEM micrograph of stomach content from a second sea otter that died from acute DA toxicosis. Postmortem stomach content and urine were strongly positive for DA (≥5,000 ppb) and a fragment of *Pseudo-nitzschia* frustule was obtained from the GI tracts of sand crabs recovered from the stomach of this sea otter (Bar = 4 µm). **(E)** Reference *Pseudo-nitzschia australis* frustules showing the characteristic pennate shape and complex ribbed morphology (Bar = 20 µm).
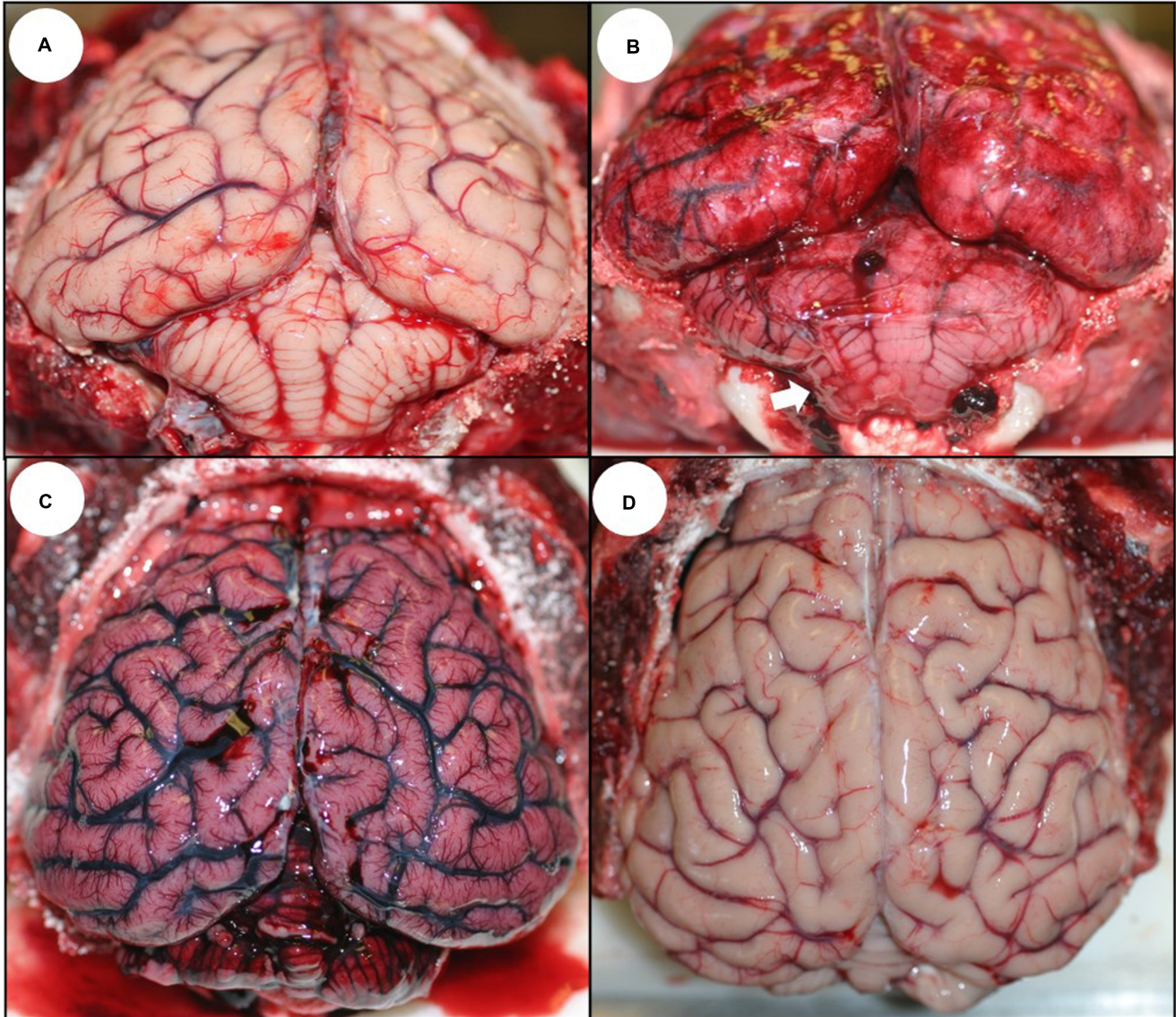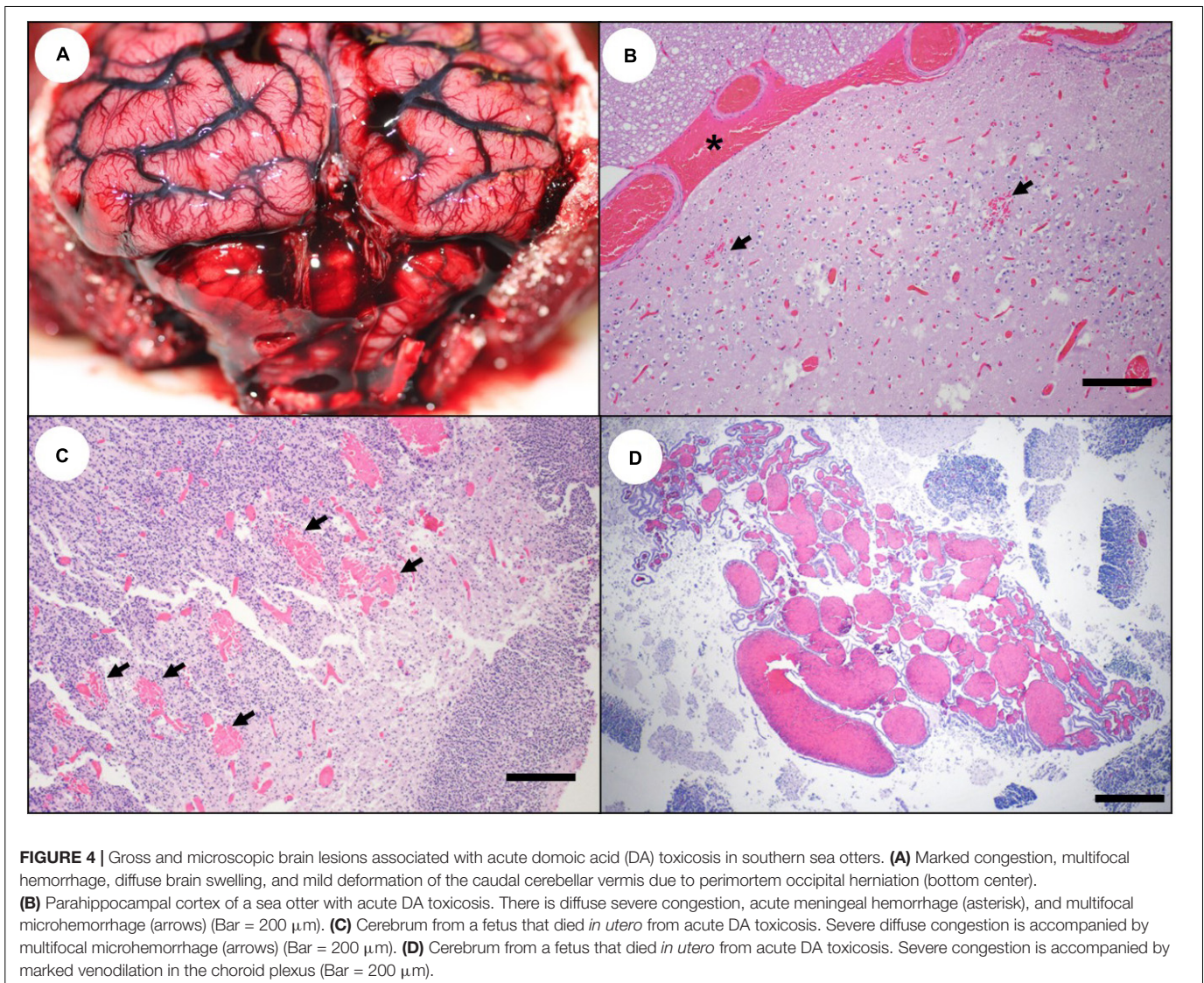

FIGURE 3 | Gross appearance of the southern sea otter central nervous system following domoic acid (DA) toxicosis. **(A)** Normal sea otter brain; the outer meninges (dura and arachnoid) were removed to show the brain surface. **(B)** Brain (with dura and arachnoid) from a sea otter that died from acute DA toxicosis showing severe diffuse meningeal congestion, multifocal acute hemorrhage, and mild deformation of the caudal cerebellar vermis (arrow) due to diffuse brain swelling that resulted in perimortem occipital herniation. **(C)** Brain (without dura and arachnoid) from a sea otter that died from acute DA toxicosis; there was severe diffuse congestion, multifocal hemorrhage, and mild to moderate diffuse swelling. **(D)** Brain (without dura and arachnoid) from a sea otter that died from chronic DA-associated cardiomyopathy (chronic DA post-exposure case); the brain is mildly atrophied with flattened gyri and pale tan neuropil.

FIGURE 4 | Gross and microscopic brain lesions associated with acute domoic acid (DA) toxicosis in southern sea otters. **(A)** Marked congestion, multifocal hemorrhage, diffuse brain swelling, and mild deformation of the caudal cerebellar vermis due to perimortem occipital herniation (bottom center). **(B)** Parahippocampal cortex of a sea otter with acute DA toxicosis. There is diffuse severe congestion, acute meningeal hemorrhage (asterisk), and multifocal microhemorrhage (arrows) (Bar = 200 μm). **(C)** Cerebrum from a fetus that died *in utero* from acute DA toxicosis. Severe diffuse congestion is accompanied by multifocal microhemorrhage (arrows) (Bar = 200 μm). **(D)** Cerebrum from a fetus that died *in utero* from acute DA toxicosis. Severe congestion is accompanied by marked venodilation in the choroid plexus (Bar = 200 μm).

hemorrhage, fibrin deposition, and malacia were also observed in some acute and subacute DA cases (**Figures 5B–F**). Severe congestion of the choroid plexus was common (**Figure 4D**), and necrosis of the choroidal epithelium and ventricular ependyma was suspected (**Figures 9A–E**), although postmortem autolysis precluded confirmation. Ependymal swelling, cytoplasmic eosinophilia, and sloughing were consistent findings throughout the ventricles (**Figures 9A–E**) and spinal cord central canal.

Severe congestion, spongiosis, and occasional microhemorrhage were apparent in all circumventricular organs (CVOs) examined microscopically (**Table 2**), including the area postrema (**Figure 10B**; please also see **Figure 10A** as a normal comparison image), median eminence, pineal, and pituitary gland (**Figures 11B–D**; please also see **Figure 11A** as a normal comparison image). The microscopic appearance of the pituitary gland was especially striking in acute DA cases: when bisected along the median sagittal plane, the pars distalis and pars nervosa were severely congested,

while the pars intermedia was relatively unremarkable (**Table 2** and **Figures 11B–D**). Multifocal microhemorrhage and spongiosis were also common in the pars nervosa (**Figures 11C,D**, **12F**). Pituitary congestion was often so extreme that it was visible on subgross examination. Although congestion and spongiosis were also observed in the pineal gland and area postrema (**Figures 10B–D**), the pattern was less visually striking when compared with the pituitary gland.

Cardiovascular system

Sea otters with acute DA toxicosis commonly had mild diffuse venodilation (**Figure 1B**), and the atria had a mildly dilated appearance (**Table 1** and **Figures 13B**, **14A**; please also see **Figure 13A** as a normal comparison image) grossly. The ventricular myocardium was diffusely wet, brown, and mildly translucent (**Figures 13B**, **14A**), accompanied by a mild increase in pericardial fluid (≤2 ml is normal at necropsy) that had a slight brownish tinge.
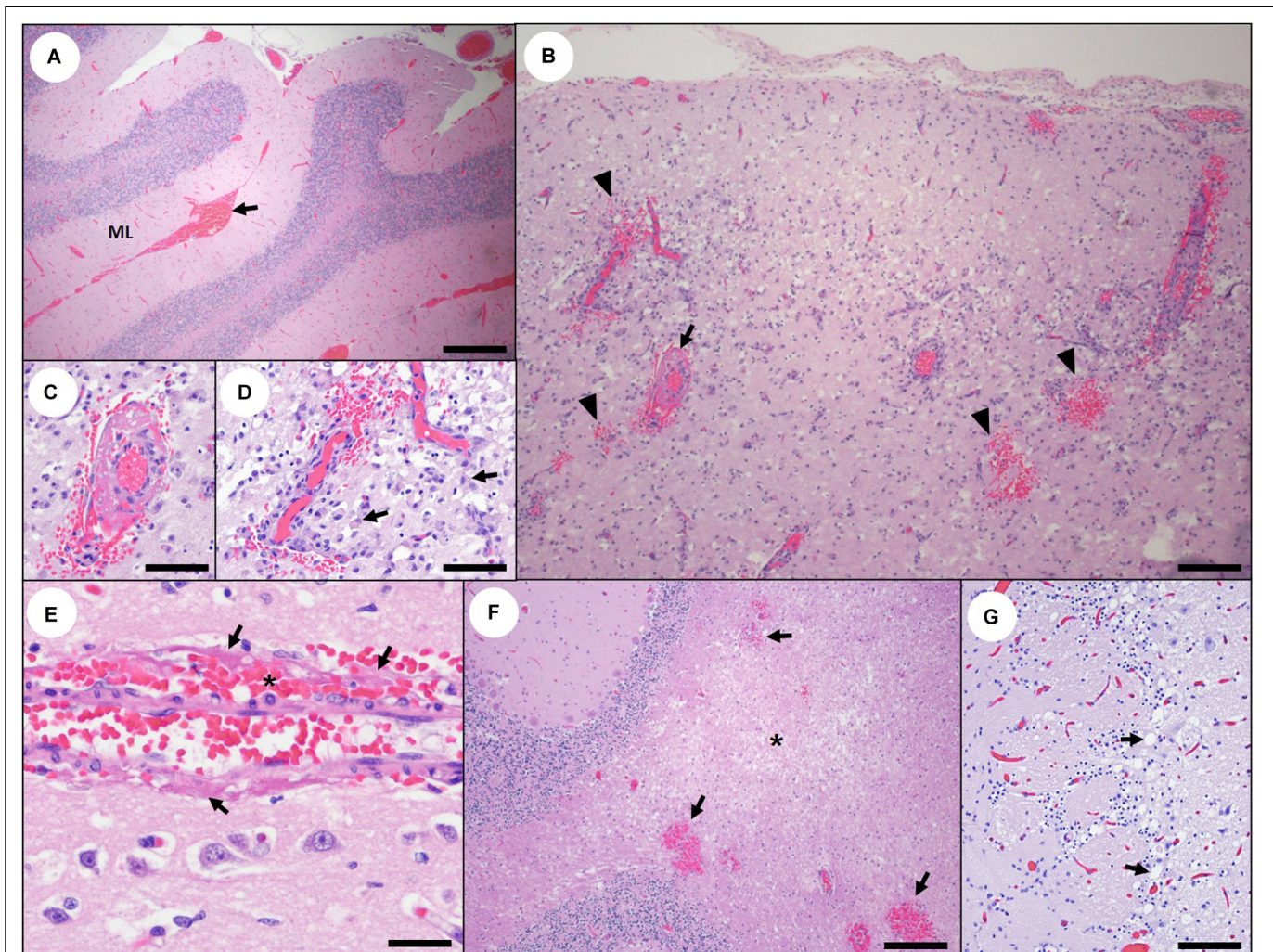
FIGURE 5 | Acute and subacute cerebral and cerebellar pathology associated with domoic acid (DA) toxicosis in southern sea otters. **(A)** Diffuse, severe cerebellar congestion in a sea otter with acute DA toxicosis. The congestion is often most visible in the molecular layer (ML), often accompanied by multifocal meningeal hemorrhage (arrow) (Bar = 200 µm). **(B)** Parahippocampal gyrus in a sea otter with subacute DA toxicosis. Malacia, astrogliosis, perilesional microhemorrhage (arrowheads), and vascular mural and perivascular fibrin (arrow) are occasionally observed in the brain of sea otters with subacute DA toxicosis (Bar = 100 µm). **(C,D)** Higher magnification of **(B)** showing perivascular fibrin deposition, hemorrhage, malacia, and perivascular gliosis (arrows) (**C**,**D**: Bar = 40 µm). **(E)** Vascular mural and perivascular fibrin deposition (arrows) and hemorrhage (asterisk) in the parahippocampal gyrus of a sea otter with subacute DA toxicosis (Bar = 20 µm). **(F)** Spongiosis and malacia (asterisk), and multifocal microhemorrhage (arrows) in the cerebellar white matter of a sea otter with subacute DA toxicosis (Bar = 200 µm). **(G)** Olfactory lobe of a sea otter with acute or subacute DA toxicosis. There is diffuse congestion, mild patchy spongiosis, and linear bands of swollen, pale cytoplasmic vacuoles (presumptive astrocytic processes; arrows) (Bar = 60 µm).
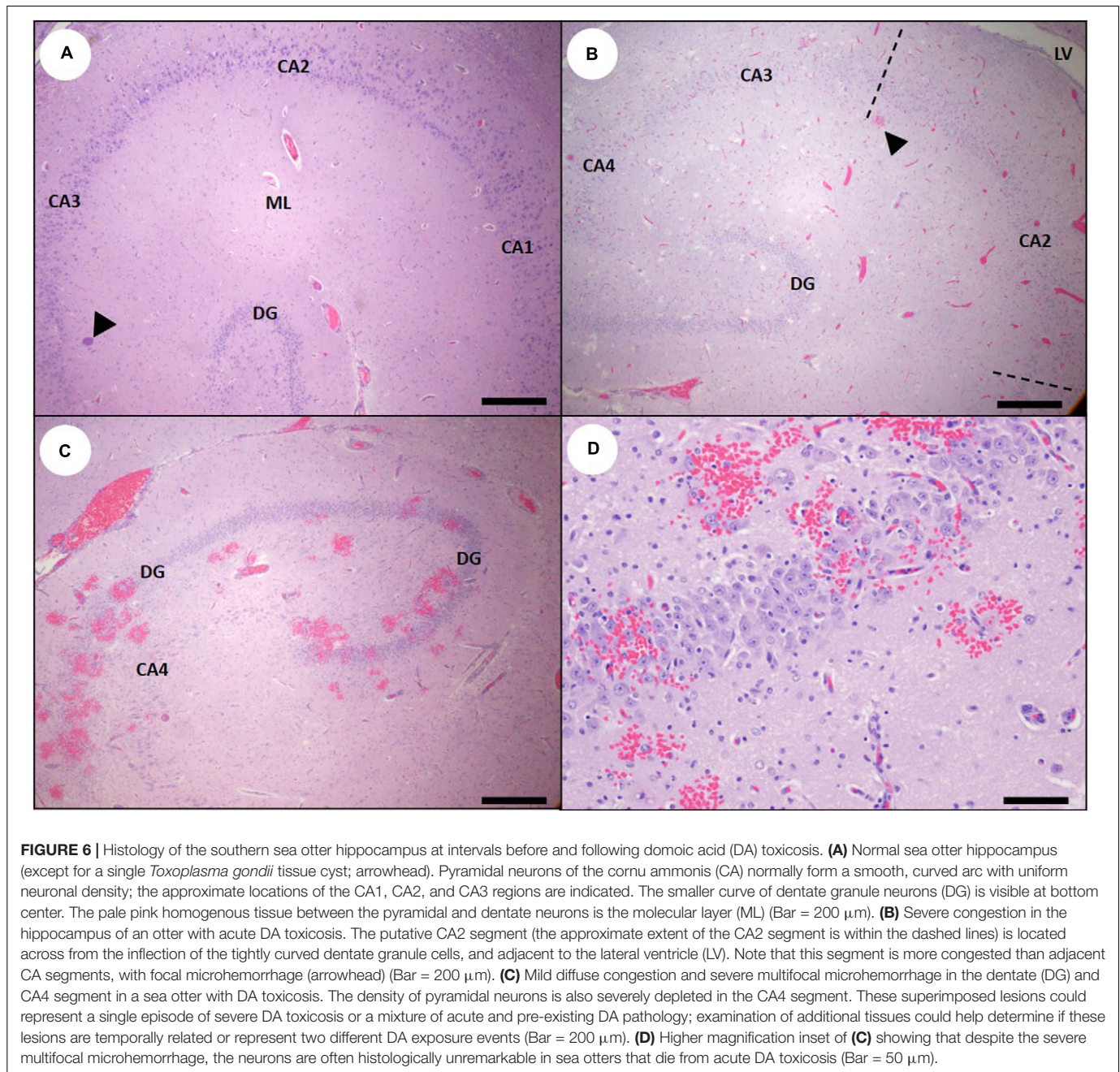
Acute cardiac pathology was subtle on histopathology and affected mainly the myocardium, coronary vasculature, and, to a lesser extent, the Purkinje fibers. Severe diffuse congestion (**Figures 14C**, **15A**) was often accompanied by patchy cardiomyocyte hyper-eosinophilia, swelling and vacuolation, linear bands of contracted cardiomyocytes, and swelling and cytoplasmic vacuolation of Purkinje fibers (**Table 2**). Small and medium-sized arterioles in areas of cardiomyocyte damage often had mural smooth muscle cell swelling and cytoplasmic hyper-eosinophilia, accompanied by mural and perivascular edema and microhemorrhage (**Figures 16A–C**). Perivascular and interstitial microhemorrhage and edema were apparent in areas of cardiomyocyte pathology (**Table 2** and

Figures 14B,C, **15B,C**), especially the perivascular interstitium, the papillary, epicardial and, endocardial myocardium, the apex, and along the atrioventricular border near the base of the valve leaflets. Acute inflammation was usually minimal or absent.

Subacute DA Toxicosis
Central nervous system
Gross CNS lesions were often less visually striking in sea otters with subacute DA toxicosis when compared with acute DA cases (**Table 1**). Subacute DA cases were characterized by less severe vascular congestion and the appearance of significant neuronal, glial, and stromal histopathology (**Table 2**).

FIGURE 6 | Histology of the southern sea otter hippocampus at intervals before and following domoic acid (DA) toxicosis. **(A)** Normal sea otter hippocampus (except for a single *Toxoplasma gondii* tissue cyst; arrowhead). Pyramidal neurons of the cornu ammonis (CA) normally form a smooth, curved arc with uniform neuronal density; the approximate locations of the CA1, CA2, and CA3 regions are indicated. The smaller curve of dentate granule neurons (DG) is visible at bottom center. The pale pink homogenous tissue between the pyramidal and dentate neurons is the molecular layer (ML) (Bar = 200 μm). **(B)** Severe congestion in the hippocampus of an otter with acute DA toxicosis. The putative CA2 segment (the approximate extent of the CA2 segment is within the dashed lines) is located across from the inflection of the tightly curved dentate granule cells, and adjacent to the lateral ventricle (LV). Note that this segment is more congested than adjacent CA segments, with focal microhemorrhage (arrowhead) (Bar = 200 μm). **(C)** Mild diffuse congestion and severe multifocal microhemorrhage in the dentate (DG) and CA4 segment in a sea otter with DA toxicosis. The density of pyramidal neurons is also severely depleted in the CA4 segment. These superimposed lesions could represent a single episode of severe DA toxicosis or a mixture of acute and pre-existing DA pathology; examination of additional tissues could help determine if these lesions are temporally related or represent two different DA exposure events (Bar = 200 μm). **(D)** Higher magnification inset of **(C)** showing that despite the severe multifocal microhemorrhage, the neurons are often histologically unremarkable in sea otters that die from acute DA toxicosis (Bar = 50 μm).

Swollen, brightly eosinophilic hippocampal pyramidal neurons (i.e., "red dead" neurons) were infrequent in southern sea otters with DA toxicosis (**Table 2** and **Figures 7B**, **17B**), as opposed to other species where this lesion is commonly reported (Silvagni et al., 2005; Pulido, 2008). More frequently, there was discrete shrinkage of pyramidal neurons and cytoplasmic hyperchromasia, vacuolation and pallor, and neuronal loss (**Table 2** and **Figures 7E,F**, **17A**, **18A–C**). Also common were gemistocytic astrocytes (**Figures 7C,D**), elongated angular hyperchromic neurons (**Figure 7E**), and tiny linear eosinophilic cytoplasmic processes or punctate spots (putative dendrites, axons and/or astrocytic processes; **Figure 7F**), accompanied

by gliosis and spongiosis of the hippocampal molecular layer (**Figures 18B,C**).

As with other species (Silvagni et al., 2005; Pulido, 2008; Lefebvre et al., 2010; McHuron et al., 2013; Buckmaster et al., 2014), DA-associated damage to the hippocampal pyramidal neurons was usually segmental, with severe neuronal loss in some CA segments while adjacent areas remained intact (**Table 2** and **Figures 6B**, **18A,B**). The earliest and most severe pyramidal neuron lesions were centered on the hippocampal CA segment located directly opposite the curved inflection of the granule cells of the dentate gyrus (**Figures 6B**, **18B**), which appears to correspond with the CA2 segment in
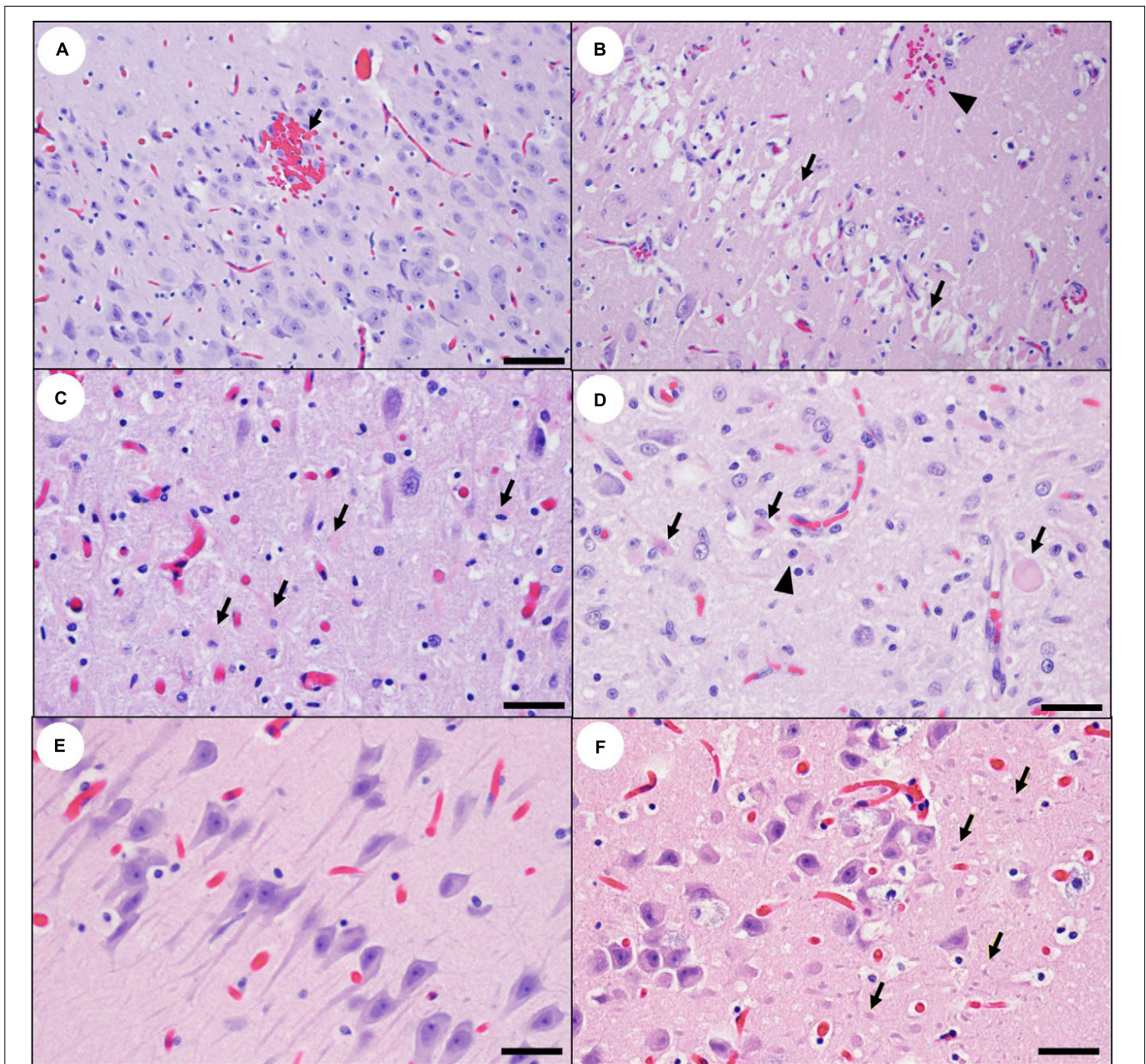
FIGURE 7 | High magnification views of the southern sea otter hippocampus illustrating acute and subacute domoic acid (DA)-associated pathology.
(A) Hippocampal cornu ammonis (CA) in a sea otter with acute DA toxicosis. There is moderate diffuse vascular congestion and focal microhemorrhage (arrow). Pyramidal neurons are histologically unremarkable at this early stage. Views **(B)** through **(E)** illustrate subacute hippocampal pathology in sea otters: **(B)** Considered a classic lesion for other mammals with DA toxicosis, severe segmental necrosis of pyramidal neurons (i.e., "red dead" neurons; arrows) is uncommon in sea otters with subacute DA toxicosis, possibly because this lesion is ephemeral and rapidly disappears. The severe neuropil congestion that characterizes acute DA cases is no longer present in this subacute case, but a focal microhemorrhage is visible (arrowhead) (Bar = 40 μm). **(C)** Pyramidal neuron degeneration is often accompanied by hyperplasia of plump, gemistocytic astrocytes (arrows) (Bar = 20 μm). **(D)** Concurrent pyramidal neuron necrosis (arrows) and astrogliosis (arrowhead) (Bar = 20 μm). **(E)** DA-affected neurons can vary greatly in appearance, from the swollen eosinophilic cells shown above, to angular and elongated hyperchromic neuronal profiles with prominent axons and dendrites (Bar = 20 μm), or **(F)** shrunken hyperchromic neurons surrounded by numerous tiny non-nucleated cell profiles (possible axons, dendrites or astrocytic processes; arrows) (Bar = 20 μm).

other animals. Lesions appeared to spread along the CA segments and into adjacent tissue in subacute cases, and they sometimes encompassed the CA1 through CA4 segments (**Figures 17A**, **18C**). Dentate granule neurons were less commonly affected

(**Figures 17A**, **18C**). Gemistocytic astrocytes were numerous in areas of pyramidal neuron pathology (**Figures 7C,D**) and were accompanied by variable spongiosis, gliosis, and, occasionally, mild non-suppurative inflammation (**Figures 18B,C**).
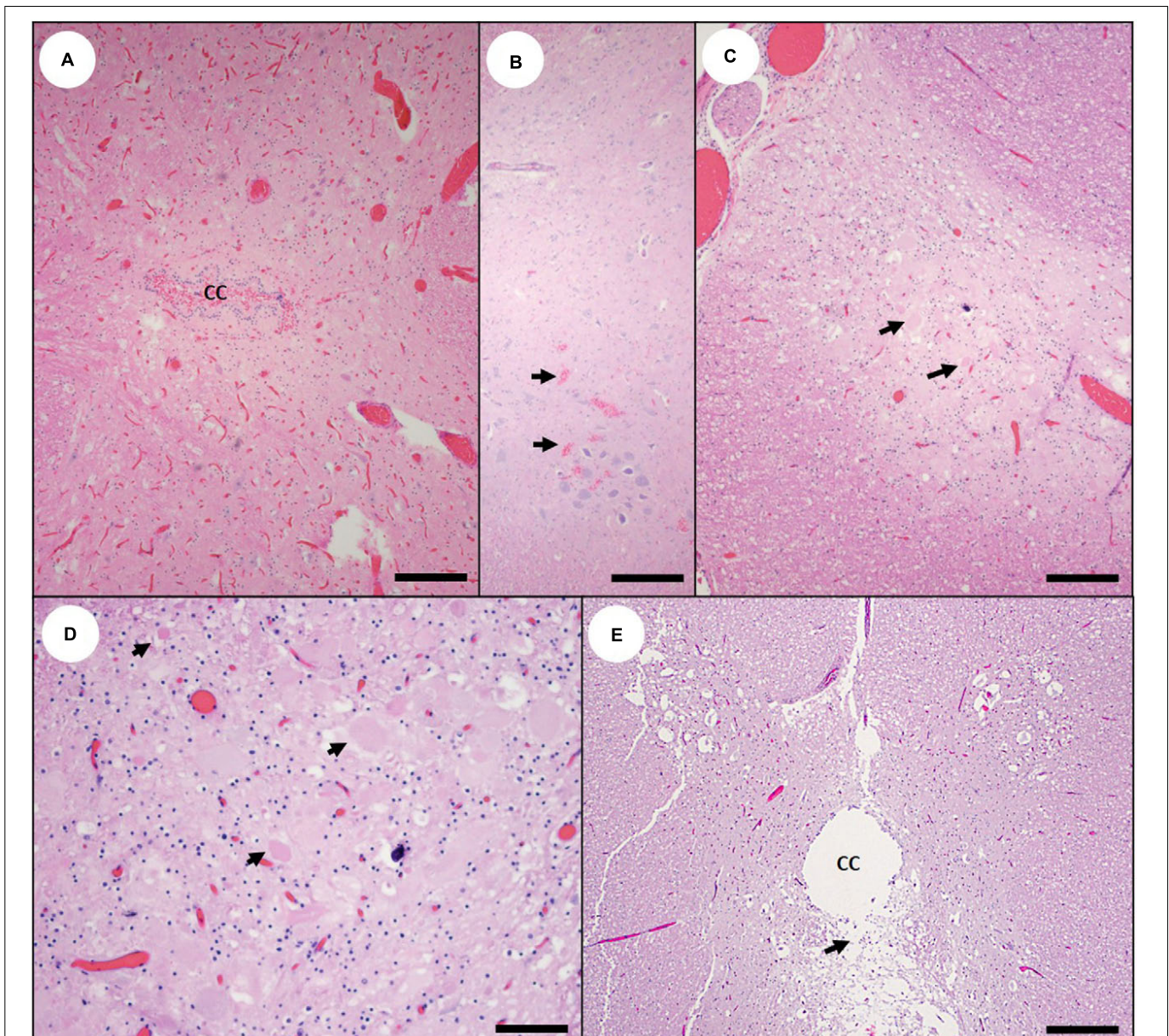
FIGURE 8 | Spinal cord pathology in southern sea otters with domoic acid (DA) toxicosis. **(A)** Diffuse, severe congestion and mild hemorrhage into the central canal (CC) of the spinal cord from a sea otter with acute DA toxicosis (Bar = 200 μm). **(B)** Multifocal acute microhemorrhage in the gray matter (arrows) of the spinal cord of a sea otter with acute DA toxicosis (Bar = 100 μm). **(C)** Mild congestion, spongiosis, and neuronal necrosis and/or astrogliosis (arrows) in the dorsal horn of the spinal cord of a sea otter with subacute DA toxicosis (Bar = 100 μm). **(D)** Higher magnification view of **(C)**; (image rotated due to space constraints) showing congestion, spongiosis, and neuronal necrosis or astrogliosis (arrows) (Bar = 40 μm). **(E)** Spinal cord from a sea otter with chronic DA toxicosis; the central canal (CC) is moderately dilated, with extensive ependymal loss and spongiosis of the periventricular neuropil (arrow) (Bar = 200 μm).

Ependymal loss, abortive ependymal regeneration, and ventricular scarring were observed in subacute and chronic DA cases (**Figures 9C–E**, **12C,D**) and were characterized by a discontinuous ependymal lining, an irregular "moth-eaten" appearance of the ventricular walls, ventricular mural adhesions, and entrapment of small islands of ependyma below a fibrillar, variably thickened, and acellular ventricular surface (**Figures 12C,D**). Ventricular luminal dilation was apparent in severe subacute and chronic DA cases (**Figures 8E**,

12C,D, **19B**, **20**; please also see **Figure 19A** as a normal comparison image).

Severe lesions were often located in the peri-ventricular brain tissue next to regions of ependymal and ventricular pathology. As acute congestion and microhemorrhage (**Figures 9A,B**) normalized in subacute cases, the sub-ependymal neuropil became spongiotic and edematous, with numerous gemistocytic astrocytes (**Figures 9C–E**, **10C,D**, **12E**) and neuronal loss in periventricular gray matter. In the cerebellum, subacute
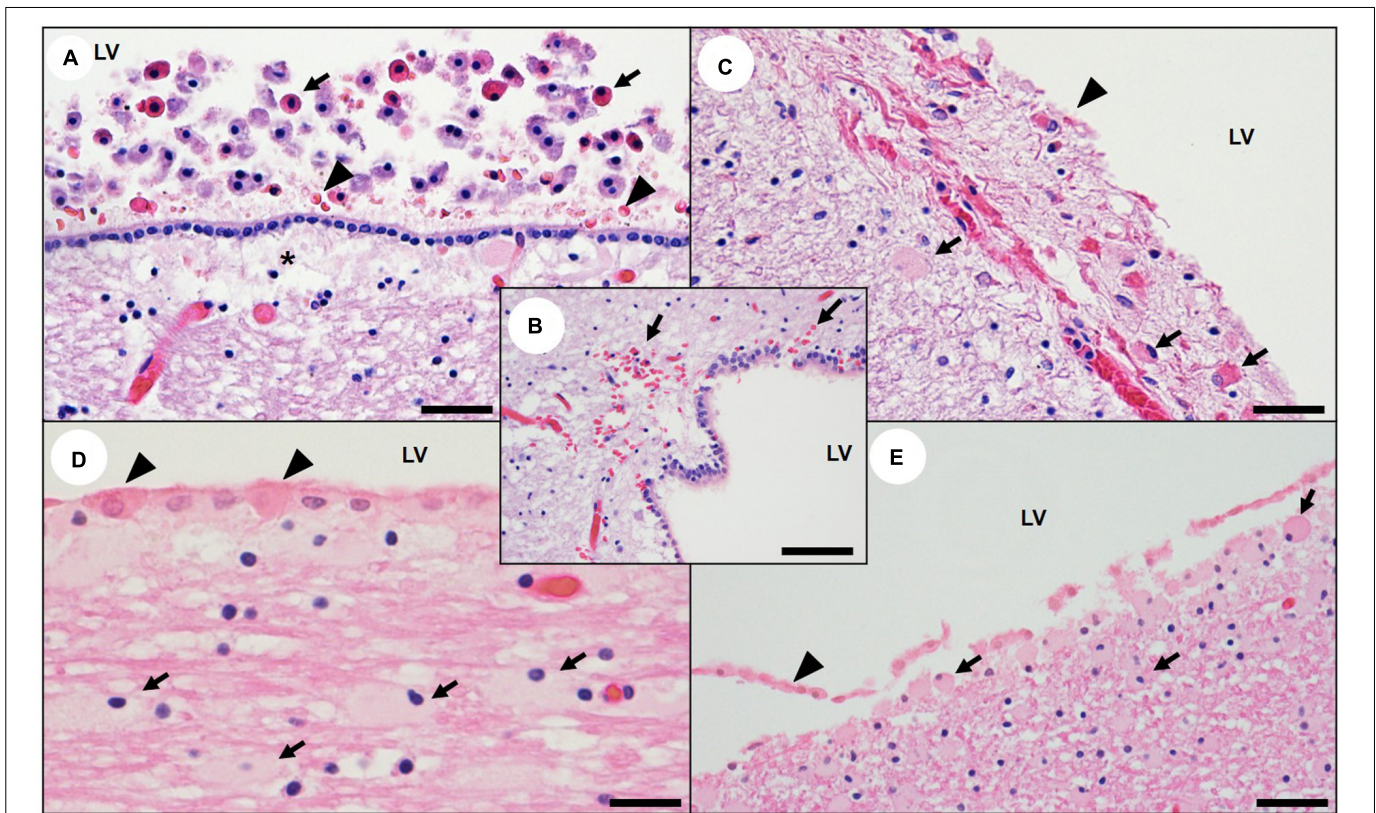
FIGURE 9 | Central nervous system ventricular and periventricular pathology associated with domoic acid (DA) toxicosis in southern sea otters. **(A)** Edge of the lateral ventricle (LV) of a sea otter with acute DA toxicosis. The ventricular lumen contains swollen, rounded, free-floating nucleated cells with brightly eosinophilic cytoplasm (possible sloughed necrotic or apoptotic choroid plexus epithelium and/or ependyma; arrows) and sparse hemorrhage (arrowheads). Moderate intercellular edema is visible in the sub-ependymal neuropil (asterisk) (Bar = 40 μm). **(B)** Lateral ventricle from a sea otter with acute DA toxicosis. The subependymal neuropil is congested and spongiotic with multifocal microhemorrhage (arrows) (Bar = 40 μm). Images **(C)** through **(E)** are examples of the lateral ventricle (LV) from sea otters with subacute to acute DA toxicosis; there is scattered ependymal necrosis or apoptosis and sloughing (**C–E**: arrowheads), and the sub-ependymal neuropil is congested and spongiotic **(C)**, with numerous gemistocytic astrocytes (**C–E**; arrows). Due to rapid autolysis, assessment of ependymal and choroid pathology should be attempted only on minimally decomposed carcasses (**C**: Bar = 100 μm), (**D**: Bar = 20 μm), and (**E**: Bar = 40 μm).

cases were characterized by mild Purkinje cell shrinkage, hyperchromasia, vacuolation and loss, and swelling and cytoplasmic vacuolation of adjacent astrocyte processes. The neuropil damage was usually temporally concordant across all areas of the CNS; examination of multiple consistently trimmed areas helped to facilitate DA diagnosis and assessment of the post-exposure interval.
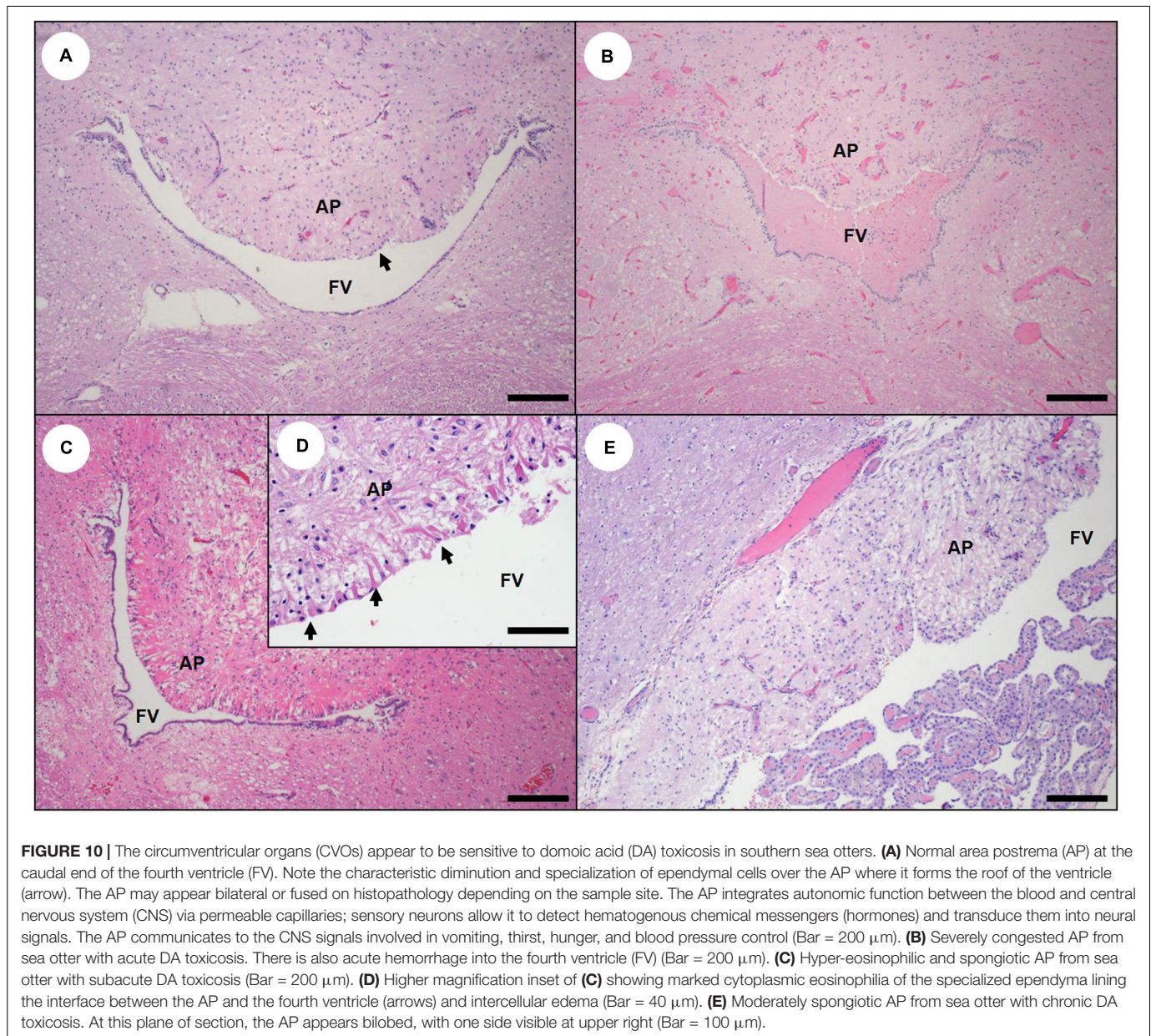
Fewer spinal cords were examined microscopically in this study, but DA-associated subacute lesions were observed in the gray matter, periventricular neuropil, and central canal, occasionally with severe neuronal degeneration, loss and astrogliosis (**Table 2** and **Figures 8C–E**). The central canal was sometimes dilated, especially in the cervical spinal cord, with partial or complete ependymal loss and a motheaten appearance to the wall, similar to other ventricular spaces (**Figure 8E**).

Cardiovascular system

The hearts of subacute DA cases were variably enlarged and rounded at gross necropsy with pale tan to light, orange-mottled ventricular myocardium (**Table 1** and **Figure 13C**). Irregular pale streaks radiated from the cardiac apex or the

interventricular junction to the atrioventricular border, especially along the left ventricular free wall (**Figure 13C**). Progressive dilation of epicardial veins was accompanied by proliferation of tortuous collateral venules (**Figures 13C,D**) and moderate serofibrinous pericardial effusion, especially in sea otters that died due to congestive heart failure. Severe cardiomegaly with luminal expansion of both atria and ventricles was observed in severely affected sea otters (**Figure 13D**).

On histopathology, myocardial congestion was less prominent in subacute cases (**Table 2** and **Figure 15D**). Instead, there was substantial cardiomyocyte pathology characterized by multifocal cardiomyocyte necrosis or apoptosis, loss, stromal collapse, and fatty or fibrous replacement (**Figures 15D,E**, **21B–E**). These lesions corresponded with the grossly apparent ventricular mottling and streaking (**Figures 13C,D**, **21A**). Hyperplastic cardiomyocytes with karyomegaly and/or nuclear rowing (attempted regeneration) occurred in some areas. Severe lesions were most common in the apex, left heart (ventricular and atrial free wall and papillary muscle), and interventricular septum, although a global distribution also occurred. Lesions were often concentrated in the sub-epicardial and sub-endocardial

FIGURE 10 | The circumventricular organs (CVOs) appear to be sensitive to domoic acid (DA) toxicosis in southern sea otters. **(A)** Normal area postrema (AP) at the caudal end of the fourth ventricle (FV). Note the characteristic diminution and specialization of ependymal cells over the AP where it forms the roof of the ventricle (arrow). The AP may appear bilateral or fused on histopathology depending on the sample site. The AP integrates autonomic function between the blood and central nervous system (CNS) via permeable capillaries; sensory neurons allow it to detect hematogenous chemical messengers (hormones) and transduce them into neural signals. The AP communicates to the CNS signals involved in vomiting, thirst, hunger, and blood pressure control (Bar = 200 μm). **(B)** Severely congested AP from sea otter with acute DA toxicosis. There is also acute hemorrhage into the fourth ventricle (FV) (Bar = 200 μm). **(C)** Hyper-eosinophilic and spongiotic AP from sea otter with subacute DA toxicosis (Bar = 200 μm). **(D)** Higher magnification inset of **(C)** showing marked cytoplasmic eosinophilia of the specialized ependyma lining the interface between the AP and the fourth ventricle (arrows) and intercellular edema (Bar = 40 μm). **(E)** Moderately spongiotic AP from sea otter with chronic DA toxicosis. At this plane of section, the AP appears bilobed, with one side visible at upper right (Bar = 100 μm).

ventricular myocardium and the papillary muscles, and they occasionally formed discrete, well-demarcated areas of cardiomyocyte loss (**Figures 15D,E**, **21B**). Cell swelling and cytoplasmic vacuolation were observed in the Purkinje fibers and other components of the cardiac conduction system, as reported for California sea lions (Zabka et al., 2009). Ventricular arterioles (especially in the left ventricular free wall) had progressive mural smooth muscle cell swelling, hyper-eosinophilia, necrosis or apoptosis, loss, patchy mural hyalinization and thickening, and dystrophic mineralization (**Figures 16C–F**), accompanied by mild endothelial cell regeneration and hyperplasia (**Figures 16C,D**). Estimates of lesion chronicity in the heart usually matched those in the CNS (**Supplementary Table 2**), providing helpful metrics to confirm DA toxicosis and estimate the post-exposure interval.

For subacute DA cases, perilesional inflammation was usually mild, but occasionally it was severe, possibly reflecting both host response to DA-mediated tissue damage and concurrent protozoal myocarditis (Kreuder et al., 2005; Miller et al., 2020). Domoic acid-associated cardiac pathology was typically more regional, affecting the sub-epicardial and subendocardial tissues, apex, and papillary muscles (**Figures 15D,E**, **21B,D,E**), while definitive protozoal lesions containing intracytoplasmic parasites were often randomly distributed. Reactive inflammation associated with myocardial pathology due to DA often contained a mixture of macrophages and lymphocytes, while *T. gondii*-associated myocarditis was predominantly lymphoplasmacytic. Sea otters with myocardial sarcocystosis had mixtures of mononuclear leukocytes and sparse neutrophils or eosinophils. Bacterial myocarditis and endocarditis were characterized by
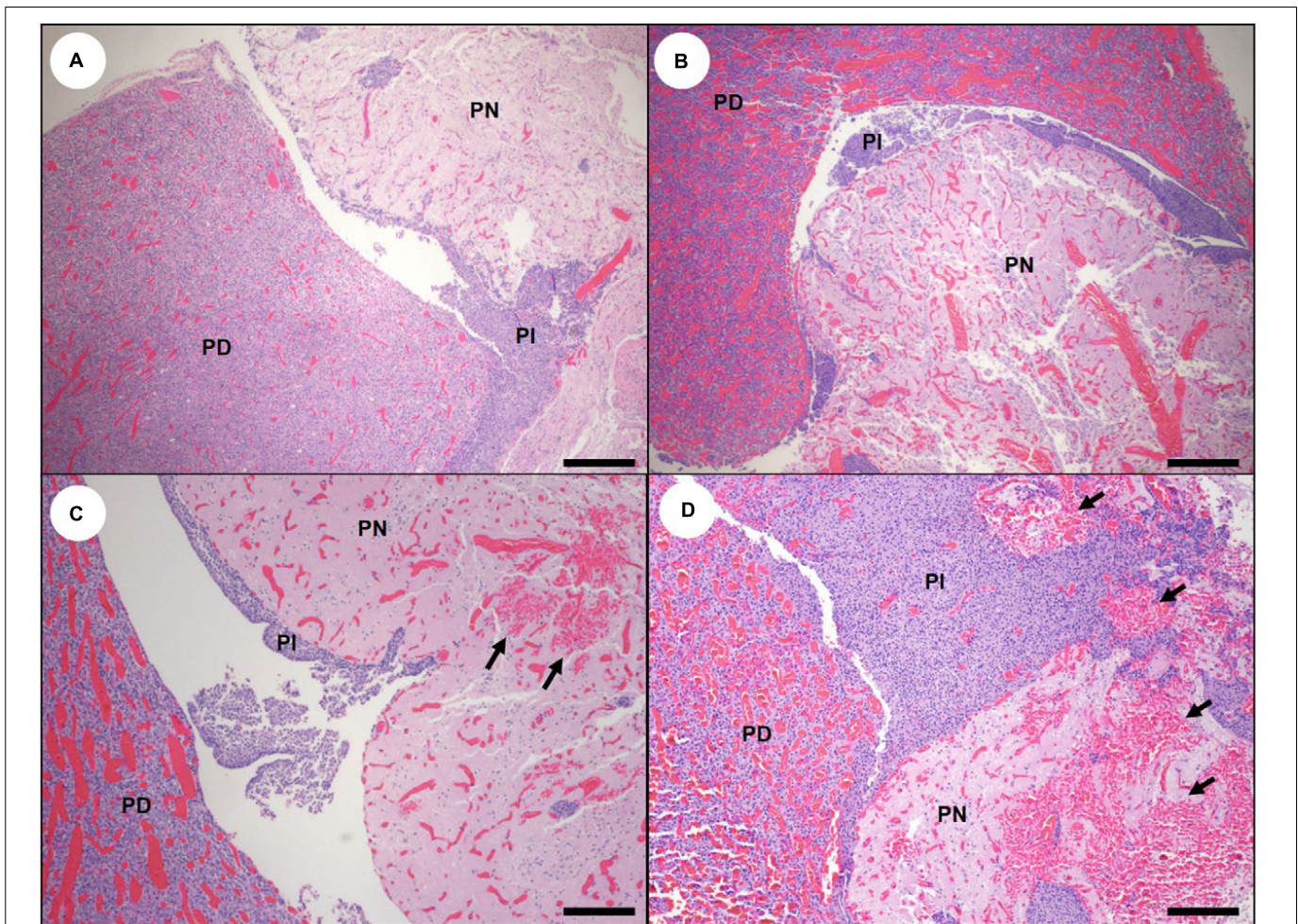
FIGURE 11 | Pituitary gland histopathology in southern sea otters with acute domoic acid (DA) toxicosis. **(A)** Normal sea otter pituitary gland bisected along the sagittal midline to reveal the pars distalis (PD), pars intermedia (PI), and pars nervosa (PN) (Bar = 200 μm). **(B)** Pituitary gland from sea otter with acute DA toxicosis. There is severe congestion of the pars distalis and pars nervosa, while the pars intermedia is histologically unremarkable (Bar = 200 μm). **(C,D)**; The pituitary congestion is often accompanied by microhemorrhage in the pars nervosa (arrows) but not the pars distalis or pars intermedia (**C**,**D**: Bar = 100 μm).

miliary suppurative inflammation. Subacute or chronic DA-associated myocardial pathology was sometimes difficult to distinguish from persistent protozoal and bacterial lesions.

Chronic DA Toxicosis

Central nervous system

Chronic lesions had the same CNS distribution as acute and subacute cases but were relatively quiescent, reflecting prior DA-associated pathology with some progressive and healing responses. Severely damaged brains were atrophied with diffuse tan discoloration, flattened gyri, and deep sulci (**Table 1** and **Figure 3D**); postmortem sampling commonly yielded an increased volume of CSF (>2 ml). In severe cases, one or both hippocampal profiles were shrunken with corresponding dilation of the lateral ventricles (**Figures 19B**, **20**).

On histopathology, hippocampal degeneration was characterized by flattening of the normally convex curve of the CA, and expansion of the lateral ventricle (**Table 2** and **Figure 22B**). Severely damaged CA segments had extensive pyramidal neuron loss, mild astrogliosis, and neuropil rarefaction and scarring (**Figures 22C,D**). Scar maturation and tissue retraction often resulted in angular deformation of the normal smooth arc of CA pyramidal neurons (**Figure 22B**). Previously damaged CA sectors were often slightly retracted toward the dentate gyrus, resulting in segmental inflection of the linear band of pyramidal cells (**Figures 18D**, **22A**). Chronic hippocampal lesions were often accompanied by patchy scarring of the ventricles (**Figures 12C,D**) and peri-hippocampal white matter. Intralesional gemistocytic astrocytes and microglia were sparse in chronic cases, making mild lesions possible to miss on histopathology (**Figures 18B,D**, **22A**).

A similar but less visually striking pattern was noted in the olfactory, parahippocampal and entorhinal cortex, CVOs, olfactory bulbs, diencephalon, mesencephalon, periventricular neuropil, pons, medulla, brainstem, and spinal cord (**Table 2** and **Figures 5G**, **8E**, **10E**, **12A–F**, **22C,D**). Areas of bilaterally symmetrical gray and white
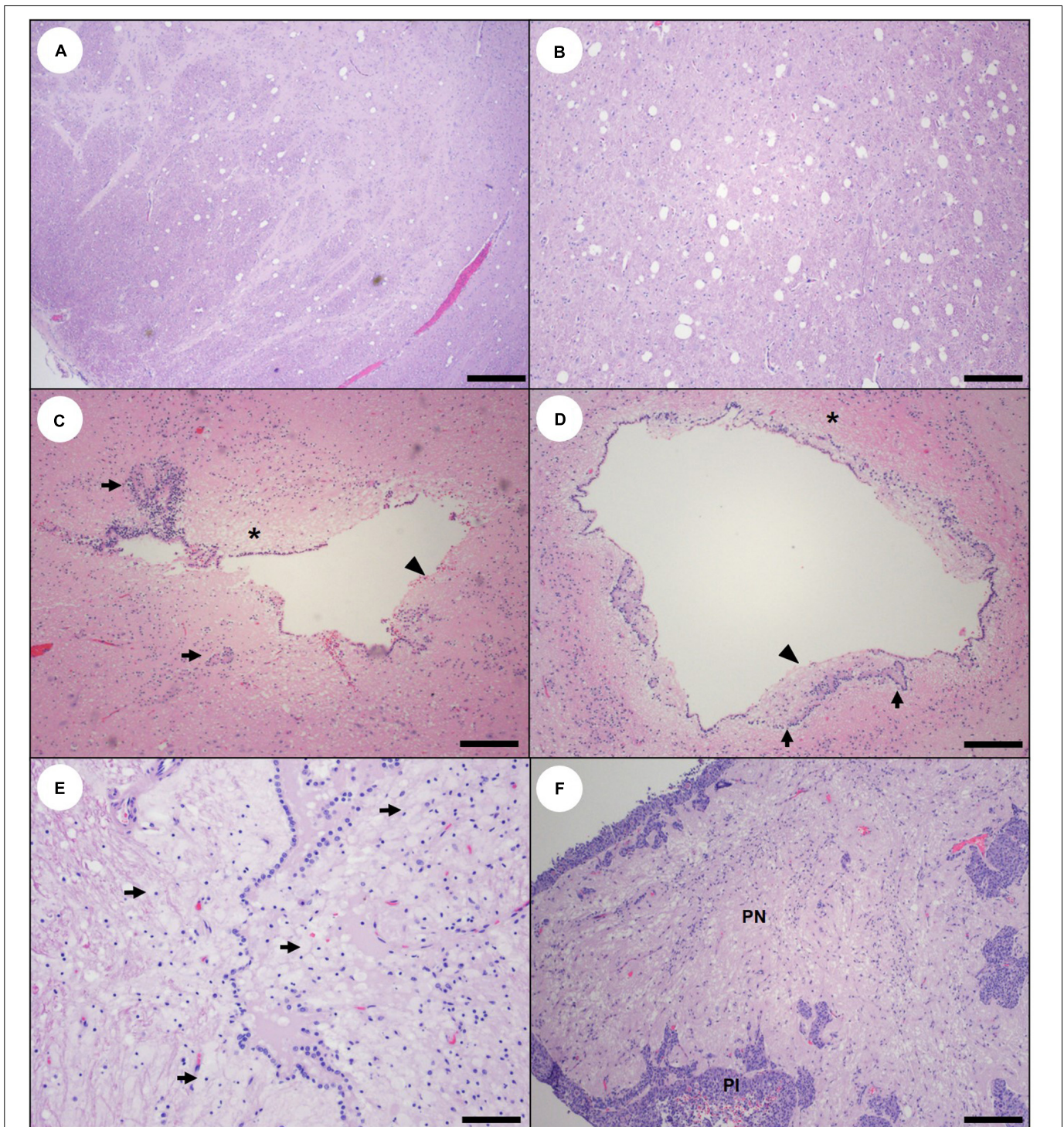
FIGURE 12 | Pathology suggestive of chronic (prior sublethal) domoic acid (DA) toxicosis in southern sea otters. **(A,B)** Large, sharp-walled vacuoles are scattered throughout the gray and white matter in the diencephalon from a sea otter with chronic sublethal DA toxicosis. These large vacuoles are common in the thalamus, hypothalamus, and periventricular neuropil, and are usually bilaterally symmetrical (**A**: Bar = 200 μm), (**B**: Bar = 100 μm). **(C,D)**: Scarred, mis-shapen ventricles from sea otters with chronic sublethal DA toxicosis. Prior damage to the ventricular wall is indicated by adhesions **(C)**, clusters of ependymal cells trapped below the irregularly thickened ventricle wall (arrows), a discontinuous ependymal lining (arrowheads) and periventricular spiongiosis and astrogliosis (asterisks) (**C,D**: Bars = 100 μm). **(E)** Ventricle from a sea otter with chronic sublethal DA toxicosis. There is partial disruption of the ventricle wall and massive proliferation of gitter cells and/or astroglia in the periventricular neuropil (arrows) (Bar = 40 μm). **(F)** Pituitary gland from a sea otter with subacute or chronic DA toxicosis. There is spongiosis and mild gliosis of the pars nervosa (PN), while the pars intermedia (PI) is histologically unremarkable (Bar = 100 μm).
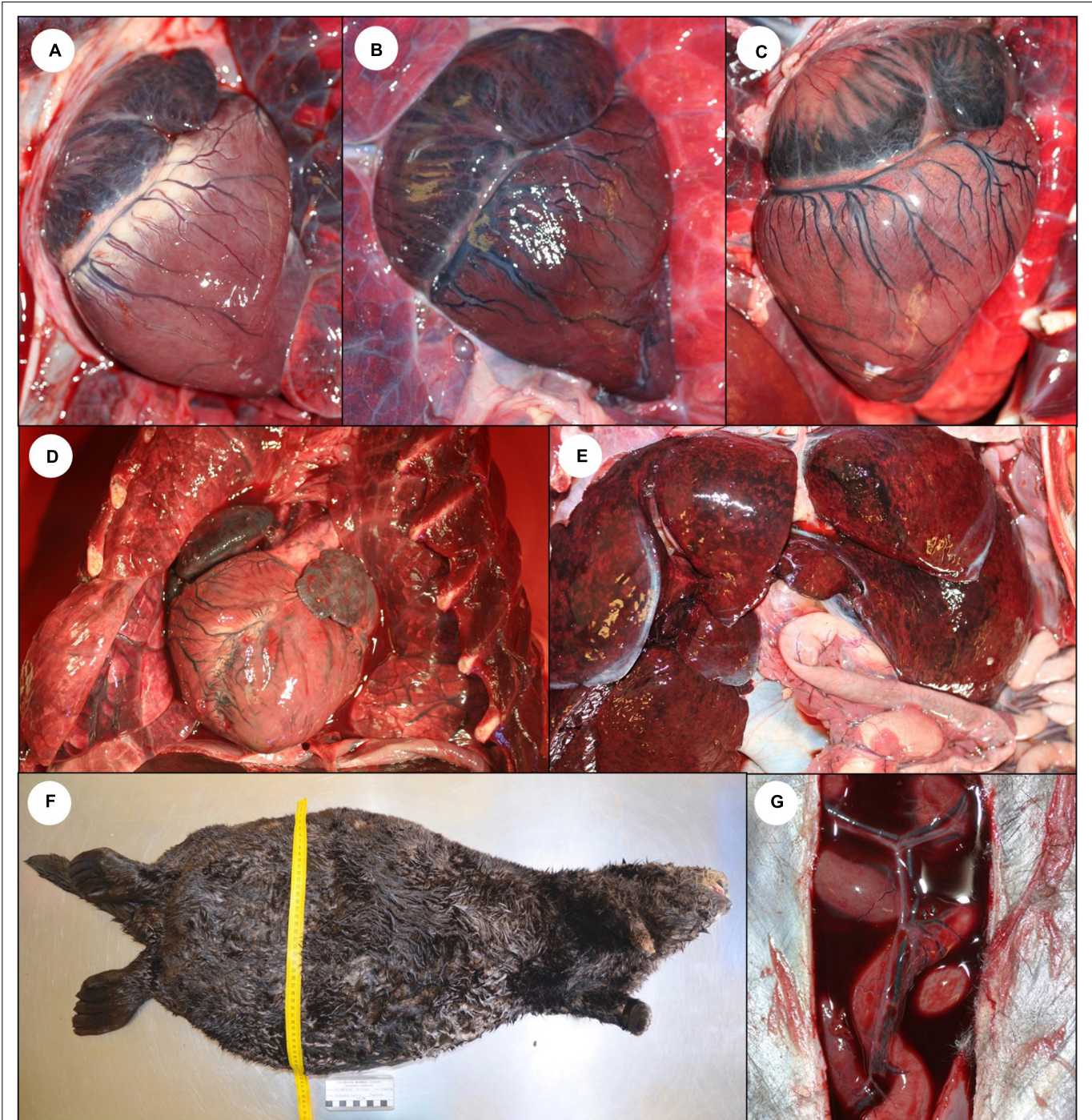
FIGURE 13 | Gross cardiac pathology suggestive of domoic acid (DA) toxicosis in southern sea otters. **(A)** Normal sea otter heart. **(B)** Heart from a sea otter with acute DA toxicosis. The myocardium is wet, shiny, and mildly translucent. There is diffuse brown discoloration of the ventricular myocardium and diffuse venodilation. Although the heart is not enlarged, the atria appear "full." **(C)** Heart from a sea otter with subacute DA toxicosis. The brown discoloration has transitioned to patchy myocardial pallor (tan or white spots or streaks), which are often most severe in the apex and left ventricular free wall. **(D)** Heart from a sea otter with chronic DA toxicosis. There is severe myocardial streaking, pallor, and cardiomegaly. **(E)** Enlarged and congested liver from a sea otter with subacute or chronic cardiomyopathy. **(F)** Peritoneal cavity distended with ascitic fluid in a sea otter with severe cardiomyopathy and congestive heart failure. **(G)** Blood-tinged serous peritoneal effusion secondary to congestive right heart failure.
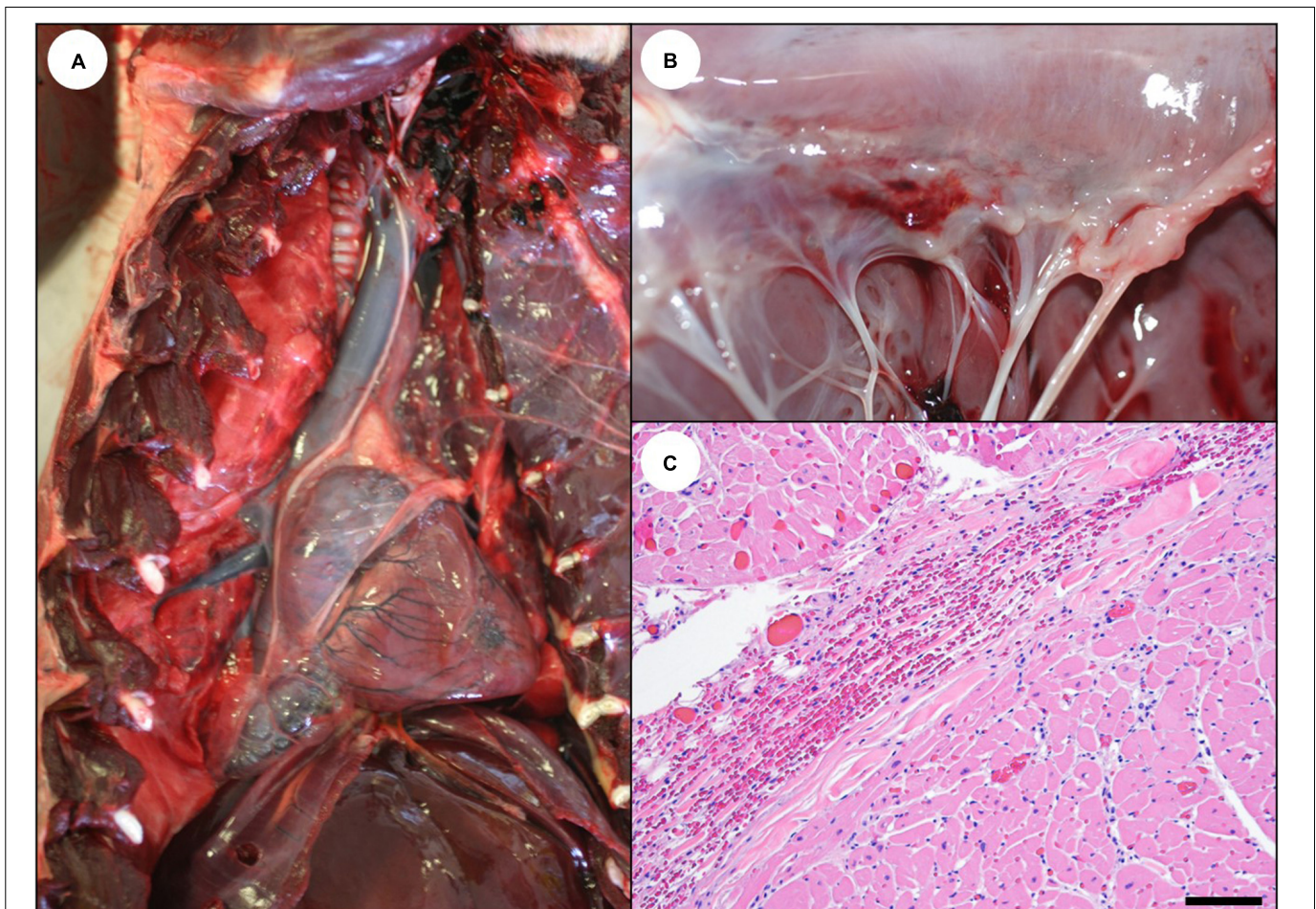
FIGURE 14 | Cardiac pathology suggestive of acute domoic acid (DA) toxicosis in southern sea otters. **(A)** Heart from a sea otter with acute DA toxicosis. The ventricular myocardium is mildly brown-discolored, shiny, and wet, and the right atrium and cranial vena cava appear "full." **(B)** Acute DA cases sometimes have grossly apparent acute cardiac hemorrhages, especially in the epicardium near the coronary groove, the endocardium near the base of the valves, the left papillary muscles, and the left ventricular endocardium. This is an example of endocardial hemorrhage at the base of the mitral valve. **(C)** Microhemorrhage is common in these same areas on histology (Bar = 100 μm).

matter vacuolation were sometimes apparent in areas of neuropil with prior primary insult; these large, sharply defined vacuoles were associated with mild neuronal depletion in some neuronal nuclei and were especially common in the diencephalon (thalamus and hypothalamus) of otters with chronic DA-associated CNS pathology (**Figures 12A,B**).

Cardiovascular system

The most common finding at gross necropsy for sea otters with chronic DA toxicosis was congestive heart failure (**Table 1**). Lesions suggestive of heart failure included severe diffuse venodilation and congestion (**Figures 1B–D**), hepatomegaly and chronic passive hepatic congestion (**Figure 13E**, **23A**), severe ascites (**Figures 13F,G**), pulmonary septal edema, pleural effusion, pulmonary septal and pleural fibrosis, and peritoneal and thoracic venous shunts. The heart was round with massive dilation (eccentric hypertrophy) of all four chambers and a prominent double apex indicative of severe right ventricular

dilation (**Figure 13D**). In the ventricles, occasional areas of severe cardiomyocyte loss resulted grossly in extensive pallor (**Figure 21A**) and depressed, variably translucent foci. The left atrial free wall was often mildly thickened and opaque (**Figure 21C**). Marked (>4–16 ml) serofibrinous, mildly red-tinged pericardial effusion was common for sea otters that died due to congestive heart failure. A few otters with subacute or chronic right-sided congestive heart failure died acutely due to hepatic vein thrombosis and massive hepatic necrosis (**Figures 23A–F**); this condition was often indicated grossly by perihilar hepatic capsular fibrin exudation (**Figure 23B**).

Chronic cardiac lesions resembled subacute cases, but they were more severe and quiescent on histopathology (**Table 2**). Intersecting bands of severe stromal collapse, fatty replacement, and peripheral cardiomyocyte hypertrophy were indicative of a chronic process (**Figure 15F**). Severe cardiomyocyte loss and stromal collapse were associated with fatty replacement or fibrosis (**Figures 15D–F**, **21D,E**).
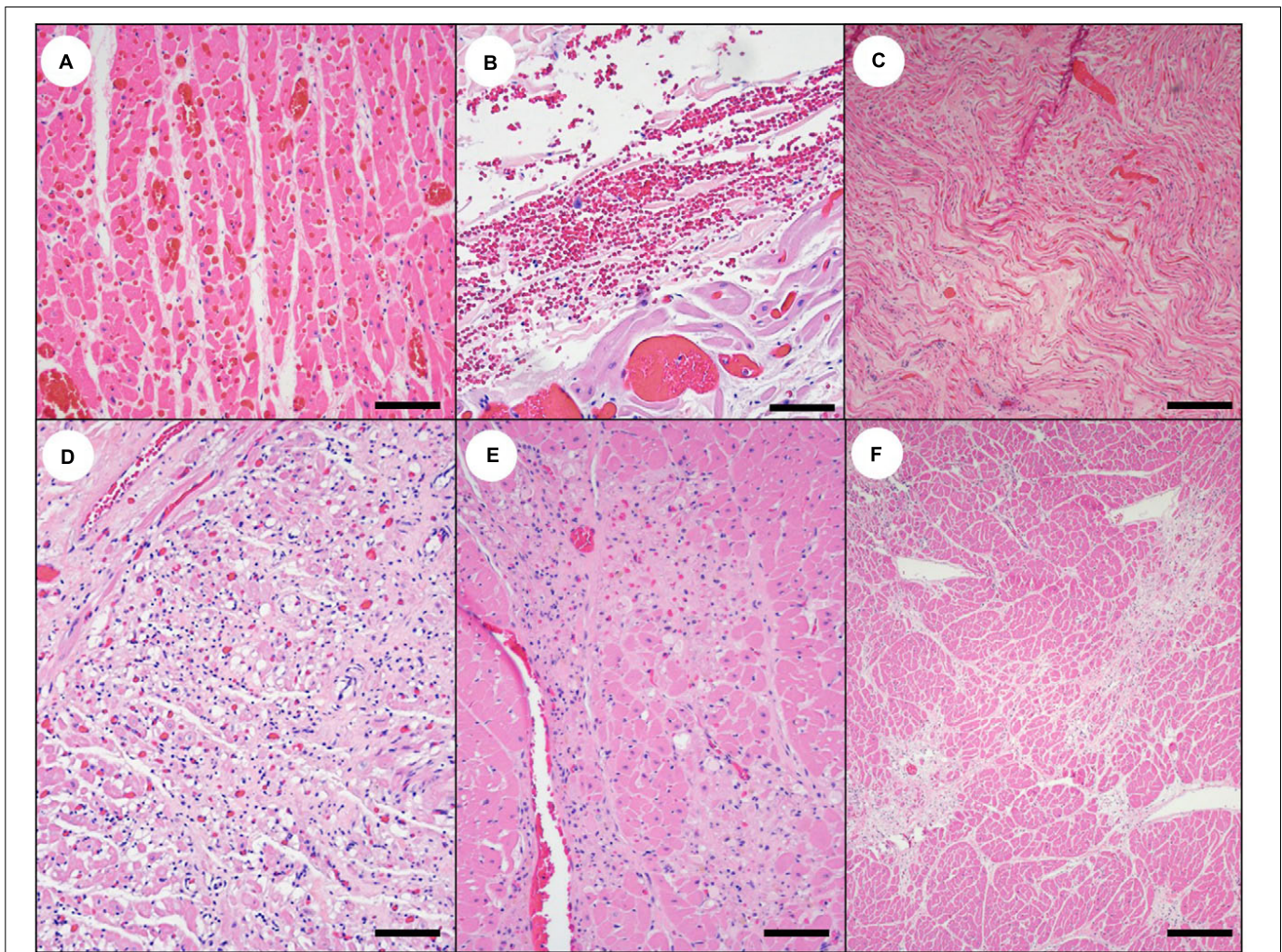
FIGURE 15 | Cardiac histopathology suggestive of domoic acid (DA) toxicosis in southern sea otters. **(A)** The first sign of acute DA toxicosis on cardiac histopathology is severe, diffuse congestion (Bar = 100 μm), and **(B)** multifocal microhemorrhage (Bar = 40 μm). Also common is **(C)** patchy interstitial edema that often corresponds with the brown-discolored myocardium observed grossly (Bar = 150 μm). **(D)** Subacute DA-associated cardiac pathology is characterized by regional cardiomyocyte vacuolation, necrosis or apoptosis, depletion, stromal collapse, fatty replacement, interstitial fibrosis, and, occasionally, non-suppurative myocarditis (Bar = 100 μm). **(E)** As the acute myocardial congestion normalizes over time, the cardiac lesions progressively expand (Bar = 100 μm). **(F)** For sea otters with chronic DA toxicosis, grossly apparent foci of myocardial pallor and streaking correspond histologically with intersecting bands of cardiomyocyte depletion, stromal collapse, fatty replacement, and interstitial fibrosis (Bar = 200 μm).

Cardiomyocyte necrosis and non-suppurative inflammation were usually mild. Coronary arteriolar hyalinization and sclerosis were often severe in the left ventricular free wall, papillary muscles, and apex (**Figure 16F**).

Estimating the Interval Between DA Exposure and Death Based on Lesion Chronicity

For 54 sea otters that were independently assessed for DA-associated pathology in the CNS and heart, the temporal stage of DA-associated CNS pathology matched with DA-associated cardiac pathology in most cases (87%; $n = 47/54$) (**Supplementary Table 2**). Seven otters (13%; $n = 7/54$) exhibited mixed patterns of acute, subacute, and chronic DA pathology in the CNS and heart on histopathology, suggestive of multiple episodes of DA toxicosis.

Domoic Acid-Associated Pathology of Other Tissues

In addition to the CNS and heart, severe diffuse vascular congestion was common in the liver, intestines, lungs, mesentery, adrenal glands, and kidneys (**Table 1** and **Figures 1B–D**, **23A**). Severe diffuse congestion of the choroid, retina, and ciliary body of both eyes was both common and distinctive for sea otters with acute DA toxicosis (**Table 2** and **Figures 24B,D**; please also see **Figures 24A,C** as normal comparison images). The ocular congestion was often accompanied by grossly apparent or microscopic hyphema (**Figure 24D**) and multifocal microhemorrhage. As with the pituitary gland, microscopic

FIGURE 16 | Coronary arterial histopathology associated with domoic acid (DA) toxicosis in southern sea otters. (A) through (D); cardiac tissue of sea otters with acute to subacute DA toxicosis often exhibits perivascular microhemorrhage and edema (A: arrowhead). Adjacent coronary arterioles often exhibit mural pathology, including shrunken or swollen mural smooth muscle cells with eosinophilic cytoplasm, pyknotic nuclei and intercellular edema (asterisks), and transient endothelial sloughing (A,B: arrows) or hyperplasia (C,D: arrowheads) (A,B: Bar = 40 μm), (C: Bar = 20 μm). (D: Bar = 40 μm). (D) through (F) Sea otters with subacute to chronic DA toxicosis often exhibit progressive coronary arteriosclerosis, characterized by decreased smooth muscle density, progressive mural hyalinization, sparse dystrophic mineralization, and patchy endothelial hyperplasia, clumping, or rounding (arrowhead). The wall of affected arterioles is markedly thickened, hypocellular, and hyalinized (E,F: Bars = 100 μm). These sections have artifactual section folds that reflect the density of the severely scarred arterioles.

examination of the eyes facilitated diagnosis of sea otters with acute DA toxicosis.

Severe diffuse uterine congestion, placental necrosis, and patchy placental hemorrhage were noted for some pregnant southern sea otters with acute DA toxicosis (**Table 2** and **Figure 25A**). On histopathology the myometrium had discrete bands of hypercontracted, swollen, and markedly eosinophilic smooth muscle cells with variable cytoplasmic vacuolation, accompanied by mild proteinaceous pericellular edema and microhemorrhage (**Figures 25B–E**). Arteriolar mural smooth muscle cell necrosis or apoptosis was also observed in the myometrium,

accompanied by vascular mural and perivascular edema and microhemorrhage (**Figures 25F,G**). Glutamate receptors (potential sites for DA binding) have been detected in the female reproductive tract, including the myometrium, endometrium, and ovary in other species (Pulido, 2008).

Fetal gross and microscopic pathology resembled that of mothers with acute DA toxicosis and included severe congestion, brown-discolored ventricular myocardium, pericardial effusion, mild diffuse venous dilation, and microhemorrhage in the heart, brain, eyes, and kidneys. DA-associated reproductive and fetal pathology reported in pinnipeds, primates, fish,
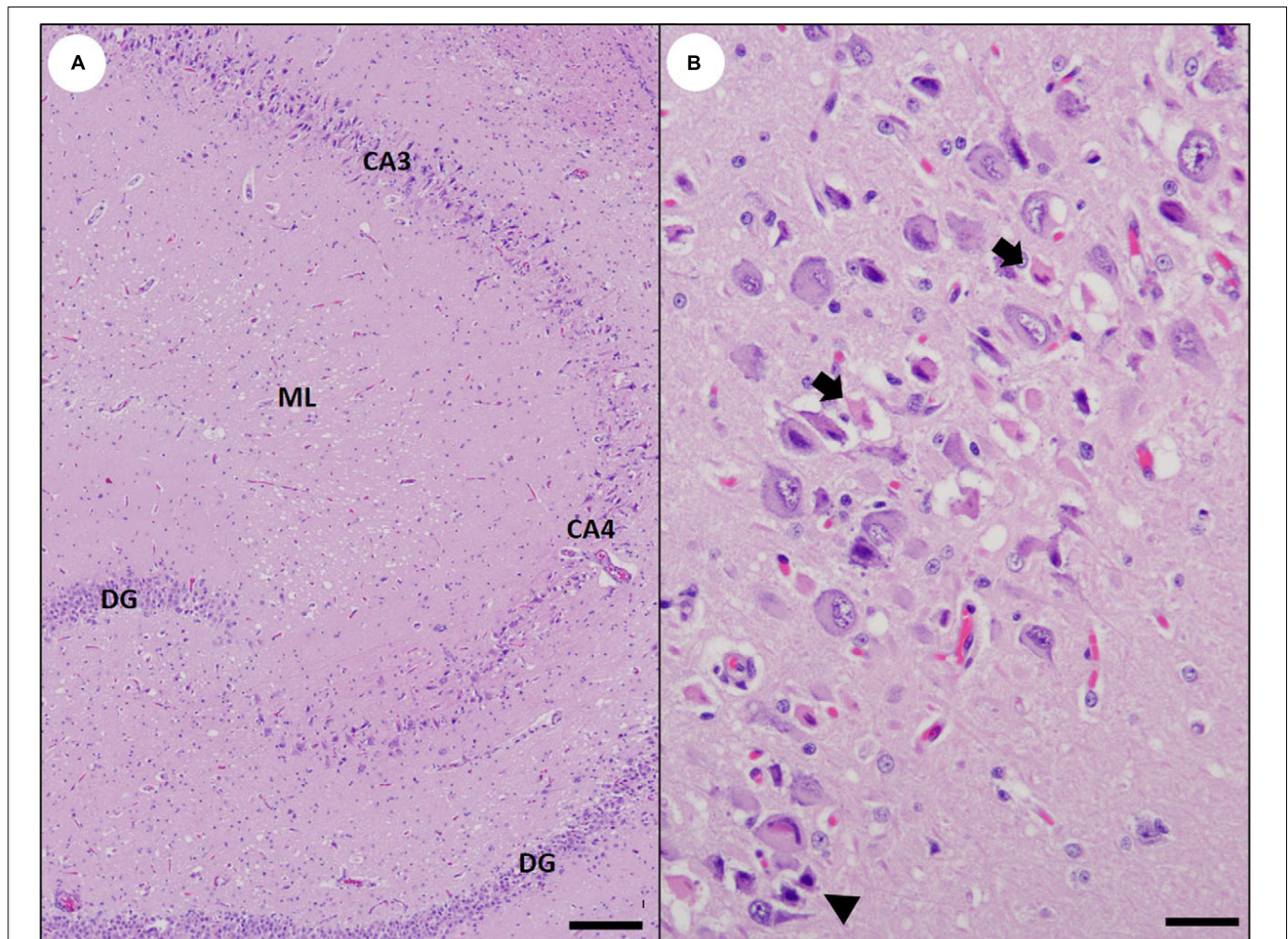
FIGURE 17 | Subacute domoic acid (DA) pathology in the southern sea otter hippocampus. **(A)** Pyramidal neurons of the cornu ammonis (CA) segments CA3 and CA4 are condensed and hyperchromic, and many appear elongated, with increased prominence of axons and dendrites. There is also moderate spongiosis of the molecular layer (ML). Note that the dentate granule neurons (DG) are histologically unremarkable (Bar = 200 μm). **(B)** High magnification view of the CA2 region of the hippocampus from a sea otter with subacute DA toxicosis. Some pyramidal neurons have bright red cytoplasm and condensed, pyknotic nuclei (arrows); these classical "red dead" hippocampal neurons are relatively uncommon in sea otters with fatal DA toxicosis. Pyramidal neurons that are shrunken, angular, and have diffusely hyperchromic cytoplasm and pyknotic nuclei (arrowhead) are more common in the CNS of sea otters with subacute DA toxicosis (Bar = 20 μm).

and laboratory animals includes abortion, fetal resorption, stillbirth, uterine torsion, and chronic post-natal health impacts (Tiedeken et al., 2005; Brodie et al., 2006; Maucher and Ramsdell, 2007; Ramsdell and Zabka, 2008; Goldstein et al., 2009; Burbacher et al., 2019). Although abortion and uterine torsion were observed in sea otters with DA toxicosis, our sample size was small: over 21 years (1998–2018), we performed detailed necropsy and histopathology on 266 minimally decomposed adult and aged adult female southern sea otters, and only 39 animals (15%) were visibly post-implantation pregnant at the time of necropsy, with 21 fetuses receiving detailed gross and microscopic examinations (**Supplementary Table 1**).

Some female sea otters with acute or subacute DA toxicosis had indications of perimortem copulation during non-estrus periods, suggesting that males were forcibly mating with females that had severe neurological impairment (**Table 1**). One animal had lesions consistent with forced copulation during near-term abortion or parturition that resulted in multifocal hematomas on the head of the fetus within the vaginal canal. Severe perimortem fight trauma was also apparent for some males with DA toxicosis. Paraphimosis was also observed, which could be indicative of DA-associated spinal cord pathology.

Sea otters with acute DA toxicosis commonly had copious red- or green-tinged seromucoid fluid leaking from the nares and oropharynx that often stained the peri-oral and peri-nasal pelage (**Table 1** and **Figure 1A**); this finding was suggestive of nausea and hypersalivation, and/or diffuse pulmonary hypersecretion. Both conditions have been reported in humans and other animals with acute DA toxicosis (Pulido, 2008). Diffuse pulmonary edema and pleural effusion were common and could reflect
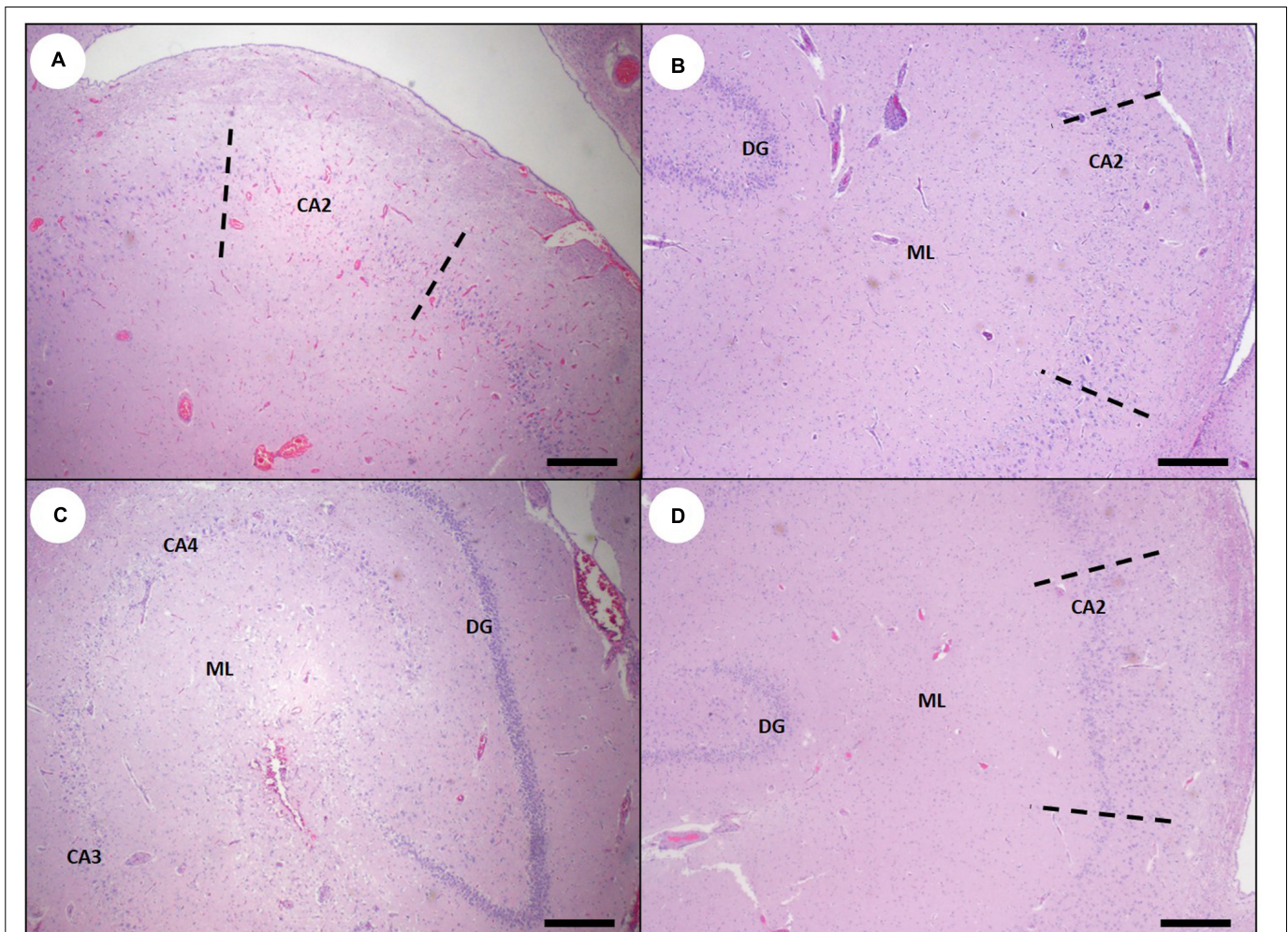
FIGURE 18 | Hippocampal histopathology in southern sea otters with subacute or chronic domoic acid (DA) toxicosis. **(A)** For cases of subacute DA toxicosis, progressive resolution of the severe congestion is associated with histologically apparent segmental pyramidal neuron degeneration and depletion, especially around the cornu ammonis (CA) segment CA2 (area between the dashed lines). During the subacute phase, DA-associated pyramidal lesions often expand and encompass additional CA segments. The extent of lesion expansion varies, possibly due to variation in the DA dose, the number of prior DA exposure events, and other factors (Bar = 200 μm). **(B)** In milder cases, segmental pyramidal neuron depletion is partial and limited to the putative CA2 segment (area between the dashed lines). At higher magnification, the remaining neurons often appear histologically abnormal (e.g., elongated or shrunken and hyperchromic; please see **Figure 7** for examples). As the congestion resolves, mild gliosis develops, as indicated by increased cellular density in the molecular layer (ML) (Bar = 200 μm). **(C)** Hippocampus from a sea otter that died from severe subacute DA toxicosis; there is marked, diffuse pyramidal neuron loss along the entire CA (CA3 and CA4 shown) and severe spongiosis of the molecular layer (ML). Note that the dentate granule neurons (DG) are relatively unaffected (Bar = 200 μm). **(D)** Pyramidal neurons from a sea otter that died with mild chronic hippocampal damage are mildly depleted and less clearly organized into a single homogenous linear band; the most severely damaged area (CA2; area between the dashed lines) is mildly displaced toward the dentate granule neurons (DG). Mild gliosis is also apparent in the molecular layer (ML). While mild chronic lesions are hard to detect, especially in cases with autolysis or concurrent brain pathology, standardized trimming of formalin-fixed tissue can facilitate lesion identification (Bar = 200 μm).

hypersecretion, systemic cardiovascular impacts, or terminal seawater aspiration.

The GI tract of sea otters with acute DA toxicosis often contained minimally or partially digested prey (**Table 1** and **Figure 2A**) that was high DA-positive (Miller et al., 2020). In contrast, emesis and comparatively empty GI tracts are common for humans and other animals with acute DA toxicosis (Tryphonas et al., 1990; Pulido, 2008; Grant et al., 2010). Other than the peri-oral staining and hypersalivation, we found no clinical reports of emesis in live-stranded sea otters, although some cases had ingested prey in the upper GI tract, trachea, bronchi, and lungs.

Domoic acid exposure has been associated with development of gastric ulcers in laboratory rodents (Glavin et al., 1990). Although GI erosions and melena were common in sea otters that died from DA toxicosis, this lesion is ubiquitous in stranded sea otters and could be a non-specific indicator of stress (Miller et al., 2020). Although we observed diffuse mucosal and serosal congestion, ileus, intestinal intussusception, and gastric or intestinal torsion in otters with DA toxicosis (**Table 1**), we could

FIGURE 19 | Unilateral hippocampal atrophy following domoic acid (DA) toxicosis in a southern sea otter. Transverse sections of formalin-fixed sea otter brain centered on the hippocampus. **(A)** Normal sea otter hippocampus (bottom center). The cornu ammonis (CA; arrow) has a smooth convex curve along the border with the lateral ventricle (arrowhead). **(B)** Opposite cerebral hemisphere from the same sea otter. There is extensive hippocampal atrophy resulting in severe flattening of the lateral aspect of the CA (arrow) and dilation of the lateral ventricle (arrowhead).

not confirm that these findings were DA-associated due to our limited sample size.

No unique patterns of DA-associated renal pathology were observed in sea otters other than diffuse, marked parenchymal congestion and occasional interstitial microhemorrhage in acute DA cases (**Table 2**). Because we focused mainly on investigating DA-associated pathology of the CNS and cardiovascular system, subtle kidney lesions could have been missed. DA-associated renal pathology has been reported in other species (Pulido, 2008; Funk et al., 2014) and glutamate receptors have been identified in renal tissue (Gill and Pulido, 2005).

Pseudo-nitzschia Frustule Detection in Prey Items and Stomach Content

Scanning electron microscopy analysis of the GI tracts of sand crabs ingested by two sea otters with acute DA toxicosis and high DA concentrations in their urine and gastric content revealed ingested *Pseudo-nitzschia* spp. frustules (**Figures 2C,D**). Similar frustules were recovered from the GI tracts of free-living sand crabs collected in Monterey Bay, California during a toxic *Pseudo-nitzschia* bloom (**Figure 2B**). These frustules matched morphologically with the reference *P. australis* strain (**Figure 2E**).

DISCUSSION

Patterns of DA-Associated Pathology

Domoic acid-associated clinical signs, gross pathology and biochemical data in southern sea otters are summarized in

Table 1, and histopathology findings are summarized in **Table 2**; example lesions from the figures are referenced in column 1 of the full-scale, printable versions of **Tables 1**, **2** that are available in **Supplementary Presentation 1**. CNS pathology in southern sea otters was similar to reports for other marine mammals, laboratory animals, and primates with DA toxicosis (Silvagni et al., 2005; Goldstein et al., 2008; Pulido, 2008; Burbacher et al., 2019), although there were some differences. Similarities include concurrent CNS and cardiovascular impacts (Pulido, 2008; Zabka et al., 2009), and a bimodal pattern of clinical signs and pathology: For sea otters, severe acute DA cases typically presented with CNS and/or systemic vascular clinical signs and lesions predominating, while chronic DA toxicosis cases were more likely to present with severe cardiovascular signs and lesions (**Tables 1**, **2**); subacute DA toxicosis cases were intermediate, presenting with CNS, cardiovascular, or both processes concurrently. Our ability to histologically diagnose DA toxicosis and estimate the post-exposure interval improved when the brain, eyes, and heart were all assessed at the same time.

Blood vessels appeared to be an early DA target for southern sea otters with acute DA toxicosis. The predominant lesion for otters with acute DA toxicosis was severe diffuse congestion and multifocal microhemorrhage with edema and tissue injury, especially in the CNS, eyes, and heart. These findings suggest that vascular mural pathology, regional or systemic edema, transient hypo- or hypertension, or vascular shock could contribute to the acute clinical signs of DA-associated neurotoxicity. These lesions were consistently observed in otters with the highest DA concentrations in urine and

FIGURE 20 | Bilateral hippocampal atrophy following domoic acid (DA) toxicosis in a southern sea otter. Transverse section of formalin-fixed sea otter brain at the level of the hippocampus. On the left side the hippocampus is mildly atrophied with mild flattening of the lateral aspect of the cornu ammonis (CA; arrow) and mild dilation of the lateral ventricle (arrowheads on left). On the right side there is marked hippocampal atrophy and the CA is severely flattened (arrow) with marked dilation of the lateral ventricle (arrowheads on right). The mesencephalic duct (surrounded by dashed line at center) is also mildly dilated. Partial formalin fixation at the time of tissue trimming is indicated by the elliptical area of pink tissue at center left.

GI content (≥500 ppb), and preceded development of microscopically apparent neuronal and glial pathology. Although the finding of severe congestion as a predictor of acute DA toxicosis in sea otters seems to contradict published reports of DA-associated pathology in other species (Silvagni et al., 2005: Pulido, 2008), retrospective case review suggests that a similar pattern may occur in California sea lions with acute DA toxicosis (T. Zabka, unpublished data).

Subacute DA toxicosis was characterized by transitional gross and microscopic pathology, reflecting toxic injury, progressive lesion expansion, vascular mural damage, and robust host response to injury. In the CNS, characteristic lesions included multifocal neuronal degeneration, gliosis, and spongiosis. In the heart there was progressive cardiomyocyte loss, stromal collapse, and interstitial fatty replacement and fibrosis. Where present, intra- or perilesional inflammation often appeared to be a response to tissue damage. Similar cardiac lesions have been reported in California sea lions following DA toxicosis and were attributed to pathology mediated via the cardiac conduction system (Zabka et al., 2009). DA-associated cardiac pathology had a similar anatomical distribution in otters and sea lions, but atrial wall pathology was more common in sea otters.

For sea otters with chronic DA toxicosis, clinical signs and pathology attributable to severe cardiac pathology and congestive heart failure were usually the most obvious findings clinically, grossly, and on histopathology. Mild chronic CNS

lesions were often challenging to discern on histopathology, whereas severe cases had massive neuronal loss, scarring, and atrophy affecting one or both hippocampal profiles. Death due to cardiovascular decompensation was common for some subacute and most chronic DA cases. The cardiovascular and CNS lesion distribution was similar for acute, subacute, and chronic cases, but chronic lesions were dominated by atrophy, scars, and gliosis that reflected damage that was initiated months to years before death. Although chronic lesions appeared to be relatively quiescent on histopathology, the cumulative impacts on cardiovascular function were often severe.

Although hippocampal pathology is a diagnostic feature of DA toxicosis in humans and other species (Sutherland et al., 1990; Gulland, 2000; Silvagni et al., 2005), the lesion distribution is variable (Pulido, 2008). While dentate granule cells are an important DA target in humans (Pulido, 2008), they are less severely affected in California sea lions than pyramidal neurons (Silvagni et al., 2005; Goldstein et al., 2008). In most mammals, the CA2 segment of hippocampal pyramidal neurons is relatively unaffected by DA in comparison to other segments (Silvagni et al., 2005; Goldstein et al., 2008; Pulido, 2008). While humans usually develop bilateral hippocampal pathology (Sutherland et al., 1990), California sea lions can develop unilateral or bilateral lesions (Silvagni et al., 2005; Goldstein et al., 2008; Buckmaster et al., 2014).

Contrary to reports in other animals (Silvagni et al., 2005; Pulido, 2008), southern sea otters with severe DA toxicosis
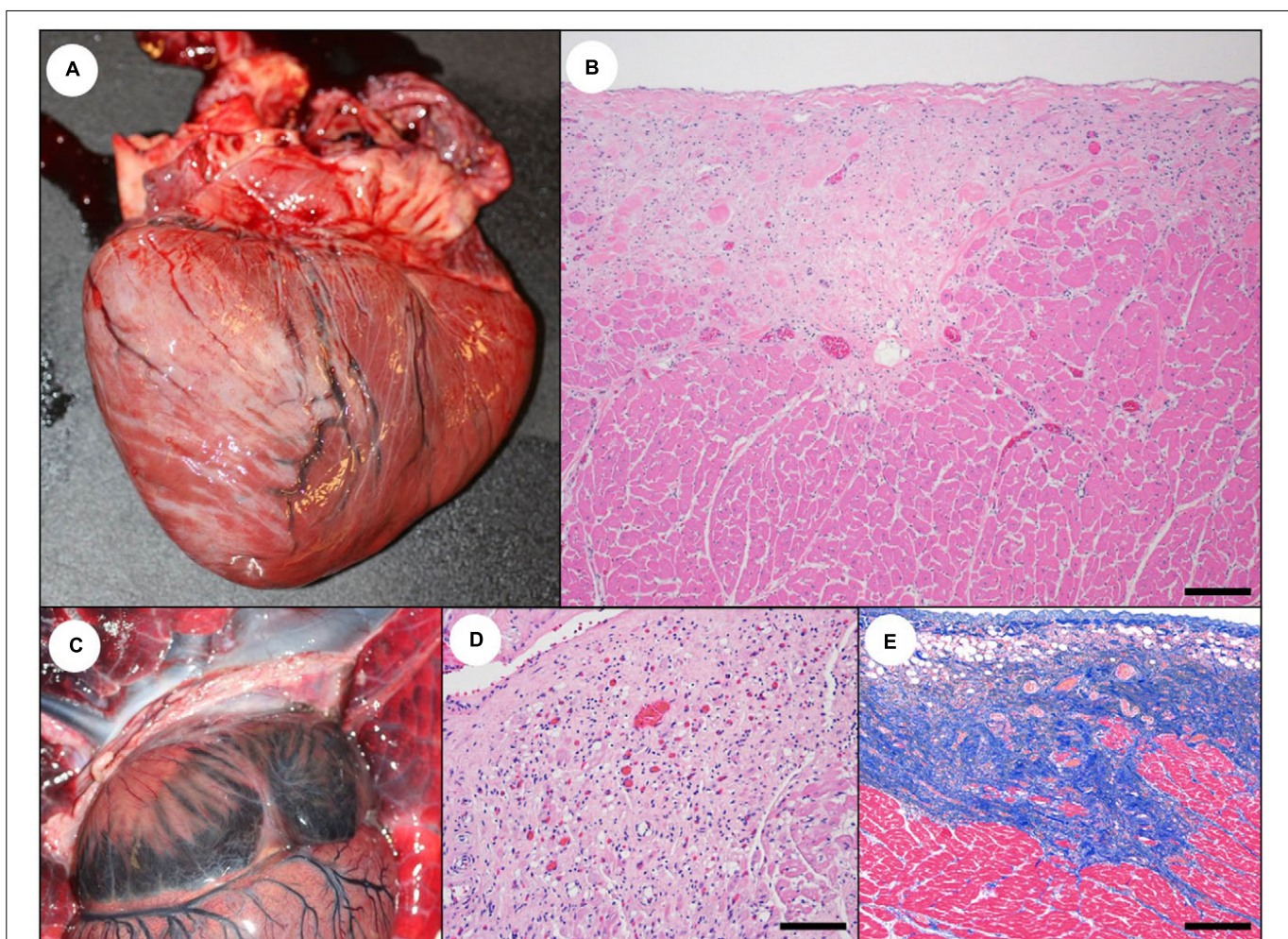
FIGURE 21 | Cardiac pathology suggestive of subacute to chronic domoic acid (DA) exposure in southern sea otters. **(A)** As DA-associated cardiac pathology (cardiomyopathy) progresses, prominent white or pale tan streaks often develop, especially on the epicardium of the left ventricle and the apex. These lesions are often opaque, light tan to white, and are sometimes slightly depressed relative to adjacent tissue. **(B)** These streaks correspond histologically with areas of cardiomyocyte depletion, mild non-suppurative myocarditis, stromal collapse, and fibrosis, and they often have a sub-epicardial and sub-endocardial distribution on histopathology (Bar = 200 μm). **(C)** In addition to the ventricular streaks, the atria (especially the left atrial free wall) often become progressively opaque and white to light tan. **(D)** On histopathology, the atrial pallor corresponds with cardiomyocyte depletion, stromal collapse, fatty degeneration, fibrosis, and mild non-suppurative myocarditis (Bar = 200 μm). **(E)** As shown in this Masson's Trichrome stain of the left ventricular free wall, in severe cases cardiomyocyte depletion and scarring can efface large expanses of myocardium, accompanied by stromal collapse and fibrosis (Bar = 200 μm).

rarely had swollen, brightly eosinophilic hippocampal pyramidal neurons or dentate granule cells on histopathology, suggesting that this commonly described DA lesion is more ephemeral in sea otters. Like sea lions, DA-exposed sea otters developed unilateral or bilateral hippocampal damage (**Table 2** and **Figures 19B**, **20**), with relative sparing of dentate granule cells (**Figures 17A**, **18B,C**). However, the earliest and most severe pyramidal cell lesions in sea otters were in the putative CA2 segment (**Figures 6B**, **18A,B**), while sea lions often show more severe damage to pyramidal neurons in other sectors; this difference could reflect anatomical variation or differential impacts of DA in sea otters. We also identified DA-associated spinal cord pathology in sea otters; this lesion could be under-recognized in all species because the spinal cord is not routinely examined microscopically.

The findings of this study suggest that some effects of DA toxicosis could be mediated through CVO damage (**Table 2** and **Figures 10B–E**, **11B–D**). Although CVOs have been proposed as potential targets for DA toxicity, there is limited information on this topic (Bruni et al., 1991). These highly vascularized structures are distributed along the sagittal midline near ventricles, and most are located outside of the blood-brain barrier. The CVOs serve as critical interfaces between the brain and systemic circulation, and regulate cardiovascular, renal, and GI function, emesis, blood osmolality, and endocrine homeostasis (Bruni et al., 1991; Duvernoy and Risold, 2007). Given these critical functions, DA-mediated CVO damage could amplify localized effects of DA toxicosis and cause systemic impacts. Given the importance of CVOs in vascular homeostasis (Duvernoy and Risold, 2007), the severe congestion observed in sea otters with
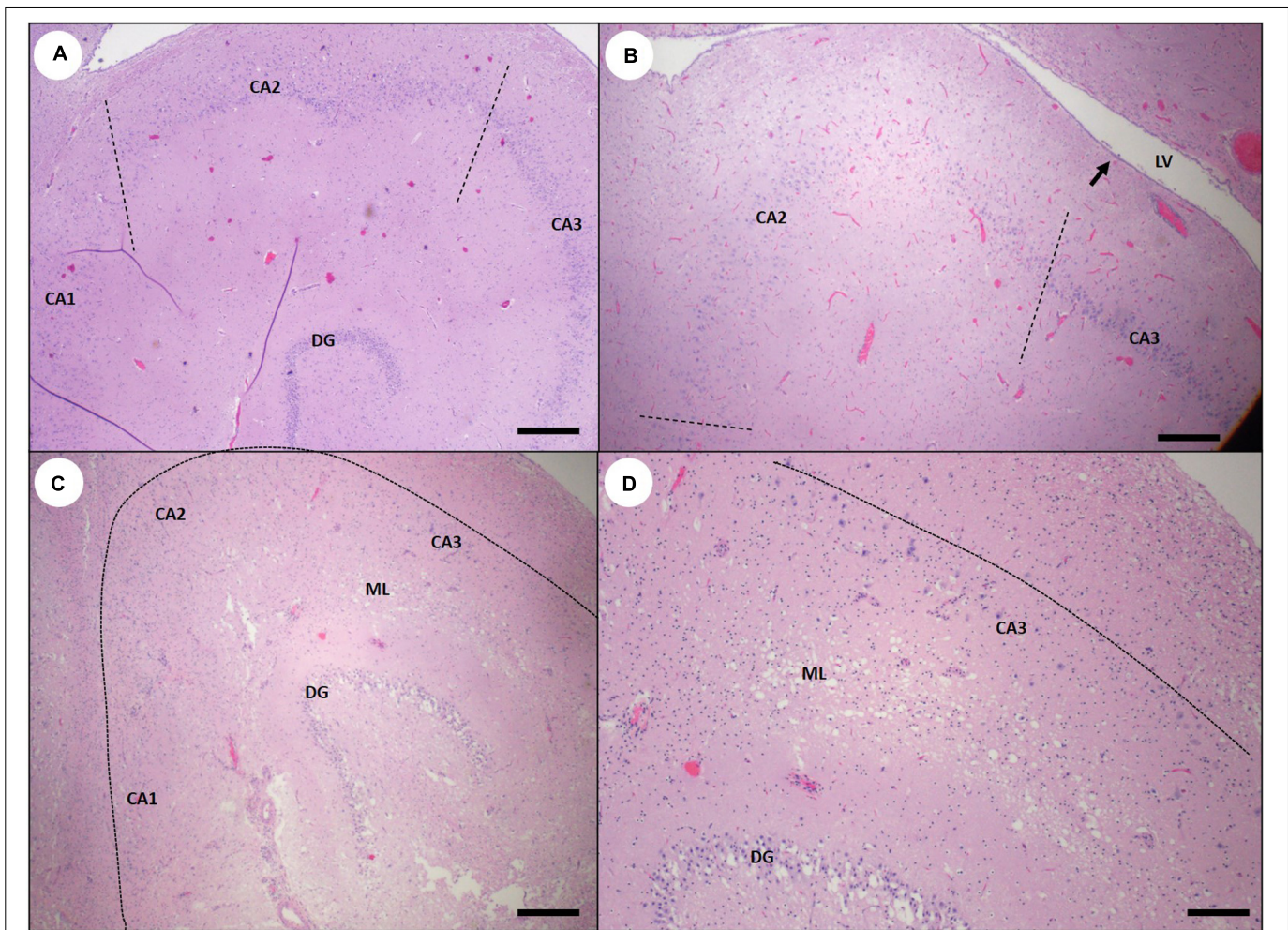
FIGURE 22 | Sea otter hippocampus showing variable tissue damage and scarring associated with subacute or chronic domoic acid (DA) toxicosis.
(A) Hippocampus from a sea otter with chronic DA toxicosis. Pyramidal neurons are segmentally depleted and less evenly distributed into a single linear band. The most severely affected cornu ammonis (CA) segment CA2 (area between the dashed lines) is mildly displaced toward the dentate granule neurons (DG) (Bar = 200 μm). **(B)** Marked segmental depletion of CA2 pyramidal neurons (area between the dashed lines). Hippocampal atrophy has resulted in the development of a concave surface (arrow) and mild luminal expansion of the corresponding lateral ventricle (LV). The normally smooth convex curve of pyramidal neurons has also become sharper and more angular (compare with normal hippocampus: **Figure 6A**) (Bar = 200 μm). **(C)** Severely damaged hippocampus with massive depletion of pyramidal neurons in all CA segments (pyramidal neurons should normally be visible just inside of the dashed line). The dentate granule cells (DG) were also partially depleted in this severe case. There is also diffuse, marked gliosis and spongiosis in the molecular layer between the dentate and the CA (ML) (Bar = 200 μm). **(D)** Higher magnification inset of **(C)** showing near-total depletion of pyramidal CA neurons (normally visible just inside of the dashed line), severe gliosis and spongiosis of the molecular layer (ML), and partial depletion of dentate granule neurons (DG) (Bar = 100 μm).

acute DA toxicosis could be reflective of primary cardiac or vascular insult, or secondary systemic insult from CVO damage.

Because of their location, function, rich vascular supply, and exclusion from the blood-brain barrier, CVOs could also serve as portals for DA passage from the systemic circulation into the brain and CSF (Bruni et al., 1991). Biochemical testing has confirmed that DA enters the ventricular system in sea otters, with concentrations as high as 1,244 ppb in CSF (M. Miller, unpublished data). Potential routes of DA entry into the CSF include the choroid plexus, ependyma, CVOs, DA-mediated vascular leakage, damage to periventricular neuropil, and ventricular hemorrhage. We have identified potential DA-associated pathology in all of these anatomic regions. This research also suggests that DA entry into the CSF may facilitate toxin spread throughout the CNS. Interestingly, CSF transport has also been postulated as a means of expediting DA clearance from the CNS; CSF volume is replaced approximately every 4 h in rats (Fuquay et al., 2012). If a similar clearance interval occurs in sea otters, detection of high DA concentrations in CSF could be diagnostic for acute DA toxicosis.

The pituitary gland has been described as a highly vascularized secretory CVO or an extension of the median eminence, another CVO (Bruni et al., 1991; Duvernoy and Risold, 2007; Pulido, 2008). Given the close anatomic and functional relationship of the pituitary gland to the CVOs, we have included it with the CVOs. As with other CVOs, the pituitary gland
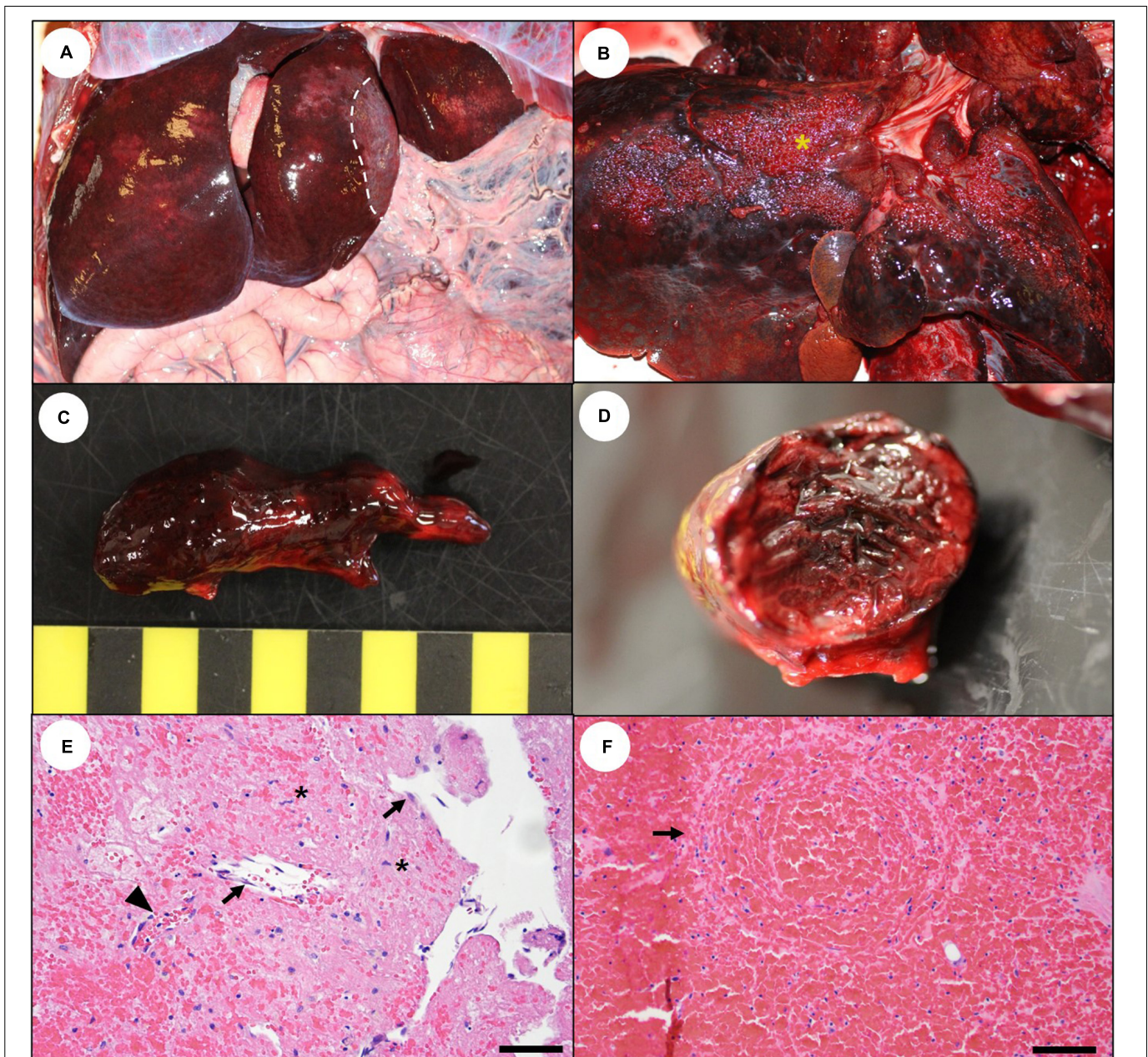
FIGURE 23 | Budd-Chiari-like syndrome: Cardiomyopathy-associated hepatic vein thrombosis in southern sea otters with subacute to chronic domoic acid (DA) toxicosis. Some sea otters with DA-associated subacute or chronic cardiomyopathy develop hepatic vein thrombi, leading to acute exacerbation of congestive right heart failure. **(A)** An enlarged, congested, red-black mottled liver from a sea otter with hepatic vein thrombosis. This sea otter survived a prior episode of thrombosis, as indicated by focally extensive, regional hepatic atrophy (area of liver lobe to the right of the dashed line, center right). **(B)** Hepatic perihilar raised fibrin plaques with a "Turkish towel" appearance (asterisk) are suggestive of hepatic vein thrombosis; the liver should be carefully searched for venous thrombi. **(C)** Hepatic vein thrombi are often large, firm, branched, and loosely attached to the wall of larger and smaller branches of the hepatic vein. **(D)** The thrombi have a layered or lamellated appearance on cross-section. **(E)** Microscopic examination often reveals surface endothelium (arrows), fibroblast proliferation (asterisks), and capillary buds (arrowhead), confirming that this is an antemortem thrombus (Bar = 40 μm). **(F)** On histopathology, congested livers with dilated, blood-filled central veins containing concentric bands of lamellated fibrin and red blood cells (arrow) are indicative of hepatic vein thrombosis (Bar = 100 μm).

appears to be a sensitive target for DA in southern sea otters (**Table 2** and **Figures 11B–D**). When other causes of pituitary gland congestion and hemorrhage were excluded (e.g., sepsis, endotoxemia, and trauma), detection of severe diffuse congestion of the pars distalis and pars nervosa, but not the pars intermedia,

was indicative of acute DA toxicosis. Lack of congestion in the pars intermedia could be due to lower susceptibility to DA, or because the pars intermedia has a comparatively low capillary density and separate vascular supply from the pars distalis (Duvernoy and Risold, 2007). Because the pituitary gland
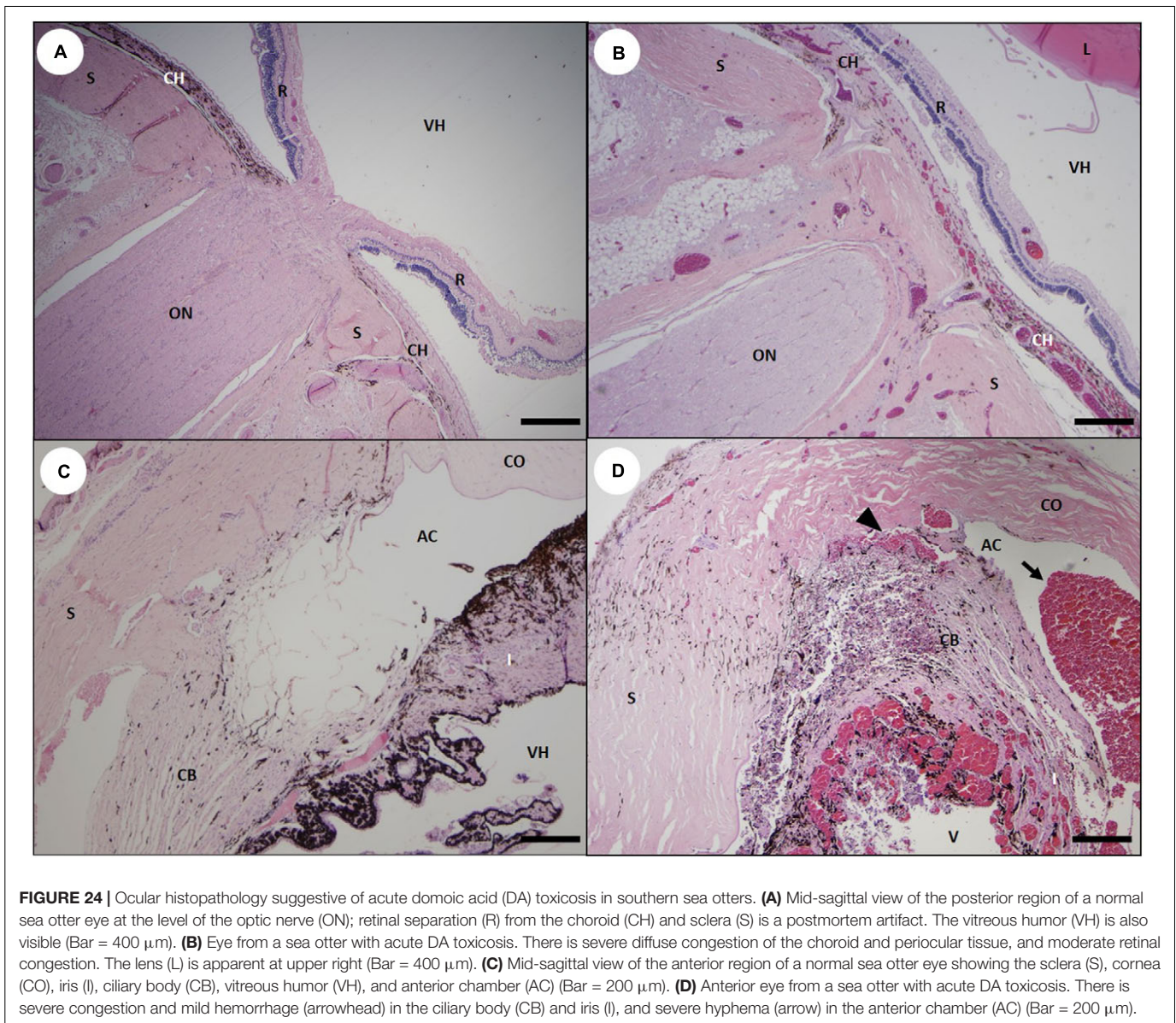
FIGURE 24 | Ocular histopathology suggestive of acute domoic acid (DA) toxicosis in southern sea otters. **(A)** Mid-sagittal view of the posterior region of a normal sea otter eye at the level of the optic nerve (ON); retinal separation (R) from the choroid (CH) and sclera (S) is a postmortem artifact. The vitreous humor (VH) is also visible (Bar = 400 μm). **(B)** Eye from a sea otter with acute DA toxicosis. There is severe diffuse congestion of the choroid and periocular tissue, and moderate retinal congestion. The lens (L) is apparent at upper right (Bar = 400 μm). **(C)** Mid-sagittal view of the anterior region of a normal sea otter eye showing the sclera (S), cornea (CO), iris (I), ciliary body (CB), vitreous humor (VH), and anterior chamber (AC) (Bar = 200 μm). **(D)** Anterior eye from a sea otter with acute DA toxicosis. There is severe congestion and mild hemorrhage (arrowhead) in the ciliary body (CB) and iris (I), and severe hyphema (arrow) in the anterior chamber (AC) (Bar = 200 μm).

is easy to find at necropsy when compared with other CVOs, we recommend routine pituitary histology as part of DA case assessment. Bisecting the gland along the mid-sagittal plane is essential to observe the distinct pattern of differential congestion on histopathology (**Supplementary Image 1B**).

Although our sample size was small, assessment of DA-associated lesion chronicity in the CNS and heart from 54 necropsied sea otters demonstrated strong temporal concordance (87%) for DA-associated pathology in the CNS and heart (**Supplementary Table 2**). These findings suggest that the CNS and cardiac pathology was initiated by a common cause (e.g., DA toxicosis). The simultaneous presence of acute, subacute and chronic, DA-associated pathology in the CNS and heart of 13% of examined otters suggests recurrent DA toxicosis. Concurrent microscopic examination of the CNS and cardiovascular system can facilitate confirmation of DA

toxicosis, temporal assessment of lesion chronicity, and detection of recurrent DA toxicosis in sea otters.

The findings of this study (**Tables 1**, **2** and **Supplementary Table 2**) strongly support other reports of a link between DA toxicosis and cardiomyopathy in sea otters (Kreuder et al., 2005; Miller et al., 2020; Moriarty et al., 2021b). As CNS lesions became more difficult to detect in subacute and chronic cases, the cardiovascular lesions were usually more severe and obvious, illustrating the value of combined assessment. Associations between DA exposure and cardiovascular pathology have been reported for sea lions (Zabka et al., 2009), sea otters (Kreuder et al., 2005; Miller et al., 2020, Moriarty et al., 2021a,b), laboratory animals (Gao et al., 2007; Vieira et al., 2016), and primates, including humans (Perl et al., 1990a; Gessner et al., 1997; Pulido, 2008; Vranyac-Tramoundanas et al., 2011). In a recent comprehensive southern sea otter
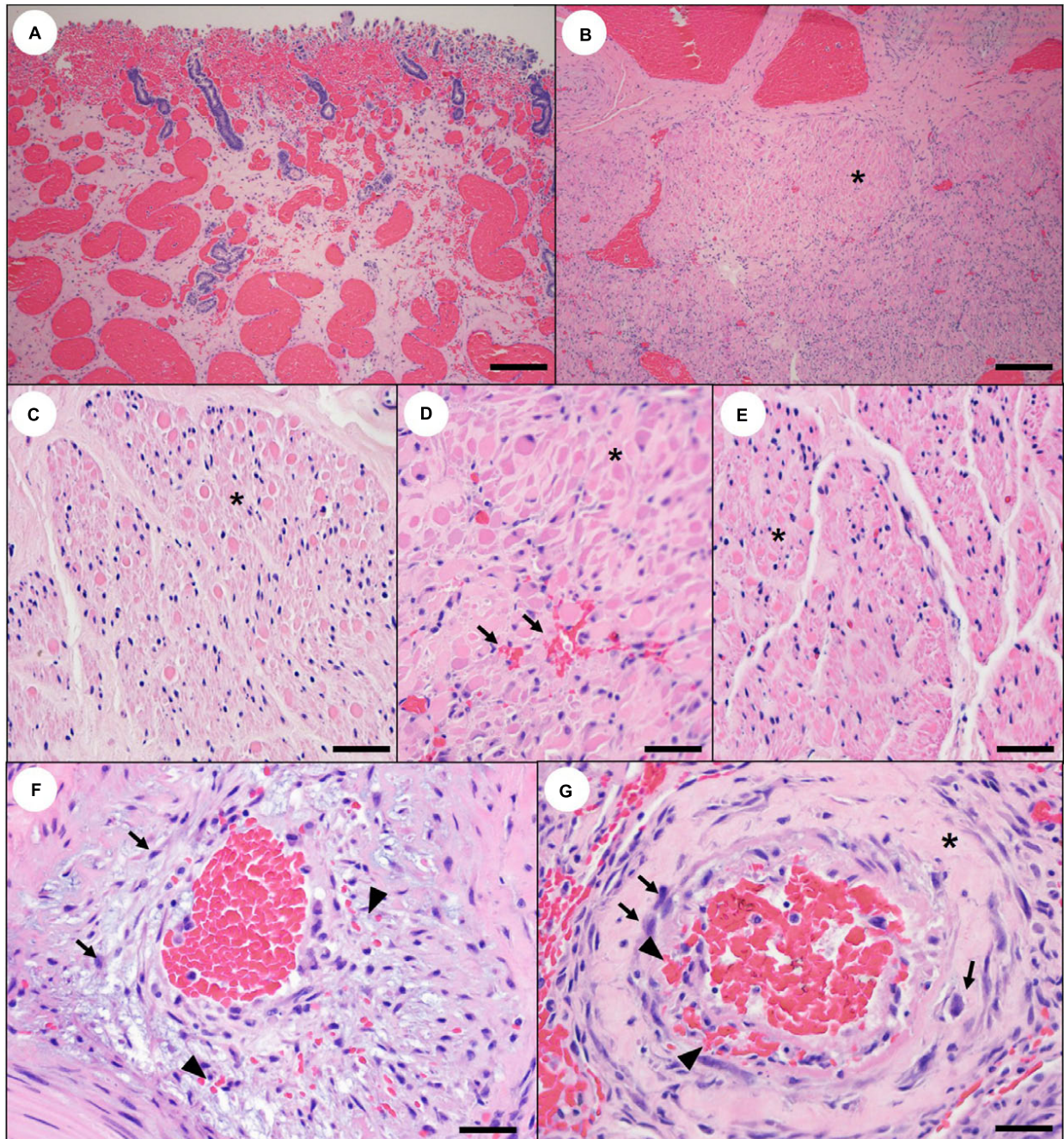
FIGURE 25 | Reproductive histopathology that may reflect domoic acid (DA) toxicosis in southern sea otters. **(A)** Through **(E)** severe diffuse congestion and hemorrhage may be observed in the uterine wall of pregnant sea otters with acute DA toxicosis (**A**: Bar = 100 μm). **(B)** Through **(G)** the myometrium of pregnant sea otters with acute or subacute DA toxicosis may exhibit congestion, multifocal microhemorrhage (**D**: arrows), and patchy smooth muscle cell necrosis or apoptosis (**B** through **E**: asterisks) (**B**: Bar = 100 μm, **C–E**: Bar = 40 μm). **(F,G)** Myometrial arterioles also appear to be affected in sea otters with fatal DA toxicosis. Similar to the coronary arterioles, there is often mural smooth muscle swelling, cytoplasmic eosinophilia, and necrosis or apoptosis (arrows). Vascular mural and perivascular edema, fibrin and hemorrhage (arrowheads), and sparse mural hyalinization (asterisk) are also visible (**F**,**G**: Bar = 20 μm).

mortality investigation (Miller et al., 2020), DA toxicosis was a significant risk factor for fatal cardiomyopathy along with older age and protozoal infection, supporting prior assessments that cardiomyopathy is a complex, multifactorial condition (Kreuder et al., 2005).

In contrast with humans and other animals (Pulido, 2008; Zabka et al., 2009), DA-associated cardiomyopathy is common as a cause of death for southern sea otters (Kreuder et al., 2005; Miller et al., 2020; Moriarty et al., 2021b). The earliest DA-associated cardiovascular lesions were severe diffuse

congestion, brown-discolored myocardium, and multifocal microhemorrhage (**Tables 1**, **2** and **Figures 13B**, **14A–C, 15A,B**). To our knowledge, this is the first report of these lesions in relation to DA exposure in any species. When present, the brown-discolored myocardium supported a diagnosis of acute DA toxicosis, although artifact from autolysis or euthanasia must also be considered. While the cause is unknown, this discoloration may reflect myoglobin leakage from DA-mediated cardiomyocyte damage. Interestingly, high DA concentrations (up to 829 ppb) have been detected in pericardial fluid of sea otters with DA toxicosis (M. Miller, unpublished data). Subacute and chronic cardiac pathology was accompanied by progressive myocardial adaptation (e.g., cardiac dilation), and, ultimately, congestive heart failure (**Table 1**). Although chronic cardiac lesions were easy to identify on histopathology, temporally compatible CNS lesions could usually be found on careful inspection (**Table 2**).

Congestive heart failure-associated hepatic vein thrombosis and massive hepatic necrosis (**Tables 1**, **2** and **Figures 23A–F**) have not been previously reported in association with DA toxicosis in humans and other animals. This condition appears similar to Budd–Chiari-like syndrome due to caudal vena cava thrombosis in domestic dogs (Dennis et al., 2010); in both dogs and sea otters the impeded venous blood flow can acutely exacerbate right-sided congestive heart failure. The most likely cause of this condition is sea otters is impeded venous return secondary to right-sided congestive heart failure, leading to blood stasis in the hepatic vein and caudal vena cava, and activation of clotting factors and platelets.

Although hypertension has been reported in humans with acute DA toxicosis (Gessner et al., 1997) and the cardiac conducting system and blood vessels express glutamate receptors that could facilitate DA binding (Mueller et al., 2003; Gill and Pulido, 2005; Gill et al., 2007), the pathophysiology of DA-mediated cardiac damage is poorly understood (Pulido, 2008). Potential pathways for cardiotoxicity include centrally mediated (CNS) processes (Pulido, 2008; Zabka et al., 2009), oxidative, mitochondrial, and/or ischemic impacts (Boldyrev et al., 2004; Vranyac-Tramoundanas et al., 2011; Vieira et al., 2016), and systemic renal, vascular and hormonal dysfunction (Arufe et al., 1995; Pulido, 2008; Funk et al., 2014). Domoic acid-mediated myocardial pathology could involve multiple pathways that are directly or indirectly initiated by DA toxicosis, including vasopressive or vasotoxic effects, shock, ischemia, dysrhythmia, osmotic dysregulation, endocrine disruption, mitochondrial damage, and cytokine cascades that culminate in cellular necrosis or apoptosis (Kreuder et al., 2005; Pulido, 2008; Zabka et al., 2009). Because the CVOs regulate blood volume, plasma osmolality, electrolytes, hormones, and cardiac function (Fry and Ferguson, 2009), DA-associated CVO damage could also be a contributing factor.

Sea otters with DA toxicosis also had substantial vascular mural pathology (**Table 2**), especially in the coronary arterioles (**Figures 16A–F**), which has not been reported in humans or other animals. Based on their microscopic appearance, acute lesions were suggestive of DA-mediated cytotoxicity for vascular mural smooth muscle cells and endothelium, which could be associated with regional or systemic hypotension

and vascular shock. The observed arterial lesions coincided spatially and temporally with regions of extensive cardiomyocyte loss, suggesting that the coronary pathology could accelerate cardiomyocyte loss through chronic hypoxia.

The findings of this study indicate that ocular examination and histopathology can facilitate diagnosis of acute DA toxicosis in sea otters. Severe hyphema and congestion, affecting the choroid, retina, and ciliary body, were common in sea otters with acute DA toxicosis (**Tables 1**, **2** and **Figures 24B,D**), and visual deficits have been noted in some live-stranded otters with DA toxicosis. Glutamate receptors are present in mammalian ocular tissue (Thoreson and Witkovsky, 1999; Yang, 2004; Gill and Pulido, 2005), providing potential binding sites for DA. Domoic acid-associated retinal pathology has been reported in sea lions and laboratory animals (Olney, 1982; Todd, 1993; Silvagni et al., 2005). The extended postmortem interval and the type of tissue fixation used in the current study limited assessment of retinal histopathology; future research may also identify DA-associated retinal lesions in sea otters.

Challenges of Broad-Scale Assessment of DA Toxicosis in Sea Otters

Postmortem assessment of DA toxicosis is challenging in free-ranging wildlife due to limited clinical history, unknown toxin dose and frequency, variable time intervals between DA exposure and death, and artifact due to postmortem scavenging and autolysis. In addition to fatal acute toxicosis, understanding the sublethal effects of DA is important, yet under-recognized. Domoic acid-associated pathology in California sea lions can propagate from initial sites of damage over time (Silvagni et al., 2005; Goldstein et al., 2009). These cascades of tissue damage in the brain, heart, vasculature, and other tissues can cause chronic health impacts (Silvagni et al., 2005; Pulido, 2008; Goldstein et al., 2009). Although these sublethal effects are less well characterized, lifelong illness can result from one-time, episodic, or chronic DA exposure (Goldstein et al., 2008; Pulido, 2008). Fetal DA exposure can also cause lifelong disease and reduce fitness (Ramsdell and Zabka, 2008; Grant et al., 2010). Given the frequency of toxic *Pseudo-nitzschia* blooms in California (Lewitus et al., 2012; Smith et al., 2018) and the importance of DA as a cause of acute and chronic CNS and cardiovascular disease (Miller et al., 2020), this potent neurotoxin has the potential to hinder southern sea otter population recovery (Moriarty et al., 2021b; Tinker et al., in Press).

Several unique biological characteristics put sea otters at high risk for DA toxicosis (Jessup et al., 2004, 2007). As the smallest marine mammal with no insulating blubber (Riedman and Estes, 1990), sea otters consume 25% of their body weight in prey each day to meet baseline metabolic requirements (Kenyon, 1969; Yeates et al., 2007). Because the diets of southern sea otters can include a high proportion of filter-feeding and detritus-feeding benthic invertebrates (Riedman and Estes, 1990; Tinker et al., 2008), high DA exposure may occur during or after a toxic bloom event, as DA-containing diatoms sink into deeper water and persist in sediment and invertebrates (Wekell et al., 1994; Sekula-Wood et al., 2009; Schultz et al., 2013). As a result, sea

otters with DA toxicosis often strand weeks after DA-exposed pinnipeds during toxic bloom events. California sea lions are highly mobile predators that feed on planktivorous fish, while sea otters have greater site fidelity, smaller home ranges, and feed on invertebrates. Domoic acid toxicosis in these two species likely reflects trophic transfer of the toxin in the pelagic and nearshore food webs, respectively. Although there can be spatiotemporal overlap of DA-associated mortality events in sea lions and sea otters (Kreuder et al., 2005), this is not always the case and is likely due to their different life histories and the ecological complexity of DA events.

Indistinct associations between *Pseudo-nitzschia* blooms and DA-associated sea otter deaths could also reflect the tendency for this toxin to persist in sediment and invertebrates long after blooms dissipate (Wekell et al., 1994; Sekula-Wood et al., 2009; Schultz et al., 2013). Although stranding patterns for sea otters and other marine species often increase during or after *Pseudo-nitzschia* blooms (Scholin et al., 2000; Kreuder et al., 2005; De La Riva et al., 2009), DA detection in tissues and body fluids and DA-associated sea otter deaths occur year-round in California (Miller et al., 2020). Similar results have been reported for free-ranging sea lions, including during the winter season when blooms are unlikely (Akmajian et al., 2017).

Several factors likely influence disease outcome following DA exposure, including the toxin dose, exposure frequency, age at exposure, and relative competency of the blood-brain barrier (Pulido, 2008). Other potential influences on outcome include prior DA-associated tissue damage, nutritional status, concurrent disease, and renal competence, since urinary excretion is a major route of DA clearance (Suzuki and Hierlihy, 1993; Pulido, 2008). Baseline CNS, vascular, and cardiac health are also important based on the case definitions presented herein and reports in other species (Goldstein et al., 2008; Zabka et al., 2009; Lefebvre et al., 2010; McHuron et al., 2013).

Reproductive status may also affect outcome; fetal fluids can act as a "sink" for maternally ingested DA, thereby slowing toxin excretion and prolonging both maternal and fetal exposure (Ramsdell and Zabka, 2008; Goldstein et al., 2009; Lefebvre et al., 2018). Prey preference also poses risks; some invertebrates such as razor clams (*Siliqua patula*) readily concentrate and retain DA in their tissues for weeks to months after toxic bloom events (Trainer et al., 2002; Goldberg, 2003; Kvitek et al., 2008). *In vitro* studies have also revealed that DA-exposed mussels can increase production of endogenous excitatory neurotransmitters, which could potentiate neurotoxic effects (Novelli et al., 1992). Interaction among risk factors is likely and could explain observations of varying disease expression, lesion patterns, and survival.

Summary

In this study, case definitions for acute, subacute, and chronic pathological findings for DA toxicosis were reported in a large cohort of necropsied southern sea otters. Although DA toxicosis has previously been reported in southern sea otters (Kreuder et al., 2003; Miller et al., 2020; Moriarty et al., 2021a,b), it is important to establish criteria for diagnosis so cases can be accurately identified, and DA-associated mortality can be factored into population monitoring and management efforts. *Pseudo-nitzschia* blooms that produce DA are common in California (Trainer et al., 2000; Lewitus et al., 2012; Wells et al., 2015; Smith et al., 2018), and bloom severity and frequency appear to be accentuated by climate change (Wells et al., 2015; Lefebvre et al., 2016; McKibben et al., 2017). A robust dataset encompassing hundreds of southern sea otters necropsied over 20 years has provided a unique opportunity to evaluate and describe pathology associated with DA toxicosis in this keystone species (Estes and Palmisano, 1974) and environmental sentinel (Jessup et al., 2004). Standardized necropsy and histopathology, sample collection, processing, and testing facilitated recognition of DA-associated lesion patterns in the brain, vasculature, heart, eyes, and other tissues, and aided identification of acute, subacute, and chronic impacts.

This work represents the first concerted effort to develop a rigorous case definition for DA toxicosis in sea otters. Diagnosing this common but often occult condition is important for improving clinical care of live-stranded sea otters and provides some of the necessary tools to assess the population-level impacts of DA for this federally listed, threatened subspecies. This work will also facilitate monitoring of DA-associated disease prevalence in southern sea otters in relation to periodic El Niño-Southern Oscillation events, climate change, and other environmental perturbations.

These provisional case definitions should be further refined and improved through prospective case review and biochemical testing, and the temporal estimates put forth can be further evaluated as part of ongoing research. Although mitigating the effects of DA on sea otters would be challenging, improving case recognition is a critical first step. Because humans, sea otters, and other marine wildlife consume similar marine foods, efforts to characterize acute, subacute, and chronic health effects of DA toxicosis for southern sea otters will provide strong collateral benefits for the health and well-being of humans and other animals. Documentation of cases in the absence of bloom events can also highlight the importance of DA retention in ecosystems and biota, accentuating exposure of all secondary consumers.

DATA AVAILABILITY STATEMENT

The raw data supporting the conclusions of this article will be made available by the authors, without undue reservation.

ETHICS STATEMENT

Ethical review and approval was not required for the animal study because the study was performed using dead southern sea otters submitted for necropsy to the California Department of Fish and Wildlife as per a federal MOU.

AUTHOR CONTRIBUTIONS

FUNDING

ACKNOWLEDGMENTS

SUPPLEMENTARY MATERIAL

The Supplementary Material for this article can be found online at: https://www.frontiersin.org/articles/10.3389/fmars.2021.585501/full#supplementary-material

REFERENCES

Akmajian, A. M., Scordino, J. J., and Acevedo-Gutiérrez, A. (2017). Year-round algal toxin exposure in free-ranging sea lions. *Mar. Ecol. Prog. Ser.* 583, 243–258. doi: 10.3354/meps1234

Arufe, M. C., Arias, B., Duran, R., and Alfonso, M. (1995). Effects of domoic acid on serum levels of TSH and thyroid hormones. *Endocr. Res.* 121, 671–680. doi: 10.1080/07435809509030482

Bargu, S., Silver, M., Goldstein, T., Roberts, K., and Gulland, F. (2010). Complexity of domoic acid-related sea lion strandings in Monterey Bay, California: foraging patterns, climate events, and toxic blooms. *Mar. Ecol. Prog. Ser.* 418, 213–222. doi: 10.3354/meps08816

Bejarano, A. C., Van Dolah, F. M., Gulland, F. M., Rowles, T. K., and Schwacke, L. H. (2008). Production and toxicity of the marine biotoxin domoic acid and its effects on wildlife: a review. *Hum. Ecol. Risk Assess.* 14, 544–567. doi: 10.1080/10807030802074220

Boldyrev, A., Bulygina, E., and Makhro, A. (2004). Glutamate receptors modulate oxidative stress in neuronal cells. A mini-review. *Neurotox. Res.* 6, 581–587. doi: 10.1007/BF03033454

Brodie, E. C., Gulland, F. M. D., Greig, D. J., Hunter, M., Jaakola, J., St. Leger, J., et al. (2006). Domoic acid causes reproductive failure in California sea lions (*Zalophus californianus*). *Mar. Mamm. Sci.* 22, 700–707. doi: 10.1111/j.1748-7692.2006.00045.x

Bruni, J. E., Bose, R., Pinsky, C., and Glavin, G. (1991). Circumventricular organ origin of domoic acid-induced neuropathology and toxicology. *Brain Res. Bull.* 26, 419–424. doi: 10.1016/0361-9230(91)90016-D

Buckmaster, P. S., Wen, X., Toyoda, I., Gulland, F. M. D., and Van Bonn, W. (2014). Hippocampal neuropathology of domoic acid-induced epilepsy in California sea lions (*Zalophus californianus*). *J. Comp. Neurol.* 522, 1691–1706. doi: 10.1002/cne.23509

Burbacher, T. M., Grant, K. S., Petroff, R., Shum, S., Crouthamel, B., Stanley, C., et al. (2019). Effects of oral domoic acid exposure on maternal reproduction and infant birth characteristics in a preclinical nonhuman primate model. *Neurotoxicol. Teratol.* 72, 10–21. doi: 10.1016/j.ntt.2019.01.001

Cendes, F., Andermann, F., Carpenter, S., Zatorre, R. J., and Cashman, N. R. (1995). Temporal lobe epilepsy caused by domoic acid intoxication: evidence for glutamate receptor-mediated excitotoxicity in humans. *Ann. Neurol.* 37, 123–126. doi: 10.1002/ana.410370125

Cook, P. F., Reichmuth, C., Rouse, A., Dennison, S., Van Bonn, B., and Gulland, F. (2016). Natural exposure to domoic acid causes behavioral perseveration in Wild Sea lions: neural underpinnings and diagnostic application. *Neurotoxicol. Teratol.* 57, 95–105. doi: 10.1016/j.ntt.2016.08.001

Cook, P. F., Reichmuth, C., Rouse, A. A., Libby, L. A., Dennison, S. E., Carmichael, O. T., et al. (2015). Algal toxin impairs sea lion memory and hippocampal connectivity, with implications for strandings. *Science* 350, 1545–1547. doi: 10.1126/science.aac5675

De La Riva, G. T., Johnson, C. K., Gulland, F. M., Langlois, G. W., Heyning, J. E., Rowles, T. K., et al. (2009). Association of an unusual marine mammal mortality event with *Pseudo-nitzschia* spp. blooms along the southern California coastline. *J. Wildlife Dis.* 45, 109–121. doi: 10.7589/0090-3558-45.1.109

Dennis, R., Kirberger, R. M., Barr, F., and Wrigley, R. H. (2010). "Chapter 7, Cardiovascular system," in *Handbook of Small Animal Radiology and Ultrasound*, 2nd Edn, eds R. Dennis, R. M. Kirberger, F. Barr, and R. H. Wrigley (New York, NY: Elsevier Ltd), 175–198. doi: 10.1016/C2009-0-43690-0

Doucette, T. A., Bernard, P. B., Husum, H., Perry, M. A., Ryan, C. L., and Tasker, R. A. (2004). Low doses of domoic acid during postnatal development produce permanent changes in rat behaviour and hippocampal morphology. *Neurotox Res.* 6, 555–563. doi: 10.1007/BF03033451

Duvernoy, H. M., and Risold, P. Y. (2007). The circumventricular organs: an atlas of comparative anatomy and vascularization. *Brain Res. Rev.* 56, 119–147. doi: 10.1016/j.brainresrev

Estes, J. A., and Palmisano, J. F. (1974). Sea otters: their role in structuring nearshore communities. *Science* 185, 1058–1060.

Fritz, L., Quilliam, M. A., Wright, J. L. C., Beale, A. M., and Work, T. M. (1992). An outbreak of domoic acid poisoning attributed to the pennate diatom *Pseudonitzschia australis. J. Phycol.* 28, 439–442. doi: 10.1111/j.0022-3646.1992.00439.x

Fry, M., and Ferguson, A. V. (2009). Ghrelin modulates electrical activity of area postrema neurons. *Am. J. Physiol.* 296, R485–R492. doi: 10.1152/ajpregu.90555.2008

Funk, J. A., Janech, M. G., Dillon, J. C., Bissler, J. J., Siroky, B. J., and Bell, P. D. (2014). Characterization of renal toxicity in mice administered the marine biotoxin domoic acid. *J. Am. Soc. Nephrol.* 25, 1187–1197. doi: 10.1681/ASN.2013080836

Fuquay, J. M., Muha, N., Wang, Z., and Ramsdell, J. S. (2012). Elimination kinetics of domoic acid from the brain and cerebrospinal fluid of the pregnant rat. *Chem. Res. Toxicol.* 2, 2805–2809. doi: 10.1021/tx300434s

Gao, X., Xu, X., Pang, J., Zhang, C., Ding, J. M., Peng, X., et al. (2007). NMDA receptor activation induces mitochondrial dysfunction, oxidative stress and apoptosis in cultured neonatal rat cardiomyocytes. *Physiol. Res.* 56, 559–569.

Gessner, B. D., Bell, P., Doucette, G. J., Moczydlowski, E., Poli, M. A., Van Dolah, F., et al. (1997). Hypertension and identification of toxin in human urine and serum following a cluster of mussel-associated paralytic shellfish poisoning outbreaks. *Toxicon* 35, 711–722. doi: 10.1016/S0041-0101(96)00154-7

Gill, S., and Pulido, O. (2005). "Glutamate receptors in peripheral tissues: Distribution and implications for toxicology," in *Glutamate Receptors in Peripheral Tissues: Excitatory Transmission Outside the CNS*, eds S. Gill and O. Pulido (New York, NY: Kluwer Academic Plenum Press), 3–26.

Gill, S., Veinot, J., Kavanagh, M., and Pulido, O. (2007). Human heart glutamate receptors - implications for toxicology, food safety, and drug discovery. *Toxicol. Pathol.* 35, 411–417. doi: 10.1080/01926230701230361

Giordano, G., White, C. C., Mohar, I., Kavanagh, T. J., and Costa, L. G. (2007). Glutathione levels modulate domoic acid induced apoptosis in mouse cerebellar granule cells. *Toxicol. Sci.* 100, 433–444. doi: 10.1093/toxsci/kfm236

Glavin, G. B., Pinsky, C., and Bose, R. (1990). Gastrointestinal effects of contaminated mussels and putative antidotes thereof. *Can. Dis. Wkly. Rep.* 16(Suppl. IE), 111–115.

Goldberg, J. (2003). *Domoic Acid in the Benthic Food Web of Monterey Bay, California.* Master's thesis, California State University, Moss Landing, CA.

Goldstein, T., Mazet, J. A. K., Zabka, T. S., Langlois, G., Colegrove, K. M., Silver, M., et al. (2008). Novel symptomatology and changing epidemiology of domoic acid toxicosis in California sea lions (*Zalophus californianus*): an increasing risk to marine mammal health. *P. R. Soc. B* 275, 267–276. doi: 10.1098/rspb.2007.1221

Goldstein, T., Zabka, T. S., DeLong, R. L., Wheeler, E. A., Ylitalo, G., Bargu, S., et al. (2009). The role of domoic acid in abortion and premature parturition of California sea lions (*Zalophus californianus*) on San Miguel Island, California. *J. Wildlife Dis.* 45, 91–108. doi: 10.7589/0090-3558-45.1.91

Grant, K. S., Burbacher, T. M., Faustman, E. M., and Grattan, L. (2010). Domoic acid: neurobehavioral consequences of exposure to a prevalent marine biotoxin. *Neurotoxicol. Teratol.* 32, 132–141. doi: 10.1016/j.ntt.2009.09.005

Grattan, L. M., Boushey, C. J., Liang, Y., Lefebvre, K. A., Castellon, L. J., Roberts, K. A., et al. (2018). Repeated dietary exposure to low levels of domoic acid and problems with everyday memory: research to public health outreach. *Toxins* 10:103. doi: 10.3390/toxins10030103

Gulland, F. M. (2000). *Domoic Acid Toxicity in California Sea Lions (Zalophus californianus) Stranded Along the Central California Coast, May-October 1998: Report to the National Marine Fisheries Service Working Group on Unusual Marine Mammal Mortality Events*, Vol. 17. Washington, DC: US Department of Commerce, National Oceanic and Atmospheric Administration, National Marine Fisheries Service.

Hatfield, B. B., Yee, J. L., Kenner, M. C., and Tomoleoni, J. A. (2019). *California Sea Otter (Enhydra lutris nereis) Census Results, Spring 2019*. Report USGS Numbered Series. Reston, VA: U.S. Geological Survey.

Jessup, D. A., Miller, M., Ames, J., Harris, M., Kreuder, C., Conrad, P. A., et al. (2004). Southern sea otter as a sentinel of marine ecosystem health. *Ecohealth* 1, 239–245. doi: 10.1007/s10393-004-093-7

Jessup, D. A., Miller, M. A., Kreuder-Johnson, C., Conrad, P. A., Tinker, M. T., Estes, J., et al. (2007). Sea otters in a dirty ocean. *JAVMA* 231, 1648–1652. doi: 10.2460/javma.231.11.1648

Jian Wang, G. J., Schmued, L. C., Andrews, A. M., Scallet, A. C., Slikker, W. H., and Binienda, Z. H. (2000). Systemic administration of domoic acid-induced spinal cord lesions in neonatal rats. *J. Spinal Cord Med.* 23, 31–39. doi: 10.1080/10790268.2000.11753506

Kenyon, K. W. (1969). The sea otter in the Eastern Pacific ocean. *N. Am. Fauna* 68:352. doi: 10.3996/nafa.68.0001

Kreuder, C., Miller, M. A., Jessup, D. A., Lowenstein, L. J., Harris, M. D., Ames, J. A., et al. (2003). Patterns of mortality in southern sea otters (*Enhydra lutris nereis*) from 1998-2001. *J. Wildlife Dis.* 39, 495–509. doi: 10.7589/0090-3558-39.3.495

Kreuder, C. M., Miller, M. A., Lowenstine, L. J., Conrad, P. A., Carpenter, T. E., Jessup, D. A., et al. (2005). Evaluation of cardiac lesions and risk factors associated with myocarditis and dilated cardiomyopathy in southern sea otters (*Enhydra lutris nereis*). *Am. J. Vet. Res.* 66, 289–299. doi: 10.2460/ajvr.2005.66.289

Kumar, V., Abbas, A. K., and Aster, J. C. (2014). "Chapter 2: Cellular responses to stress and toxic insults", and "Chapter 3: Inflammation and repair," in *Robbins & Cotran: Pathologic Basis of Disease*, 9th Edn, eds V. Kumar, A. K. Abbas, J. C. Aster (Maryland Heights, MO: Elsevier Press), 31–112.

Kvitek, R. G., Goldberg, J. D., Smith, G. J., Doucette, G. J., and Silver, M. W. (2008). Domoic acid contamination within eight representative species from the benthic food web of Monterey Bay, California, USA. *Mar. Ecol. Progr. Ser.* 367, 35–47. doi: 10.3354/meps07569

Lefebvre, K. A., Bargu, S., Kieckhefer, T., and Silver, M. W. (2002). From sanddabs to blue whales: the pervasiveness of domoic acid. *Toxicon* 40, 971–977. doi: 10.1016/S0041-0101(02)00093-4

Lefebvre, K. A., Hendrix, A., Halaska, B., Duignan, P. J., Shum, S., Isoherranen, N., et al. (2018). Domoic acid in California sea lion fetal fluids indicates continuous exposure to a neuroteratogen poses risks to mammals. *Harmful Algae* 79, 53–57. doi: 10.1016/j.hal.2018.06.003

Lefebvre, K. A., Kendrick, P. S., Ladiges, W., Hiolski, E. M., Ferriss, B. E., Smith, D. R., et al. (2017). Chronic low-level exposure to the common seafood toxin domoic acid causes cognitive deficits in mice. *Harmful Algae* 64, 20–29. doi: 10.1016/j.hal.2017.03.003

Lefebvre, K. A., Quakenbush, L., Frame, E., Burek-Huntington, K., Sheffield, G., Stimmelmayr, R., et al. (2016). Prevalence of algal toxins in Alaskan marine mammals foraging in a changing arctic and subarctic environment. *Harmful Algae* 55, 13–24. doi: 10.1016/j.hal.2016.01.007

Lefebvre, K. A., Robertson, A., Frame, E. R., Colegrove, K. M., Nance, S., Baugh, K. A., et al. (2010). Clinical signs and histopathology associated with domoic acid poisoning in northern fur seals (*Callorhinus ursinus*) and comparison of toxin detection methods. *Harmful Algae* 9, 374–383. doi: 10.1016/j.hal.2010.01.007

Levin, E. D., Pang, W. G., Harrison, J., Williams, P., Petro, A., and Ramsdell, J. S. (2006). Persistent neurobehavioral effects of early postnatal domoic acid exposure in rats. *Neurotoxicol. Teratol.* 28, 673–680. doi: 10.1016/j.ntt.2006.08.005

Lewitus, A. J., Horner, R. A., Caron, D. A., Garcia-Mendoza, E., Hickey, B. M., Hunter, M., et al. (2012). Harmful algal blooms along the North American west coast region: history, trends, causes, and impacts. *Harmful Algae* 19, 133–159. doi: 10.1016/j.hal.2012.06.009

Maucher, J. M., and Ramsdell, J. S. (2007). Maternal-fetal transfer of domoic acid in rats at two gestational time points. *Environ. Health Perspect.* 115, 1743–1746. doi: 10.1289/ehp.10446

McCabe, R. M., Hickey, B. M., Kudela, R. M., Lefebvre, K. A., Adams, N. G., Bill, B. D., et al. (2016). An unprecedented coastwide toxic algal bloom linked to anomalous ocean conditions. *Geophys. Res. Lett.* 43, 310–366.

McHuron, E. A., Greig, D. J., Colegrove, K. M., Fleetwood, M., Spraker, T. R., Gulland, F. M. D., et al. (2013). Domoic acid exposure and associated clinical signs and histopathology in Pacific harbor seals (*Phoca vitulina richardii*). *Harmful Algae* 23, 28–33. doi: 10.1016/j.hal.2012.12.008

McKibben, S. M., Peterson, W., Wood, A. M., Trainer, V. L., Hunter, M., and White, A. E. (2017). Climatic regulation of the neurotoxin domoic acid. *Proc. Natl. Acad. Sci. U.S.A.* 114, 239–244. doi: 10.1073/pnas.1606798114

Miller, M. A., Moriarty, M. E., Henkel, L., Tinker, M. T., Burgess, T., and Batac, F. I. (2020). Predators, disease, and environmental change in the nearshore ecosystem: mortality in southern sea otters (*Enhydra lutris nereis*) from 1998-2012. *Front. Mar. Sci.* 7:582. doi: 10.3389/fmars.2020.00582

Miller, P. E., and Scholin, C. A. (1998). Identification and enumeration of cultured and wild *Pseudo-nitzschia* (*Bacillariophyceae*) using species-specific LSU rRNA-targeted fluorescent probes and filter-based whole cell hybridization. *J. Phycol.* 34, 371–382. doi: 10.1046/j.1529-8817.1998.340371.x

Miller, M. A., et al. Biochemical assessment of domoic acid ingestion, absorption and distribution in southern sea otters (*Enhydra lutris nereis*) from California. In final preparation.

Moriarty, M. E., Miller, M. A., Murray, M. J., Gunther-Harrington, C. T., Duignan, P., Field, C. L., et al. (2021a). Exploration of serum cardiac troponin I as a biomarker of cardiomyopathy in southern sea otters (*Enhydra lutris nereis*). *Am. J. Vet. Res.* (in press).

Moriarty, M. E., Tinker, M. T., Miller, M. A., Tomoleoni, J. A., Staedler, M. M., Fuji, J. A., et al. (2021b). Exposure to domoic acid is an ecological driver of cardiac disease in southern sea otters. *Harmful Algae* 101:101973. doi: 10.1016/j.hal.2020.101973

Mueller, R. W., Gill, S. S., and Pulido, O. M. (2003). The monkey (*Macaca fascicularis*) heart neural structures and conducting system: an immunochemical study of selected neural biomarkers and glutamate receptors. *Tox. Path.* 31, 227–234. doi: 10.1080/01926230390183724

Novelli, A., Kispert, J., Ferna, M. T., Torreblanca, A., and Zitko, V. (1992). Domoic acid-containing toxic mussels produce neurotoxicity in neuronal cultures through a synergism between excitatory amino acids. *Brain Res.* 577, 41–48. doi: 10.1016/0006-8993(92)90535-H

Olney, J. W. (1982). The toxic effects of glutamate and related compounds in the retina and the brain. *Retina* 2, 341–359.

Perl, T. M., Bedard, L., Kosatsky, T., Hockin, J. C., Todd, E. C., McNutt, L. A., et al. (1990a). Amnesic shellfish poisoning: a new clinical syndrome due to domoic acid. *Can. Dis. Wkly. Rep.* 16(Suppl. 1E), 7–8.

Perl, T. M., Bédard, L., Kosatsky, T., Hockin, J. C., Todd, E. C., and Remis, R. S. (1990b). An outbreak of toxic encephalopathy caused by eating mussels contaminated with Domoic Acid. *N. Engl. J. Med.* 322, 1775–1780. doi: 10.1056/NEJM199006213222504

Pulido, O., Mueller, R., Truelove, J., Iverson, F., Rowsell, P. B. M., and Bujaki, M. (1995). "Neuropathology of subchronic oral administration of domoic acid in rats," in *Proceedings of the Society for Neuroscience 25th Meeting Abstract*, New York, NY.

Pulido, O. M. (2008). Domoic acid toxicologic pathology: a review. *Mar. Drugs* 6, 180–219. doi: 10.3390/md20080010

Ramsdell, J. S., and Gulland, F. M. (2014). Domoic acid epileptic disease. *Mar. Drugs* 12, 1185–1207. doi: 10.3390/md12031185

Ramsdell, J. S., and Zabka, T. S. (2008). In utero domoic acid toxicity: a fetal basis to adult disease in the California sea lion (*Zalophus californianus*). *Mar. Drugs* 6, 262–290. doi: 10.3390/md6020262

Riedman, M., and Estes, J. A. (1990). The sea otter (*Enhydra lutris*): behavior, ecology, and natural history. *Biol. Rep.* 90, 1–126.

Rust, L., Gulland, F., Frame, E., and Lefebvre, K. (2014). Domoic acid in milk of free living California marine mammals indicates lactational exposure occurs. *Mar. Mamm. Sci.* 30, 1272–1278. doi: 10.1111/mms.12117

Scholin, C. A., Gulland, F., Doucette, G. J., Benson, S., Busman, M., Chavez, F. P., et al. (2000). Mortality of sea lions along the central California coast linked to a toxic diatom bloom. *Nature* 403, 80–84. doi: 10.1038/47481

Schultz, I. R., Skillman, A., Sloan-Evans, S., and Woodruff, D. (2013). Domoic acid toxicokinetics in dungeness crabs: new insights into mechanisms that regulate bioaccumulation. *Aquat. Toxicol.* 140, 77–78. doi: 10.1016/j.aquatox.2013.04.011

Sekula-Wood, E., Schnetzer, A., Benitez-Nelson, C. R., Anderson, C., Berelson, W. M., Brzezinski, M. A., et al. (2009). Rapid downward transport of the neurotoxin domoic acid in coastal waters. *Nat. Geosci.* 2, 272–275. doi: 10.1038/ngeo472

Shumway, S. E., Allen, S. M., and Boersma, P. D. (2003). Marine birds and harmful algal blooms: sporadic victims or under-reported events? *Harmful Algae* 2, 1–17. doi: 10.1016/S1568-9883(03)00002-7

Silvagni, P. A., Lowenstine, L. J., Spraker, T., Lipscomb, T. P., and Gulland, F. M. D. (2005). Pathology of domoic acid toxicity in California sea lions (*Zalophus californianus*). *Vet. Pathol.* 42, 184–191. doi: 10.1354/vp.42-2-184

Smith, J., Connell, P., Evans, R. H., Gellene, A. G., Howard, M. D., Jones, B. H., et al. (2018). A decade and a half of *Pseudo-nitzschia* spp. and domoic acid along the coast of southern California. *Harmful Algae* 79, 87–104. doi: 10.1016/j.hal.2018.07.007

Sobotka, T. J., Brown, R., Quander, D. Y., Jackson, R., Smith, M., Long, S. A., et al. (1996). Domoic acid: neurobehavioral and neurohistological effects of low-dose exposure in adult rats. *Neurotoxicol. Teratol.* 18, 659–670. doi: 10.1016/S0892-0362(96)00120-1

Sutherland, R. J., Hoesing, J. M., and Whishaw, I. Q. (1990). Domoic acid, an environmental toxin, produces hippocampal damage and severe memory impairment. *Neurosci. Lett.* 120, 221–223. doi: 10.1016/0304-3940(90)90043-9

Suzuki, C. A. M., and Hierlihy, S. L. (1993). Renal clearance of domoic acid in the rat. *Food Chem. Toxicol.* 31, 701–706. doi: 10.1016/0278-6915(93)90140-T

Teitelbaum, J. S., Zatorre, R. J., Carpenter, S., Gendron, D., Evans, A. C., Gjedde, A., et al. (1990). Neurologic sequelae of domoic acid intoxication due to the ingestion of contaminated mussels. *N. Engl. J. Med.* 322, 1781–1787. doi: 10.1056/NEJM199006213222505

Thomas, K., Harvey, J. T., Goldstein, T., Barakos, J., and Gulland, F. (2010). Movement, dive behavior, and survival of California sea lions (*Zalophus californianus*) posttreatment for domoic acid toxicosis. *Mar. Mamm. Sci.* 26, 36–52. doi: 10.1111/j.1748-7692.2009.00314.x

Thoreson, W. B., and Witkovsky, P. (1999). Glutamate receptors and circuits in the vertebrate retina. *Prog. Retin. Eye Res.* 18, 765–810. doi: 10.1016/S1350-9462(98)00031-7

Tiedeken, J. A., Ramsdell, J. S., and Ramsdell, A. F. (2005). Developmental toxicity of domoic acid in zebrafish (*Danio rerio*). *Neurotoxicol. Teratol.* 27, 711–717. doi: 10.1016/j.ntt.2005.06.013

Tinker, M. T., Bentall, G., and Estes, J. A. (2008). Food limitation leads to behavioral diversification and dietary specialization in sea otters. *Proc. Natl. Acad. Sci. U.S.A.* 105, 560–565. doi: 10.1073/pnas.0709263105

Tinker, M. T., Carswell, L. P., Tomoleoni, J. A., Hatfield, B. B., Harris, M. D., Miller, M. A., et al. (in Press). *An Integrated Population Model for Southern Sea Otters.* Reston, VA: US Geological Survey. US Geological Survey Open-File Report No. 2021-xxxx.

Todd, E. C. (1993). Domoic acid and amnesic shellfish poisoning, a review. *J. Food Protect.* 56, 69–83. doi: 10.4315/0362-028X-56.1.69

Trainer, V. L., Adams, N. G., Bill, B. D., Stehr, C. M., Wekell, J. C., Moeller, P., et al. (2000). Domoic acid production near California coastal upwelling zones, June 1998. *Limnol. Oceanog.* 45, 1818–1833. doi: 10.4319/lo.2000.45.8.1818

Trainer, V. L., Hickey, B. M., and Horner, R. A. (2002). Biological and physical dynamics of domoic acid production off the Washington coast. *Limnol. Oceanogr.* 47, 1438–1446. doi: 10.4319/lo.2002.47.5.1438

Tryphonas, L., Truelove, J., Todd, E., Nera, E., and Iverson, F. (1990). Experimental oral toxicity of domoic acid in cynomolgus monkeys (*Macaca fascicularis*) and rats: preliminary investigations. *Food Chem. Toxicol.* 28, 707–715. doi: 10.1016/0278-6915(90)90147-F

Vieira, A. C., Cifuentes, J. M., Bermúdez, R., Ferreiro, S. F., Castro, A. R., and Botana, L. M. (2016). Heart alterations after domoic acid administration in rats. *Toxins* 8:68. doi: 10.3390/toxins8030068

Vranyac-Tramoundanas, A., Harrison, J. C., Sawant, P. M., Kerr, D. S., and Sammut, I. A. (2011). Ischemic cardiomyopathy following seizure induction by domoic acid. *Am. J. Pathol.* 179, 141–154. doi: 10.1016/j.ajpath.2011.03.017

Wekell, J. C., Gauglitz, E. J. Jr., Bamett, H. J., Hatfield, C. L., Simons, D., and Ayres, D. (1994). Occurrence of domoic acid in Washington State razor clams (*Siliqua patula*) during 1991-1993. *Nat. Toxins* 2, 197–205. doi: 10.1002/nt.2620020408

Wells, M. L., Trainer, V. L., Smayda, T. J., Karlson, B. S., Trick, C. G., Kudela, R. M., et al. (2015). Harmful algal blooms and climate change: learning from the past and present to forecast the future. *Harmful Algae* 49, 68–93. doi: 10.1016/j.hal.2015.07.009

Work, T. M., Barr, B., Beale, A. M., Fritz, L., Quilliam, M. A., and Wright, J. L. (1993). Epidemiology of domoic acid poisoning in brown pelicans (*Pelecanus occidentalis*) and Brandt's cormorants (*Phalacrocorax penicillatus*) in California. *J. Zoo Wildlife Med.* 24, 54–62.

Yang, X. L. (2004). Characterization of receptors for glutamate and GABA in retinal neurons. *Prog. Neurobiol.* 73, 127–150. doi: 10.1016/j.pneurobio.2004.04.002

Yeates, L. C., Williams, T. M., and Fink, T. L. (2007). Diving and foraging energetics of the smallest marine mammal, the sea otter (*Enhydra lutris*). *J. Exper. Biol.* 210, 1960–1970. doi: 10.1242/jeb.02767

Zabka, T. S., Goldstein, T., Cross, C., Mueller, R. W., Kreuder-Johnson, C., Gill, S., et al. (2009). Characterization of a degenerative cardiomyopathy associated with domoic acid toxicity in California sea lions (*Zalophus californianus*). *Vet. Pathol.* 46, 105–119. doi: 10.1354/vp.46-1-105

Zatorre, R. J. (1990). Memory loss following domoic acid intoxication from ingestion of toxic mussels. *Can. Dis. Wkly. Rep.* 16, 101–103.